

THESIS FOR THE DEGREE OF DOCTOR OF PHILOSOPHY

Load Modelling for Fatigue Assessment of Vehicles – a Statistical Approach

MAGNUS KARLSSON

CHALMERS | GÖTEBORG UNIVERSITY



Department of Mathematical Sciences, Chalmers University of Technology
Department of Mathematical Sciences, Göteborg University
SE-412 96 Göteborg, Sweden

Göteborg, January 2007

Load Modelling for Fatigue Assessment of Vehicles – a Statistical Approach
MAGNUS KARLSSON
ISBN 978-91-7291-887-0

© MAGNUS KARLSSON, 2007.

Doktorsavhandlingar vid Chalmers Tekniska Högskola
Ny serie nr 2568
ISSN 0346-718X

Department of Mathematical Sciences, Chalmers University of Technology
Department of Mathematical Sciences, Göteborg University
SE-412 96 Göteborg
Sweden
Telephone + 46 (0)31-772 1000
Göteborg, Sweden 2007

Load Modelling for Fatigue Assessment of Vehicles – a Statistical Approach
MAGNUS KARLSSON
Department of Mathematical Sciences, Chalmers University of Technology
Department of Mathematical Sciences, Göteborg University

Abstract

A way of modelling loads in customer usage for fatigue life considerations of vehicles is discussed. The starting point is lateral vehicle loads acting on trucks. Customer usage is described by using road classification. Within each road class the loads are assumed to be similar and a particular customer can be modelled on the basis of the distance the driver drives in each road class. A parametric model is built up to describe the lateral loads found in measurements. From this model, an explicit expression for the expected damage is derived based on the rain flow cycle count method, the Basquin equation and the Palmgren-Miner rule. This model aims to capture the external loads coming into the vehicle in the lateral direction. In particular, it focuses on the operational environment and customer behaviour. From measurements, the parameters in the model are estimated. The variation of the parameters over the measurements is studied using the analysis of variance method. In the study, the road class as well as more local factors such as market and driver are considered in order to make sure that the road class can be regarded as global. The loads in the road classes can then be modelled using the results from the analysis of variance. Practical considerations in the design of experiments to gather data for the models are taken into account. The analysis technique is applied to the load model using data from a field study made in three different markets. Conclusions are drawn on the possibilities of classifying road loads and the need for design of experiments to use field measurements more efficiently.

Keywords: Fatigue, customer correlation, road load modelling, design of experiments, vehicle independent load models, lateral loads

Acknowledgements

The research presented in this work has been financially supported by Volvo 3P and VINNOVA within its Swedish National Road Vehicle Program. This support is gratefully acknowledged.

My personal thanks go to:

Thomas Svensson, my supervisor at FCC, for his great ability of bringing up new ideas, and all the interesting discussions about my research topic and many other topics.

Bengt Johannesson, my supervisor at Volvo 3P, for his fantastic encouragement and support.

Jacques de Maré, my supervisor at the Department of Mathematical Sciences, Chalmers University of Technology/Gothenburg University, for his great efforts to create scientific environment to work in and helping me out with many scientific as well as practical details.

I would also like to thank the other members of my supervising group, Pär Johannesson, FCC, Stefan Edlund and Inge Johansson, Volvo, for their many valuable comments.

Igor Rychlik also deserves special thanks for reading the manuscript of paper II and supplying valuable comments, which greatly improved the paper. He also provided the ideas behind large parts of section 6 of the paper.

Further, Fredrik Öijer and Per-Olov Fryk as well as the other members of the CVA-Durability project team at Volvo have provided many great ideas. Thanks!

Thanks also to the people at the durability and reliability department at Volvo, the people at FCC, and the people at the Department of Mathematical Sciences at Chalmers.

Finally, I would also like to thank my family and friends for their great support. And then, of course, Lisa, thanks for making my life so much better.

Göteborg, January 2007

Magnus Karlsson

This thesis is based on the work contained in the following papers:

Paper I: Karlsson, M., (2004) “Driver Independent Road Curve Characterisation”, *Supplement to Vehicle System Dynamics*, 41, pp. 411–420.

Paper II: M. Karlsson, “Parameterisation of Lateral Fatigue Loads on Vehicles”.

Paper III: M. Karlsson, (2005) “Evaluation of Approximative Methods for Rainflow Damage of Broad-Banded Non-Gaussian Random Loads”, *Proc. of 2005 ASME International Mechanical Engineering Congress and Exposition*, Nov. 5-11, 2005, Orlando, FA.

Paper IV: M. Karlsson, “Evaluation of Road Load Classification for Fatigue Assessments”.

Table of Contents

1. Introduction	1
1.1 Fatigue	1
1.2 Statistical nature of the problem	1
2. Customer load descriptions	1
2.1 Traditional ways of describing customer loads	1
2.2 New possibilities for measuring and modelling loads	2
2.3 Modelling load data using road classes	2
3. Modelling of road classes	4
3.1 Vehicle-independent load models.....	4
3.2 An example of a parametric vehicle-independent load model.....	4
3.3 From modelling measurement to modelling road classes.....	6
4. Analysing the road classes	7
4.1 Global classification	7
4.2 Design of experiment and analysis	8
4.3 Customer modelling based on the road classes	9
5. Discussion and conclusions	9
6. Summary of appended articles.....	10
Paper I: Driver Independent Road Curve Characterisation	10
Paper II: Parameterisation of Lateral Fatigue Loads on Vehicles	10
Paper III: Evaluation of Approximative Methods for Rainflow Damage of Broad-Banded Non- Gaussian Random Loads	11
Paper IV: Evaluation of Road Load Classification for Fatigue Assessments.....	11
7. Future work	11
References	12

1. Introduction

1.1 Fatigue

One of the major reasons for structural component failures is fatigue, a phenomenon that causes failure in structures due to repeated loading [1]. This problem is ever present in vehicles where such components are common. To design against fatigue means constructing components with sufficient **strength** to withstand the **loads** that act on them during the vehicle's design life. As the demands on transport efficiency increases, the vehicle industry is, to a greater extent than before, tailor-making vehicles to customers. This means that the design task is also becoming more important as over-dimensioning may lead to less loading capacity and worse fuel economy, and under-dimensioning may lead to component failures, which in turn can cause loss of performance. Getting proper knowledge about the strength of components and the loads they are subjected to is therefore essential.

1.2 Statistical nature of the problem

Many of the problems involved in modelling both strength and loads are of a statistical nature. The strength varies due to variation in material properties and variation due to the manufacturing process. Therefore, even under the same loading conditions, the fatigue lives of two components from the same batch may differ considerably. Furthermore, the fatigue phenomenon itself is extremely complicated and depends on details that cannot be measured even in the controlled environment in a laboratory.

Also the loads vary due to several sources of variation: The operating environment differs from one truck to another. The vehicle utilisation, i.e. how the vehicle is driven, causes variation. For trucks also the transport mission will have an impact, as e.g. the gross combination weight will be different. Moreover, the specific features of the vehicle will affect the loads that a component is subjected to since the external loads are transferred dynamically in the vehicle.

How to handle the variation involved depends on the application. For safety critical components the failure risk has to be negligible. For components, whose function are critical due to price, economic consequences for the customer or brand image for the vehicle manufacturer, a very small risk can be accepted, whereas for components that are more easily exchangeable and have little impact on the performance, a higher risk can be accepted as this can be balanced by a better economy in the long run.

The variation in strength can to some degree be secured by process control, while the variation in load is more difficult to control [2]. Therefore, load modelling will be in focus.

2. Customer load descriptions

2.1 Traditional ways of describing customer loads

Due to limited possibilities of gathering and storing measurement signals, much of the traditional work on describing customer loads has been focused on anticipating as

closely as possible the extremes of field usage [3]. Proving grounds have been constructed to reproduce these extreme loads. Tests of vehicles, systems and components have been conducted on the proving grounds and in laboratories comprising all possible most damaging service load states [4]. The result is handled in such a way that if the vehicle/system/component can manage these extreme loads, then it is supposed to withstand also the loads in service usage. This holds as long as all possible loading phenomena are taken into account. The good thing about this policy is that it will most likely result in components that last the design life, which is a reasonable conclusion considering the insufficient data that has been available. The obvious problem is however that it is more or less impossible to say how long they will last, and this method has often resulted in components becoming unnecessarily overdimensioned [5]. Using this method, the statistical nature of the problem cannot be treated in other ways than to say that it is unlikely that the components will fail.

2.2 New possibilities for measuring and modelling loads

More recently, improved measurement equipment and computers have opened up a possibility to increase the information about the loads for the whole population of customers. With modern measurement equipment it is possible to measure at higher frequency with much improved reliability and consequently the accuracy of the information received from measurements has increased substantially. Furthermore, the development of computers has improved the possibility of analysing the measurements. This means that it is much easier to handle large measurement signals.

Moreover, the use of sensors in different types of electronic control systems in today's vehicles gives a possibility to register at least fairly accurate load signals in many more vehicles compared to the current practice. Although the accuracy of these sensors is lower there is still a great potential in obtaining valuable information from them.

All these improved technologies make it possible to get a much better understanding of the load situation than what was previously possible. With the increased number of measurements and the use of sound mathematical models, the description of the general customer usage can be improved. This gives a possibility to choose the best vehicle available for a certain customer, but also future differentiation of vehicle specifications can be based on such customer load information.

2.3 Modelling load data using road classes

Triggered by the better possibilities in gathering and handling load data, focus has moved from the extreme customers to a more general understanding of the whole customer population. One way of modelling customer loads that has been suggested recently [6-9], is to divide the customer usage into different classes. In such models, the loads are assumed to be similar within each class and consequently a large part of the variation in loads can be explained by these different classes. Customers can be described based on how much time they spend in each of the classes or how long a distance they drive. An assumption is made that the distance driven in each class and the loads within each class are independent of each other. The classification suggested has been based on the quality and the type of road. For instance, classes can be defined based on whether the road is considered to be uneven or smooth or whether it is a highway, a city street, or perhaps a mountain road.

Measurements have then been performed on roads belonging to different classes using different drivers. Loads acting on the test vehicles have been measured in the form of stresses, forces or strains. These loads have in most cases been summarised in terms of rain flow matrices, which is the basis for determination of the fatigue severity of a load signal. In the rain flow cycle count method, load cycles are defined, which represents hysteresis stress-strain loops. The number of cycles of each combination of minima and maxima are then counted and the numbers of the different combinations are summarised in a matrix. These rain-flow matrices can be used to describe the loads of the road classes. Further, in order to compare customers, pseudo-damage can be calculated from the rain-flow matrices using the Basquin equation and the Palmgren-Miner rule.

Information on how long a distance customers drive in different classes has usually been collected using questionnaires. This method makes it possible to get a good view of the customer population. However, there are some disadvantages:

Firstly, the use of questionnaires is very sensitive to the kind of questions asked and the subjective judgements of the participants, in this case the customers. Another difficult problem is how to treat non-responses. It is also necessary to make a random selection of customers. In the future, the use of control system sensors may make it possible to get more objective information on how long a distance the customers drive in each road class.

Secondly, an important trend in the vehicle industry is to move fatigue considerations into earlier stages of the design process. In these stages, the vehicle only exists as a computer model. It is then necessary to have a model for the external loads coming into the vehicle. When measuring, for example, forces and strains as suggested in [6-9], it is possible to get very accurate information about the particular vehicle used in the measurement. However, a general problem when using measurement data is that the vehicle that is to be designed does not exist as a test vehicle. The actual vehicle used in the test will have different dynamical responses and thus the strains and stresses will not be same. Traditionally, the loads that have been used have been estimated from older models. These loads are therefore vehicle-dependent and do not reflect how the loads change due to the design [10, 11].

Thirdly, the different road classes have to be defined. Preferably, these classes should be defined in a global sense, i.e. the roads within a class should vary in the same way independent of the market where they are located. This means that once a road classification is defined, it is necessary to verify that the definition is in fact made global.

We will here address the last two problems, i.e. the problem of verifying the classification and describing the loads within each class. We will start with the load description. The focus will primarily be on lateral loads, but the technique is also applicable to other load cases.

3. Modelling of road classes

3.1 Vehicle-independent load models

In order to deal with the problem of modelling loads, we intend to develop a **vehicle-independent model**, using statistical techniques to evaluate collected load data. An example of such implicit vehicle-independent load models is the modelling of road surface as suggested in e.g. [12-16]. By letting the virtual vehicles run over the modelled surfaces, loads are generated and transferred in the vehicle structure. A problem yet to be considered is that the road itself causes no damage as long as the vehicle does not move over the road with some speed, and therefore also the speed, i.e. the driver's behaviour, has to be included. We will here focus on lateral loads. These loads are admittedly not as important as the vertical loads, but will have a great impact on some components [2]. Due to their simplicity and the possibilities for rational studies, we will use parametric models. Methods for obtaining a proper classification will then be developed using the model and data collected from service usage.

Since we want to have a vehicle-independent description using load measurements, a first goal is to create a method for describing the load situation from a particular measurement. In order to make sure that the load situation is properly described, it is necessary to show that the parametric models can give an accurate description of the loads in terms of fatigue damage. For instance, this can be done by regarding the expected value of the cumulative damage or the range spectra for rain flow cycles and comparing with results found directly from measurements. Approximation of these entities can be made either by explicit calculations or by simulation studies.

3.2 An example of a parametric vehicle-independent load model

Our aim is to describe the lateral loads as vehicle-independent as possible. We are particularly interested in describing the operating environment and the driver's behaviour. The effect of the operating environment on the lateral loads comes mainly from two sources: the unevenness of the road surface creates a primarily high-frequent load and due to the curvature of the road there will be a load which is more low-frequent. A similar division can be found in [8]. These loads will cause dynamical effects in the lateral direction. We will here focus on the low-frequent loads due to the curvature. The vertical excitations can be treated using the methods suggested in e.g. [15-16].

In Paper I-III, a model for the low-frequent lateral loads is established. In this model, curves are detected from measurements of the yaw rate and velocity. For each curve detected an approximate curvature is found based on road construction requirements on how to build curves [17]. The curvature is modelled as a trapezoid, where the maximum curvature is considered to be the most important. The distribution of maximum curvatures in each curve is modelled using a transformed lognormal distribution with parameters μ_c and σ_c^2 . Further, the number of curves is assumed to be Poisson distributed with the parameter ν_c . These parameters are constants for a certain road, but they may differ from one road to another. The curvature and speed together will cause the lateral acceleration, which will be the external load acting on the vehicle. The speed is considered through a regression model, which says that down to a certain curvature,

there will be a linear relation between the logarithm of the curvature and the logarithm of the speed. For wider curves, the driver no longer adopts the speed to the curvature, but rather to other causes such as traffic density, speed limits, engine capacity etc. The models for curvature and speed can be combined to a model for centripetal acceleration in each curve j , which can be written as:

$$a_{w,j} = v_j^2 C_j = \begin{cases} a^2 C_j^{1-2b} e^{2\varepsilon_j}, & C_j \geq C_{\text{lim}} \\ a^2 C_{\text{lim}}^{-2b} C_j e^{2\varepsilon_j}, & C_j < C_{\text{lim}} \end{cases} \quad (1)$$

where the parameters a and b are the parameters in the regression model for the speed, and C_{lim} is the cut-off curvature mentioned above. The entities ε_j consider the variation in speed from one curve to another that is not explained by the regression model. The entities are modelled as independent zero-mean normally distributed random variables with variance σ_ε^2 . The parameters a , b , C_{lim} and σ_ε^2 may all vary depending on the particular driver.

However, even with a model of the speed and the curvature, not all lateral acceleration coming into the vehicle is explained. There is also a low-frequent load process, which is due to the driver's ability to follow the road, the more low-frequent effects of the road surface, etc. In papers II and III, this residual process is modelled as a transformed Gaussian process. In this process the two most important parameters are the frequency of cycles ν_{res} and the variance of the transformed process σ_{res}^2 and thus these will be considered in the set of parameters. This residual process is assumed to be present with the same properties both in curves and on straight parts of the road, whereas the curvature loads obviously only occur in curves. The two processes are further assumed to be independent of each other. Figure 3 below shows the measured lateral acceleration split into the two load processes:

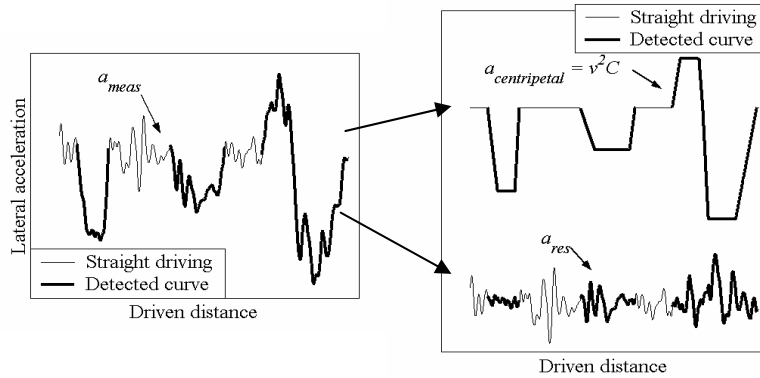


Figure 1. The measured lateral acceleration is due to the centripetal acceleration and a residual.

Using this description of the lateral acceleration, we arrive at a model containing two parameters to describe the distribution of the curvature: μ_C and σ_C^2 . We get four parameters to describe the relationship between speed and curvature a , b , C_{lim} and σ_ε^2 . We also have one parameter describing the frequency of curves: ν_C . For the

residual process, the two main parameters to consider are ν_{res} and σ_{res}^2 , the frequency of residual cycles and the variability in amplitude. The parametric model is summarised in Figure 2.

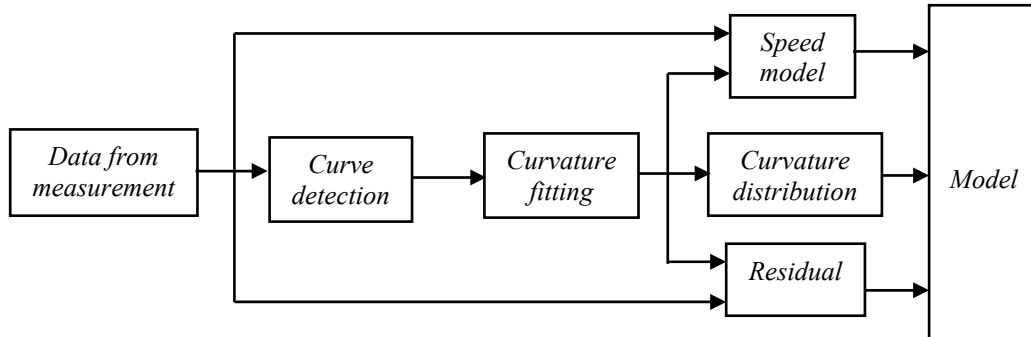


Figure 2. A summary of the parametric model

The model's accuracy has been validated through derived formulas for expected damage and expected range spectra given the parameter values. (See Paper II.) In these formulas the maximum values for the residuals in each the curve are also considered. These values are assumed to be exponentially distributed with parameter λ and to be independent.

The results of these formulas with the parameter values estimated from measurements have been compared to the pseudo-damage and the range spectra found directly from the measured load data using the rain flow cycle count method, the Basquin equation and the Palmgren-Miner rule. (See Paper II and III.) An example of such a plot can be found in Figure 3 below. In the plot, the range spectra from three different measurements are compared to the range spectra found using the fitted parameters to calculate the expected range spectra according to the procedure outlined in Paper II.

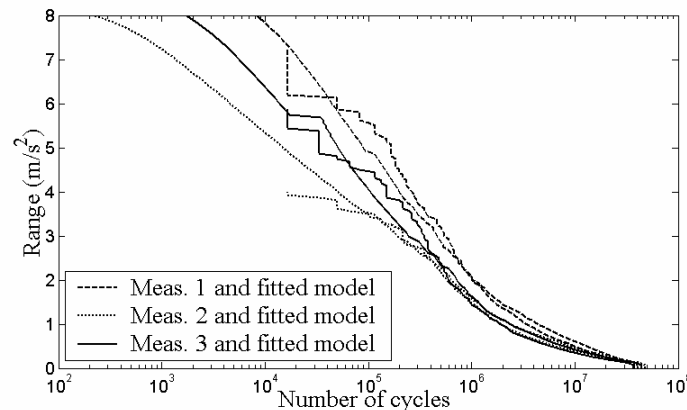


Figure 3. Example of range spectra for the model and the measured lateral acceleration

3.3 From modelling measurement to modelling road classes

From Section 3.2, we have seen that it is possible to model the loads found in one measurement using a parametric model. However, rather than modelling each measurement, we are interested in modelling the road classes. In each measurement, the parameters are assumed to be constant, i.e. given the road and the driver; the parameters

will be the same. On the other hand, driving over another road and using another driver will result in other parameters. By looking at the classes the parameters identified from each measurement will therefore be regarded as samples of random variables. In fact, as these parameters are used to model the load levels, they are in a sense measures of how severe the loads are.

Thus, a better name for the parameters when considering the road classes is **random load measures**. The loads in each class will therefore be modelled with regard to these random load measures. This means that the road classes can be modelled by studying how the load measures detected vary within the classes.

This also shows one of the advantages of the parametric description. By using a parametric representation of each measurement, it is possible to get an accurate description of the loads in the measurements, but we also get a description which is simple enough to allow us to study the variation between and within, for instance, different road classes. The alternatives to a parametric model are to use the measurement signals as they are or to use their rain flow matrices. By using the measurement signals directly, we cannot generalise the description to model the customer population, and if we were to describe a severe customer for analysis we have to choose a “representative customer” among those that are measured. Using the rain flow representation, one option is to disregard the difference within the road class and use one matrix to describe the entire road class. This appears to be a rather questionable simplification. An alternative is to regard the rain flow matrix as a parametric load description with $n \times n$ parameters, where $n \times n$ is the number of bins in the matrix. With a reasonable number of bins, this would however lead to a far too complicated load description.

4. Analysing the road classes

4.1 Global classification

One of the demands we have on the road classes is that they need to be global in the sense that as long as a vehicle is driven within the same road class, the conditions should be similar, independent of where on the planet the vehicle is driven. In order to study this and to model the variation within the road classes, a factor effect model can be constructed for the load measures.

Assume that we have p load measures, $(y^{(1)}, y^{(2)}, \dots, y^{(p)})$, in our model, which may vary between different measurements. One of these measures can, for instance, be the frequency of curves in the measurement. A simple model for one of the load measures may be the following:

$$y_{ij}^{(m)} = \mu^{(m)} + \tau_i^{(m)} + \varepsilon_{ij}^{(m)} \quad (2)$$

where $\mu^{(m)}$ is the mean level of the load measure over all road classes, $\tau_i^{(m)}$ stands for the effect of the i th road class, and $\varepsilon_{ij}^{(m)}$ is the variation due to the particular measurement. However, in this model we do not consider the effect of local factors such

as market. In order to take these into consideration, the model in eq. (2) can be extended in the following way, where we have also considered possible interactions between the different effects. In this model, we consider the effects of road classes, markets and drivers:

$$y_{ijkl}^{(m)} = \mu^{(m)} + \tau_i^{(m)} + \beta_j^{(m)} + \gamma_{k(j)}^{(m)} + (\tau\beta)_{ij}^{(m)} + (\tau\gamma)_{ik(j)}^{(m)} + \varepsilon_{(ijk)l}^{(m)} \quad (3)$$

In this model, $\mu^{(m)}$ is the mean level of the load measure over all road classes, markets and drivers. The parameters $\tau_i^{(m)}$ and $\beta_j^{(m)}$ stand for the effects of the i th road class and the j th market, respectively. The interaction effect between a road class and a market is represented by $(\tau\beta)_{ij}^{(m)}$. The effect of the driver within the market can be found in $\gamma_{k(j)}^{(m)}$ and the possible interaction between driver and road class within the market in $(\tau\gamma)_{ik(j)}^{(m)}$. Finally, the entity $\varepsilon_{(ijk)l}^{(m)}$ is the variation due to the particular measurement.

4.2 Design of experiment and analysis

In analysing the model suggested in eq. (3), data have to be gathered in such a way that the assumptions made in the factor effect model are violated as little as possible. These data are load measures detected from the measurements. To have a perfectly randomised experiment is not practically possible. A more reasonable strategy may be the following: For each market we have chosen to measure, we take a random sample of haulage contractors. Then, for each contractor, we pick two drivers at random. Each driver can then be followed over some period of time and road segments within the different road classes can be randomly picked along the route for measurements. Other aspects that are necessary to consider in the design of experiments are the length of these road segments and what sample size to choose in order to get sufficient information to draw conclusions. Information from older measurements, pre-studies and experienced engineers can be used to determine this sort of information.

If the true situation can be regarded as close to the assumptions made in the model, the load measures can be investigated using the analysis of variance method. In such an analysis, attention has to be paid to the fact that the load measures may depend on each other. As an example, consider a road with unusually many curves. For such a road it is reasonable that also the curves are narrower than what is the case on an average road. This can be dealt with using multivariate analysis techniques or by orthogonalising the load measures and using multiple univariate models as an approximate solution.

Data used in this thesis were not collected with the analysis technique sketched above in mind and they are therefore severely unbalanced. For instance, there are a large number of measurements on highways in one market, whereas there are fewer measurements in other markets and other road classes. For this reason the model used in paper IV when analysing real data is somewhat simplified compared to the one suggested in eq. (3).

From the analysis, it can be concluded whether the road classification is sufficient or not by studying how large the market effects are. If these are small enough to be considered unimportant, the road classification is sufficient. If not, the classification has to be

improved. If the classification is sufficient it may be possible to reduce the number of classes by combining classes that are found to be similar.

4.3 Customer modelling based on the road classes

A customer can be described from the model based on knowing how long a distance the vehicle is driven in each of the road classes. The loads in each road class can be considered to be stationary and thus the load process can be regarded as step-wise stationary. By using the model for each road class, a load distribution for the customer can be found. From such a load distribution, the expected damage can be found by calculating the expected damage for each of the road classes and adding these expectations to get the expected damage for the customer. The variability for the customer is also of interest. This is somewhat more difficult, but can be simulated from the load model including the variability due to the driver, and in doing this, estimates of the severe customer can be made. From the description above, the best available specification can be chosen, when selling a truck to a customer.

5. Discussion and conclusions

There are several different areas, where a vehicle-independent load model for the general population of customers is useful, but the most obvious are:

1. to be able to generate realistic input signals for computer models of a complete vehicle representing the customer population.
2. to classify customers in terms of durability severity and find possibilities for differentiation.
3. to use the models as input when updating proving ground procedures and other tests.

Above, we have indicated how the lateral loads can be modelled from measurements. Similar ideas exist for modelling vertical loads. From these models of the measurements we can get closer to a load model for the whole customer population using the road classification and modelling suggested in section 4 above and outlined in more detail in paper IV. From these models the expected damage can be approximated and by simulations we can also get information regarding the variance of the damage. Through such calculations, we can find the most suitable vehicle specification for the particular customer, but also find possibilities for new differentiation of customer classes. Using the vehicle-independent modelling, proving ground procedures may also be updated. The information provided through these vehicle-independent models are straightforward, for instance, the models contain the number of potholes and information about the speed, or the curvature of road curves.

The development of such a methodology is summarised in Figure 4 below. From field measurements the synthetic description of vehicle-independent load data is created to model the external loads entering the vehicle. From these models the signals can be generated to serve as input to finite element models. From the description we can also get input to test programs. The verification and validation of the simulations and new input from the field lead to continuous method development, which can improve and fine-tune the parametric models.

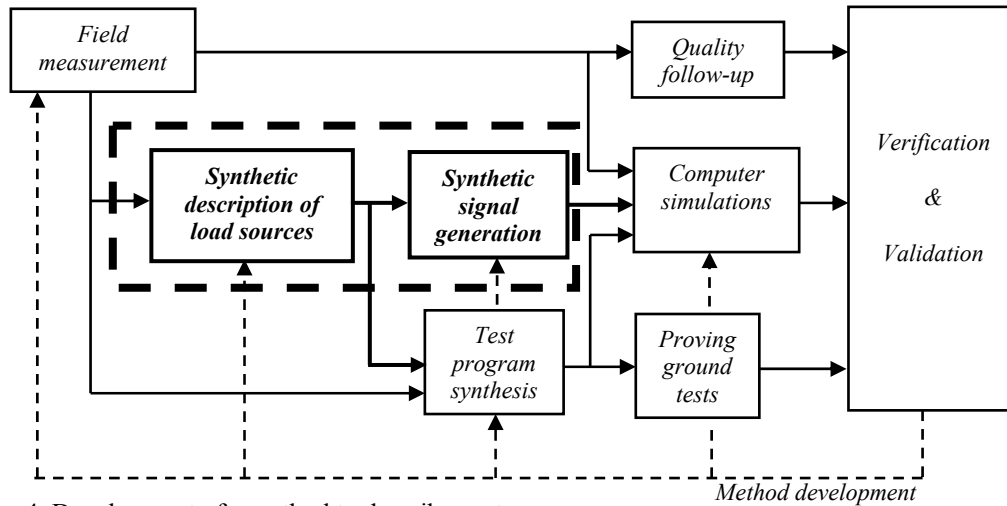


Figure 4. Development of a method to describe customers

6. Summary of appended articles

Paper I: Driver Independent Road Curve Characterisation

The method of determining the curvature of road curves from load measurements on vehicles is presented. An algorithm for detecting curves from measurements is suggested. It is verified through proving ground measurements and video recordings from field measurements. It is then explained how trapezoids can be fitted to the curvature signal, and why a trapezoid is a reasonable model. The procedure of fitting trapezoids is verified against proving ground measurements and applied to a series of measurements in Brazil with different drivers on the same road. The distributions of the curvature found in the different measurements are presented and shown to be very similar.

The residual discussed here is the curvature residual, i.e. the difference between the measured curvature and the fitted trapezoids. The variance of the residuals in the curves is used to compare the effects of different driving styles.

Paper II: Parameterisation of Lateral Fatigue Loads on Vehicles

The curvature model is discussed again and suitable distributions for measurements from different road classes such as city streets as well as highways and secondary roads are suggested. A model for the relation between the curvature and the chosen speed is investigated. A model for the acceleration residual, which assumes that the residual is a transformed normal process, is also given. The residual is assumed to be independent of the other parameters.

With these models it is possible to make an approximate calculation of the expected accumulated fatigue damage for the different parts of the measured lateral acceleration. The curvature model and the model for the speed provide a distribution for the lateral accelerations created when driving in curves. For the model of the centripetal acceleration, an explicit expression for the expected cumulative fatigue damage using rain flow cycles is given and expressions for the range spectrum are shown. For the residual, an upper bound for the expected damage is obtained. Comparisons between the

modelled loads and observed loads are made in terms of cumulative fatigue damage and range spectra. It is shown that the modelled loads give results that are very similar to the ones found in the measurements and the parametric models are therefore considered to be good. Finally, the influence of different drivers and markets are discussed.

Paper III: Evaluation of Approximative Methods for Rainflow Damage of Broad-Banded Non-Gaussian Random Loads

Different ways of modelling the residual are considered. The goal is to get a better approximation of the damage from the residual process than what was presented in paper II. Two different methods for approximating the fatigue damage of broad banded non-Gaussian random loads using the rain flow cycle count method are evaluated using the residual. Results for Gaussian loads are summarized, and transformations for non-Gaussian loads are discussed. One of the two methods is based on the spectral moments of the process, and the results are obtained as a linear combination of an upper and lower bound. The second method is based on the assumption that the sequence of turning points of the load can be considered a Markov chain, for which results can be obtained. Measurements performed on different markets are used to study the two methods. Results are presented in terms of expected damage and amplitude spectra.

Paper IV: Evaluation of Road Load Classification for Fatigue Assessments

The modelling of customer usage based on different road classes is discussed. A parametric vehicle-independent load model is assumed, where the parameters can be estimated using measurement data. The variation of the parameters over the measurements is studied using a factor effect model and the method of analysis of variance. In order to find a global description, a road classification is considered, and this is compared to the effect of more local factors such as market and driver. Practical considerations in the design of experiments to gather data for the models are addressed. To study the technique in practice, the model for lateral loads is used as a case study. The analysis technique is applied to the load model using data from a field study made in three different markets. Conclusions are drawn on the possibilities of classifying road loads and the need for design of experiments to use field measurements more efficiently.

7. Future work

An obvious goal for truck manufacturers would be to make new measurements according to the ideas outlined in Sections 2 and 3 in Paper IV. With such a design of experiments, many of the pitfalls in the current measurements can be avoided.

In the future, more data can be available through control system sensors. These data are not as accurate as the data that can be found through regular field measurements, but the possibility to collect this kind of data through the sensors used in the vast number of control systems in a large population of trucks will be of great importance. Thus, an interesting challenge in the future will be to find a rational way of updating models fitted through the current measurement type using the data from these on-board-logging activities. There is also a possibility in using warranty data as a source for updating the models. An obvious candidate technique to use is Bayesian updating.

On the basis of the easy-to-measure channels, it may also be possible to obtain more objective information on customer usage and how long a distance the customers drive in each of the road classes. This information is naturally very important for determining the load scenario for customers.

Furthermore, due to the generality of the technique, it could also be applied to other cases such as vertical loads. For most components, vertical loads are arguably more important than lateral. For vertical loads, the road classification may be based on the quality of the road rather than the type of road as used here.

An interesting topic from a more scientific point of view is to develop a better way of taking care of the dependency between the different load measures. The current solution suggested in Paper IV is approximate and it would be interesting to study this topic further to find a more exact solution.

References

- [1] Dowling N. E., *Mechanical Behavior of Materials*, 2 Ed., Prentice Hall, Upper Saddle, New Jersey (1999).
- [2] Edlund, S., Fryk P.O., "The Right Truck for the Job with Global Truck Application Descriptions", *SAE Technical Paper 2004-01-2645*, 2004.
- [3] Conle, A., and Landgraf, R. W., "A Fatigue Analysis Program for Ground Vehicle Components", *Proceedings of the International Conference on Digital Techniques in Fatigue* (SEECO '83), Society of Environmental Engineers, March 1983, London, pp. 1-28.
- [4] Berger C., Eulitz K. G., Heuler P., Kotte K. L., Naundorf H., Schütz W., Sonsino C. M., Wimmer A., Zenner H., "Betriebsfestigkeit in Germany – an overview". *Int. J. Fatigue*, 24 (2002) pp. 603-625.
- [5] Olofsson, M., "Evaluation of Estimates of Extreme Fatigue Load – Enhanced by Data from Questionnaires". Licentiate of Engineering Thesis, Chalmers University of Technology, Göteborg, Sweden, 2000.
- [6] Bignonnet, A., Thomas, J. J., "Fatigue Assessment and Reliability in Automotive Design", *SAE Technical Paper 2001-01-4061*, 2001.
- [7] Ledesma, R., Jenaway, L., Wang, Y., Shih, S., "Development of Accelerated Durability Tests for Commercial Vehicle Suspension Components", *SAE Technical Paper 2005-01-3565*, 2005.
- [8] Aoki, T., Imai, K., Watanabe, S., Yamakawa, S., Nakahara, Y., Haraguchi, M., Uchiyama, Y., "A Study of Development Indices Established Quantification of Road Load", *SAE Technical Paper 2003-01-2843*, 2003.
- [9] Panse, S. M., Awate, C. M., "Development of Accelerated Structural Durability Test Program for a Mini-truck and its Components", *SAE Technical Paper 2006-01-0085*, 2006.
- [10] Medepalli, S., Rao, R., (2000), "Prediction of Road Loads for Fatigue Design – A Sensitivity Study", *International Journal of Vehicle Design*, Vol. 23, Nos. 1/2, pp. 161-175.
- [11] Hughes, S., Jones, R. P., and Burrows, A. J., (2005), "Application of System Modeling to Road Load Data Synthesis for Automobile Product Development", *Proc. of 2005 ASME International Mechanical Engineering Congress and Exposition*, Nov. 5-11, 2005, Orlando, FA.
- [12] Ferris, J. B., (2004), "Characterising Road Profiles as Markov Chains", *International Journal of Vehicle Design*, Vol. 36, Nos. 2/3, pp. 103-115.
- [13] Dodds, C. J., Robson, J. D., "The Description of Road Surface Roughness", *J. of Sound and Vibration*, 31 (1973), pp. 175-183.
- [14] ISO 8608, "*Mechanical Vibration – Road Surface Profiles – Reporting of Measured Data*", International Organization for Standardization, Geneva, Switzerland, 1995.
- [15] Bogsjö, K., "Stochastic Modelling of Road Roughness", Licentiate of Engineering Thesis, Lund Institute of Technology, Lund, Sweden, 2005.

- [16] Öijer, F., Edlund, S., “Identification of Transient Road Obstacle Distributions and Their Impact on Vehicle Durability and Driver Comfort”, *Supplements to Vehicle System Dynamics*, 41 (2004), pp. 744-753.
- [17] Vägverket: Vägutformning-94 version S-1, del 6 Linjeföring. *Vägverket Publikation 1994-52*, Borlänge, 1994. (In Swedish).

Driver Independent Road Curve Characterisation

MAGNUS KARLSSON¹

SUMMARY

A method to determine the statistical distribution of curvature of road curves is presented. The curvature is the inverse of the radius at any point. From road construction requirements it is reasonable to model the curvature of a road curve with a trapezoid. The algorithm presented detects curves from measurements and fits a trapezoid to each curve. The residual between the fitted trapezoid and the measured curvature can be seen as the driver influence. The method is verified against proving ground measurements and applied to a series of measurements in Brazil with different drivers on the same road. The distributions of the curvature for the different drivers are presented and the variance of the residuals in the curves is used to compare the effects of the different driving styles.

1 INTRODUCTION

A major problem when predicting fatigue life for vehicle components is to determine the service loading conditions that the vehicle will experience during its life. Due to insufficient knowledge about the loading conditions the strength of components are often exaggerated through high safety factors. Many of these unnecessarily strong constructions can be avoided with a better understanding of the fatigue load in the real operating environment. The natural way to acquire information about the service loading is to make field measurements of forces, strains etc. However, it is a troublesome and expensive task, especially since there exists a great variation between different customers' way of using their vehicles.

Since the field measurements have seldom been considered long enough they have often been performed in such a way that the driver has been driving at high speed over a bad road stretch, thus guaranteeing that the measurement is severe enough. In the same way the durability test tracks have been constructed to replicate the worst-case loading conditions found during field measurements. [1]

There are other suggestions for how to get the fatigue load design specifications more related to the actual customer environment, by using for instance questionnaire surveys, (see [1-3].), but these methods do not appear to be reliable enough.

¹ *Address correspondence to:* Volvo Truck Corporation, Department 26780 A2, SE-40508 Göteborg, Sweden. Tel.: +46 31 668 286; Fax: +46 31 508 764; E-mail: magnus.k.karlsson@volvo.com

In recent years, the ambition in the automotive industry has been to design and optimise components towards a finite fatigue life. This optimisation has been based on the almost opposing requirements of lightweight design on one hand and safety and durability requirements on the other hand. It has become obvious that a more thorough understanding of the complex fatigue loading conditions is necessary.

Most techniques today directly try to describe the loading conditions in terms of forces and moments. It appears to be practice of the date to separate different kind of load origins from each other, see [4,5]. The most important loads should be those coming from driving into potholes and bumps, road vibration, curvature, braking and accelerations. These can be seen as vertical, lateral and longitudinal load origins. The vertical loads have been considered in a series of articles by Volvo, see [6-8]. This particular work focuses on the lateral loads. These loads, caused by curvature, are arguably not as great as those from the vertical loads, but will have a huge influence on, for instance, steering components.

This article will in section 2 describe a new concept for describing loads based on separation of the effects of the operating environment, driver's influence, transport mission and the vehicle design. These ideas will then be applied to lateral loads. In section 3 a mathematical description of a curve is suggested, based on road construction requirements. In section 4 an algorithm for detecting curves from measurement is described and the mathematical description of a curve is used to find the curvature for each detected curve. These methods are verified against proving ground measurement. In section 5 the ideas are applied to measurements in Brazil. The distribution of curvature is found. In section 6 some conclusions about the method are drawn.

2 A CONCEPT FOR DESCRIBING LOADS

An alternative to the idea of trying to describe the loads directly, is to ask the interesting question: "What causes the loadings?" Naturally there are several factors, but the most important should be the following:

- The operating environment: What kind of roads is the vehicle driven on?
- The vehicle utilisation: How is the driver driving the vehicle?
- The transport mission: What is the vehicle used for?
- The vehicle design: What kind of vehicle do we have?

An idea could therefore be to describe these factors separately, in order to actually understand from where the loads come, and how important the above listed sources are. The main purpose of this idea is to separate the description of the road from the influence of the driving style, the vehicle design and the effects of surrounding traffic. This means that the road description will be approximately the same irrespective of the driver and at what time the measurement is performed. The

description of today will therefore hold in the future as well. The influence of driving style can then be described separately. The method therefore gives an opportunity to study to what extent the driver influence affects the fatigue life. This can then be compared to the influence of the market where the truck is used as well as the mission of the truck. The description of the operating environment can also be of great use when performing handling and comfort analyses.

3 A SIMPLE MATHEMATICAL MODEL OF A CURVE

When constructing a curve a crucial part is to make sure that vehicles driving through the curve will not experience too high lateral accelerations. In order to avoid this and to get a smooth ride through the curve it is therefore useful to have a constant curve radius over a longer time, say a couple of seconds. One way of modelling a curve would therefore be to think of it as having a constant radius over the entire curve. However if the curve is narrow, i.e. has a small radius, it is probably better to have an area at the beginning (and the end) of the curve where the radius is adapted to the part with a small constant radius. Thus it would be easier for a driver to adjust to the smaller radius.

The Swedish National Road Administration [6] constructs curves according to the following concepts: If the radius is big (at least 900 m on a major road), the curve should follow the arc of a circle, i.e. has a constant radius. If the curve is narrow it should first have a linear change of the curvature, then the radius stays constant for a certain time and finally increases again until the road is straight.

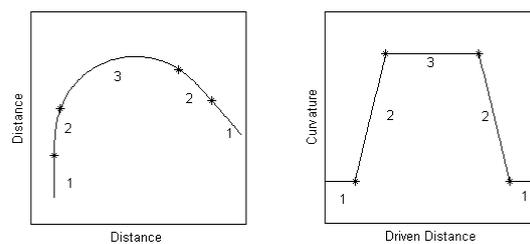


Fig. 1. To the right: A straight part before entering the curve (1), an adaptation area where the radius decreases (2), and an area of constant radius (3). To the left: The curvature for the same curve

According to these ideas it is therefore reasonable to see the curvature, here defined as the inverse of the radius at any point of the road, as following a trapezoid. See Fig. 1 above.

An equation for the trapezoid model used in this paper is as follows:

$$C(x) = \begin{cases} k \cdot (x - (x_0 - l)), & x_0 - l \leq x < x_0 - l + h/k \\ h, & x_0 - l + h/k \leq x < x_0 + l - h/k \\ k \cdot (x_0 + l - x), & x_0 + l - h/k \leq x \leq x_0 + l \end{cases} \quad (1)$$

where k is the slope of the side of the trapezoid, x_0 is the distance from the starting point of the road, l is the distance from the middle of the curve to the endpoints, and h is the height of the trapezoid. (See Fig. 2.) The trapezoid is assumed to have the same slope on both sides.

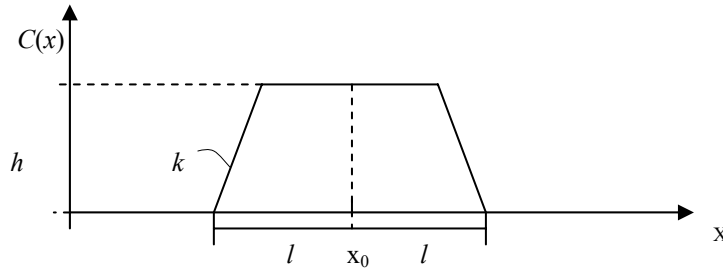


Fig. 2 A trapezoid with the parameters in the model.

4 DETECTING AND MEASURING CURVES

4.1 Different Driving Modes

Before it is possible to use real measurements to analyse the curvature of a road with the above-mentioned trapezoid method, two problems have to be solved. First we have to know where there is a curve. That is, we have to be able to automatically detect a curve simply by running the measurements through a programme. Second, we have to use the measurements to somehow estimate the curvature, where we have detected a curve.

The problem of detecting the curves can be solved in the following way. Each point of the measurements is sorted into any of the following three categories: *manoeuvres*, *curves* and *straights*. The term manoeuvres is in this case for instance parking manoeuvres or reversing for loading or unloading. The differentiation can

be made in the following way. Manoeuvres are characterised by high wheel angle and low speed. Thus the measurement is searched for points fulfilling these demands. Secondly the measurement is searched for characteristics for curves such as high lateral acceleration under a certain time, and high speed relative to the manoeuvres. What remains after these two searches is considered to be straight parts.

4.2 An Estimate of the Curvature

The curvature of the road can be found using measurements in which the yaw rate and the velocity have been recorded. The curvature can be estimated by the ratio of the yaw rate and the velocity at any point. Naturally these measurements will not exactly follow a trapezoid for each curve and then stay zero for the straights. The idea is instead that the curvature can be described as a sum of a deterministic function and a zero mean random process. The deterministic function corresponds to the trapezoid and the random process to the residual between the actual measurement and the trapezoid fit.

In practise, the trapezoid fit is made in the following way. For every curve detected, the signal corresponding to the curvature is picked out, and the distance driven is found by integrating the velocity for this particular part of the road. A trapezoid as a function of the driven distance is fitted to the measured curvature.

Under the assumption that we get the true curvature from the measurement above, how do we then explain the residual? One part can be explained by a simple measurement error. This can be seen as the high-frequency component. The low-frequency component on the other hand can be regarded as the driver's influence, such as over-compensating when taking the curve. Other possible factors causing errors are disturbances from potholes and road roughness, the dynamics of the vehicle, and the velocity. It should be possible to model the curvature (C) as a deterministic function corresponding to the trapezoids ($C_{trapezoid}$) and a stochastic process corresponding to the residual (δ), where the residual is a combination of the factors mentioned above:

$$C = C_{trapezoid} + \delta = C_{trapezoid} + \delta_{driver} + \delta_{measure} + \delta_{road} + \delta_{vehicle} + \delta_{velocity} \quad (2)$$

4.3 Reference Measurements and Verification of the Algorithm

The way of detecting curves from the measurement is naturally based on a great deal of subjective judgement. Questions like: "What is low speed?" can of course be raised. In order to verify that the method actually works, the separation of the measurement was compared to the actual situation on the road by studying video

films, which were recorded simultaneously with the measurements, as well as comparing the result with known curves at a proving ground.

The result was that it is possible to use this sort of decomposition. On the proving ground measurements, two very small curves that did not exist according to the map were detected out of a total amount of thirty-five curves. On the other hand all existing curves were detected. Since the decomposition is based on threshold values there is of course a small number of questionable cases. The most sensitive part is whether or not over-turns and such things as turning in order to avoid potholes should be considered as curves or not. In this study most of them are not. The key is how long time it should take to drive through a curve. Making this parameter smaller places the above two examples in the class of curves.

In order to verify that the method of fitting a trapezoid to each detected curve works, measurements from a proving ground with known curvature were used. The error from the measurements were found in the following way:

$$\varepsilon = \frac{r_{fitted} - r_{true}}{r_{true}} \quad (3)$$

where r_{fitted} is the smallest radius found in each curve, and r_{true} is the radius according to a map of the proving ground. The program was run over a series of such measurements, containing altogether thirty-five curves. The mean error was very close to zero (-0.0033) and thus it seems like r_{fitted} is an unbiased estimate of r_{true} . The standard deviation of ε was found to be 0.054 . To better understand these figures estimating a $r_{fitted} = 90m$ when $r_{true} = 100m$ gives an error $\varepsilon = 0.10$. Thus it seems like the estimate is good, especially if we consider the fact that the drivers do not necessarily follow the track of the road exactly, but may very well try to take a somewhat shorter way through a curve, or may have to take a longer way due to the surrounding traffic.

Another way of verifying the algorithm is to use the measurement of the curvature to find the road driven and compare that to the road that is found by using the fitted trapezoids. Although this is not the purpose of this model it should give a good hint about the quality of the model. The results come from a measurement in Brazil. As can be seen in Fig. 3, there is a rather small difference between the two estimated roads. The difference appears about halfway through the road, where the trapezoid method gives a less emphasised curve to the left than the original measurement, which is then propagated through the rest of the measurement. At the very end of the road there is also a clear mistake. Nevertheless the results seem to verify the quality of the trapezoid model. It would be of interest to compare the resulting roads curve by curve, but since the original measurement contains no information on exactly where the curves are located such a direct comparison is not

possible. It is therefore difficult to draw any further conclusions more than that it looks as if the maps are very similar.

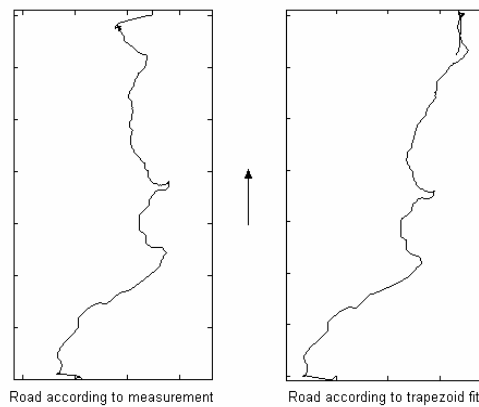


Fig. 3. The road according to the measurement and according to the fitted trapezoids. The arrow indicates the direction in which the truck was driven.

4.4 The Residual

As a first idea for a measure of the drivers' unsteadiness, the variance of the residuals in the curves can be used, thus giving us a possibility to compare the different drivers to each other. An unsteady driver gives a high variance, which will cause more damage.

5 METHOD APPLIED TO MEASUREMENTS IN BRAZIL

5.1 Description of Measurements

A series of measurements performed in Brazil was used to try out the suggested method. During these measurements five different drivers were driving the same route consisting of approximately 25 km highway, 25 km secondary road, 7 km unpaved road and 2.5 km city driving. One of the drivers was driving the stretch of roads four times, in order to see how great the variation for a single driver is.

According to the trapezoid model it should be possible to estimate the curvature of the road at every point by fitting a trapezoid to the measured curvature where a

curve has been detected. Thus when letting different drivers driving over the same route the results of the estimated curvature should, at least approximately, be the same.

The algorithm described above was used to detect curves and estimate the curvature of each detected curve for all eight measurements. Since the route was not exactly the same (some drivers skipped the city driving or parts of it), some of the most obvious curves were not included for all measurements. Nevertheless, it is still possible to study the empirical distribution of, for instance, the curvature or the curve length, which should be the same for all drivers.

5.2 Results from Measurements

In Fig. 4 the empirical distributions for the curvature for the five different drivers are plotted. As a reference the empirical distribution from another measurement performed in Brazil is also plotted. This measurement was 57 km long and consisted mainly of secondary and unpaved road. In Fig. 4 it is referred to as “reference road”.

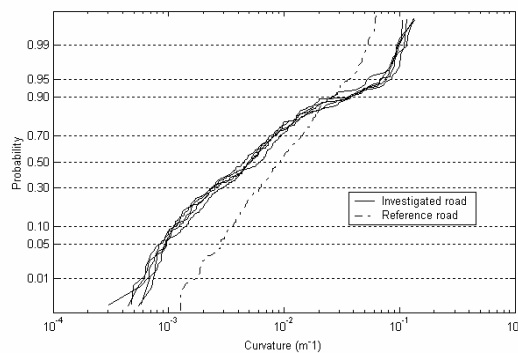


Fig. 4. Empirical distribution for the curvature for different measurements on the same road as well as a reference measurement on another road. (Plotted on lognormal paper.)

In the upper right corner of the figure an area can be seen where the distribution for the investigated road makes a bend. This part corresponds to the city driving part where the curves are narrow and similar in terms of curvature. On the other hand, in the left part of the figure the investigated road gets lower values on the curvature, than the reference road. This part comes from the highway section where the curves are designed to make it possible to drive fast. The reference road has a more homogeneous distribution of curves.

Since not all drivers took the same route the city driving part was excluded when comparing the residuals. The variance of the residuals in the remaining curves was

recorded. In Fig. 5 the variance of the residuals for the different drivers are shown normalized by the highest value. Driver No. 5 drove the route four times.

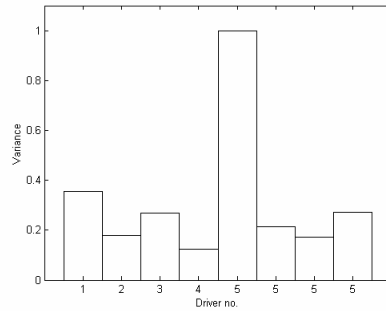


Fig. 5. The variance of the residuals for the different drivers normalized by the highest variance.

5.3 Discussion on the Results

The results from the Brazilian measurements indicate that it is possible to use the detection algorithm and the trapezoid method to measure the curvature on the roads with a fairly high precision. The empirical distributions for different drivers appear to be very similar from one driver to another, and can thus be seen as driver independent.

A co-driver from Volvo made a subjective judgement on the different drivers, which makes it possible to check the result from the variance of the residuals.

Table 1. The subjective judgement of a co-driver (a Volvo employee).

Driver no:	1	2	3	4	5
Judged as:	Fast and somewhat reckless	Fast and experienced	Careful	Careful	Fast
Nationality:	Brazilian	Brazilian	Brazilian	Brazilian	Swedish

A comparison shows that the reckless driver has the second highest variance, although he was acquainted with the course. The Swedish driver was not familiar with the Brazilian conditions during his first measurement, which is shown clearly. In the following measurements he is on the same levels as the Brazilian drivers. Notable is that one of the “careful” drivers (No. 3) did not get a very low value.

6 CONCLUSION

The results indicate that it is possible to use the above-suggested ideas to detect the curves and measure the curvature on the roads with a fairly high precision. This gives us a useful tool to detect the road conditions which is easy to use in, for instance, complete vehicle models.

The residual gives us information about to what extent a driver is driving unsteady. Thus we can find a bad driver by looking at the residual. However it should be pointed out that the most severe effect on fatigue life is the vehicle speed.

7 ACKNOWLEDGEMENTS

This work has been a joint work between Volvo Truck Corporation, Fraunhofer-Chalmers Research Centre for Industrial Mathematics (FCC), and the Department of Mathematical Statistics at Chalmers University of Technology, where the author is a graduate student. The author wishes to express his gratitude towards his supervisors Dr. Thomas Svensson, FCC, Prof. Jacques de Maré, Chalmers and Dr. Bengt Johannesson, Volvo. The project is funded by the Swedish Agency for Innovation Systems.

REFERENCES

1. Olofsson, M.: *Evaluation of Estimates of Extreme Fatigue Load – Enhanced by Data from Questionnaires*. Licentiate of Engineering Thesis, Chalmers University of Technology, Göteborg, Sweden, 2000.
2. Niemand, L.: *Probabilistic Establishment of Vehicle Fatigue Test Requirements*. Master of Engineering Thesis, University of Pretoria, Pretoria, 1996.
3. Thomas, J.J., Perroud, G., Bignonnet, A., Monnet, D.: Fatigue Design and Reliability in the Automotive Industry. In Marquis, G. Solin, J. (editors), *Fatigue Design and Reliability, ESIS Publication 23*. Oxford, UK: Elsevier Science, pp.1-12, 1999.
4. Grubisic, V., Fischer, G.: Methodology for Effective Design Evaluation and Durability Approval of Car Suspension Components. *SAE Technical Paper 970094*, 1997.
5. Fischer, G.: Design and Quality Assurance of Vehicle Components based on the Usage Related Stress Analysis. *XXIX Convegno Nazionale dell'Associazione Italiana per l'Analisi delle Sollecitazioni*, Lucca, 6-9 Sept. 2000.
6. Aurell J., Edlund S.: Operating Severity Distribution a Base for Vehicle Optimization, *11th IAVSD-Symposium on the Dynamics of Vehicles on Roads and Tracks*, Kingston, Canada, 1989.
7. Aurell J., Edlund S.: Prediction of Vibration Environment in Real Operations Described by Q-distributions, *14th IAVSD - Symposium on the Dynamics of Vehicles on Roads and Tracks*, Ann Arbor, USA, 1995.
8. Öijer, F., Edlund S.: Complete Vehicle Durability Assessments Using Discrete Sets of Random Roads and Transient Obstacles Based on Q-distributions, *17th IAVSD - Symposium on the Dynamics of Vehicles on Roads and Tracks*, Lyngby, Denmark, 2001.
9. Vägverket: Vägutformning-94 version S-1, del 6 Linjeföring. *Vägverket Publikation 1994-52*, Borlänge, 1994. (In Swedish).

Parameterisation of Lateral Fatigue Loads on Vehicles

Magnus Karlsson

Volvo Truck Corporation and
Department of Mathematical Statistics,
Chalmers University of Technology, SE-41296 Göteborg, Sweden

Abstract

A way of describing lateral acceleration for fatigue calculations is discussed. The purpose of the model is to parameterise the different sources of the fatigue load, such as the operating environment and the influence of the driver. The measured lateral acceleration is modelled with an approximative curvature, and the average speed explaining centripetal acceleration in the curve. The difference between the model and the observed lateral acceleration (the residual) is also studied. A way of extracting the curvature is presented and suitable statistical distributions for the curvature in city driving as well as driving on highways and secondary roads are suggested. A model for the relation between the curvature and the chosen speed is investigated. The acceleration residual is modelled by a transformed normal process. For the model of the centripetal acceleration an explicit expression for the expected cumulative fatigue damage using rainflow cycles is given, and expressions for the range spectrum is shown. For the residual an upper bound for the expected damage is shown. Comparison between the modelled loads and observed loads are made in terms of cumulative fatigue damage and range spectra. The influence of different drivers and markets are discussed.

1. Introduction

The truck industry is increasingly characterised by specialisation and customerisation. This means that the vehicle's specification and equipment must be tailored to suit each particular transport mission. The main focus is to optimise the performance to give the customer optimal transport efficiency, that is to maximise the productivity at the same time as the product cost is kept as low as possible.

The demands on transport efficiency (loading capacity, fuel economy etc.) and environmental friendliness have thus created a trend in vehicle development towards lightweight constructions. However, when using lightweight constructions it is necessary to make sure that the demands on reliability and durability are maintained, especially since component failures may cause loss of performance [1]. One of the major reasons for structural component failure is fatigue; therefore it is of great necessity to be able to predict what kind of loads the vehicle will experience during its intended life.

This task contains many difficulties. First of all the strength of the components varies due to variation in process and production, and secondly, and perhaps more importantly, there is a great variation in the loads depending on the application, the operating environment, the driver's behaviour and the vehicle specification. Due to insufficient knowledge about the loading conditions, the strength of components is often exaggerated through high safety factors. Many of these unnecessarily strong constructions can be avoided with a better understanding of the fatigue load in the real operating environment.

The natural way to acquire information about the service loading is to make field measurements of forces, strains etc. However, it is a troublesome and expensive task, especially since there is great variation in different customers' way of using their vehicles. Traditionally the field measurements have, via some cycle counting algorithm, been transformed into loading spectra. The loading spectra are then parameterised in different ways often using statistical techniques, and from this parameterisation, conclusions about the fatigue life are drawn. (See [2,3]) Klemenc and Fajdiga [2] treat the cycles as random variables, and try to find suitable distributions explaining the behaviour of the cycles, while Grubisic and Fischer [3] claim that they know the general shape of the loading spectra for different types of excitation mechanisms and therefore their focus is on trying to find out the maximum load and the number of cycles which give the spectra.

There are, however, some problems with the commonly used methods. Since the field measurements have seldom been considered long enough they have often been performed in such a way that the driver has been driving at high speed over a bad road stretch. However, it is very unclear just how damaging this driver and road is, and how this relates to the actual usage of a truck. In the same way the durability test tracks have been constructed to replicate the worst-case loading conditions that have been found during field measurements. [4]

There are other suggestions on how to get the fatigue load design specifications more related to the actual customer environment, for instance by using questionnaire surveys, (see [4, 5, 6].), but these methods do not appear to be reliable enough, since they are based on a subjective judgement and the results are very sensitive to the type of questions asked.

Another problem arises when trying to use the measured fatigue load at early design stages. Since the construction of prototypes when testing new components is a very expensive and time-consuming task, computer models have become very important for testing at early stages in the designing of new components. [7] However, the loads that the vehicle will experience during the measurements will to a great extent be determined by the vehicle design, and therefore there is little point in using measurements from old components, when trying to understand the loads for new components. Consequently, it would be interesting having some sort of vehicle independent description of the loads.

Rather than attempting to describe the loads as such, we here use a method based on the question: *What causes the loads?* As pointed out above there are several different factors: *the operating environment*, that is the roads that the truck will be driven on, *the driver's behaviour*, such as speed changes and manoeuvring and *the transport mission*. Also the technical design of the truck will affect the loads, i.e. *the vehicle specification*. If one could separate these different factors and describe them one by one and understand how they interact, much would be gained since the description of the operating environment would hold for any truck, the same would probably be true to a great extent for the driver's behaviour. (A reckless driver is most likely reckless no matter what truck he is driving.) It could therefore be of great interest to get a parameterisation of the actual road conditions and then model how drivers behave on these roads. Through such a description it would be possible to recreate the loads, and

the increased understanding of the origins of the loads would lead to a better understanding of the markets and applications.

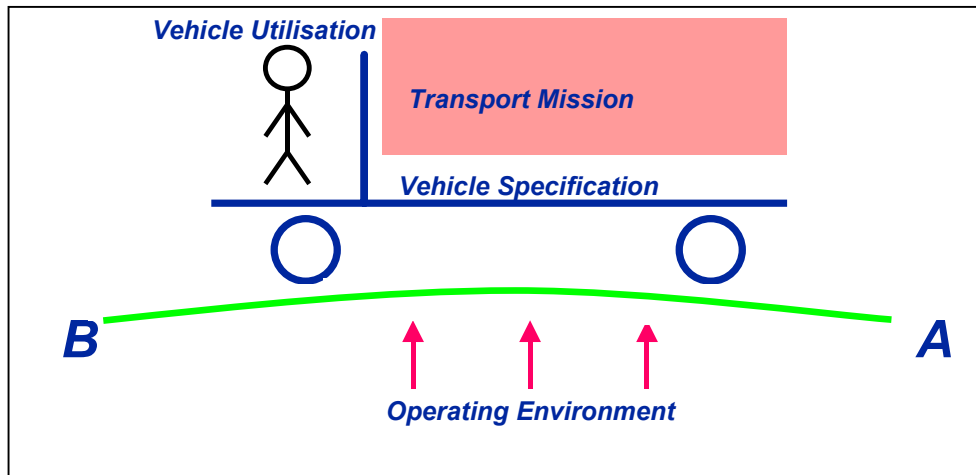


Figure 1. Different sources of fatigue load.

The loads that the truck will experience on the road come from different excitation mechanisms; some will, for instance, be due to an uneven road surface while others are due to the curvature. It appears to be current practice to separate different kinds of excitation mechanisms from each other, see [3,8,9]. One approach to the problem has been to describe different kinds of vehicle independent parameters. (See [7].)

The most important excitation mechanisms should be those coming from driving into potholes and bumps, road vibration, curvature, braking and accelerations. The potholes and bumps together with the road vibration has been considered in a series of articles by Aurell and Edlund and Öjjer and Edlund, see [10,11,12,13].

This work focuses on lateral loads. In order to describe lateral loads in terms of load origins, it is necessary to be able to describe the road, i.e. the curvature, the driver's behaviour, i.e. the speed and the driver's response to other factors than the road, as well as the vehicle's behaviour.

The paper is outlined in the following way. In section 2, the parametric model for the lateral acceleration is described. In section 3, the procedure for estimating the curvature is given, and the variability of the curvature is suggested to follow a lognormal-like distribution. In section 4, the average speed in a curve is modelled depending on the estimated curvature of the particular curve. In section 5, the models for the curvature and the speed are brought together to explain parts of the lateral acceleration. The remaining part is suggested to follow a transformed normal process. This gives us a parametric model of the lateral acceleration, in terms of road curvature, speed and response to other characteristics than the road. In section 6, the expected cumulative fatigue damage for the modelled load is devised, and an expression for range spectrum is shown. For the residual an upper bound for the expected damage is found. In section 7, results are presented in terms of range spectra for measured loads and according to the expressions in section 6. Tables of damage for the observed loads are also shown

together with damage found according to the expressions in section 6. In section 8, the results are discussed and some conclusions drawn. Finally, in section 9, some future work is suggested.

2. Model summary

The aim of this work is to parameterise the lateral loads according to the ideas outlined above, i.e. separating the different load origins, describing them one by one, and understanding their interaction. On this description, a way to classify measured load signals depending on their fatigue damage can be devised. The measurements used are related to lateral acceleration and velocity.

The cumulative fatigue damage depends on which stress the vehicle experiences. Since the stress at any point is directly proportional to the applied force, it is also proportional to the acceleration at that point. This means that the only distinction between calculating the damage from the acceleration rather than the stress should be a factor which can be determined by the proportionality. We can thus concentrate on describing the acceleration. The lateral acceleration is found by multiplying measured signals of the velocity and the yaw rate. The proportionality constants will be different from point to point on the vehicle, but the key issue here is to be able to compare damage found from the loads in one measurement to that in another. Consequently, the resulting damage number will not explain exactly how damaging the measured loads are but will rather make it possible to compare different measurements to each other.

The aim here is to describe the lateral acceleration using the concept explained above, that is separating the different load origins, describing them one by one, and understanding their interaction. According to this concept a parametric model for the lateral acceleration has to contain a description of the curvature of the road and a model for the velocity at which the driver chooses to drive through the curve. Ideally this would be enough, since the lateral acceleration can be calculated using the equation for centripetal acceleration. However, since the driver might be affected by other factors, the vehicle dynamics might affect the acceleration, and since the road surface may also lead to lateral acceleration and there may be measurement errors, the model of the lateral acceleration is constructed in the following way:

- I. A model for estimating the curvature of each curve is developed. The curvatures found are modelled statistically, given a distribution of the curvature of the measured road.
- II. A relationship between the driver's choice of speed and the curvature is explained with a regression model.
- III. The part of the measured acceleration, which cannot be described in terms of simple centripetal acceleration (which can be found from I. and II. above) is modelled with a transformed normal process.

The steps I-III give the following equation and figure:

$$a_{meas}(t) = a_{centripetal}(t) + a_{res}(t) = v^2(t)C(t) + a_{res}(t) \quad (1)$$

where C is the curvature, v is the average speed along each curve and a_{res} is the residual acceleration. We here assume that the function $v(t)$ is constant along the curve and $C(t)$ is constant along the top of the curve. See right part of Figure 2.

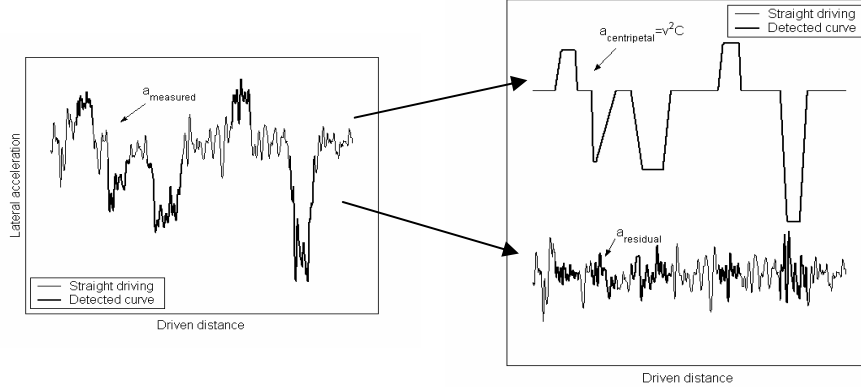


Figure 2. Separating the different parts of the acceleration.

The steps I-III above are then used to understand the cumulative fatigue damage, which the acceleration causes. Obviously (I) can be interpreted as the operating environment. (II) describes the driver's behaviour in terms of choice of speed. However, the effect of the driver can also be seen in (III), since part of this acceleration comes from the driver's response to other factors than the road. The issue is now to get a description of each of the three parts in the eq. (1) above, i.e. the curvature (C), the speed (v) and the residual (a_{res}) as functions of time or summarised in the form of distributions. These parts will, as was mentioned in the introduction, be described in section 3-5. In total there will be 9 parameters explaining the whole signal.

In the three steps (I-III) above a measurement can be described with a set of parameters. Since there is an interest in understanding how much damage the two parts of eq. (1) creates each, an approximation of the damage of the whole model is done in the following way:

$$D_{meas} \approx D_{trap} + D_{res} \quad (2)$$

where D_{meas} is the damage caused by the observed lateral load, D_{trap} is the damage caused by centripetal acceleration, i.e. the signal $C(t) \cdot v^2(t)$ in eq. (1). See also the right part of Figure 2), and D_{res} is the damage caused by the residual process, where consideration is also given to the interaction effect between the two signals. A motivation for this approach can be found in section 6.

3. The curvature model

When constructing a curve a crucial part is to make sure that vehicles driving through the curve will not experience too high lateral accelerations. In order to avoid this and to get a smooth ride through the curve it is therefore useful to have a constant curve radius over a longer time, say a couple of seconds. One way of modelling a curve would

therefore be to think of it as having a constant radius over the entire curve. However if the curve is narrow, i.e. has a small radius, it is probably better to have an area at the beginning (and the end) of the curve where the radius is adapted to the part with a small constant radius. Thus it would be easier for a driver to adjust to the smaller radius. This concept can also be seen in road construction descriptions such as [14], but has also been used in models for velocity profile planning [15].

From a mathematical point of view it turns out that it is possible to model the curvature (here defined as the inverse of the radius at any point of the road) as following a trapezoid. (See Figure 3 and [16].)

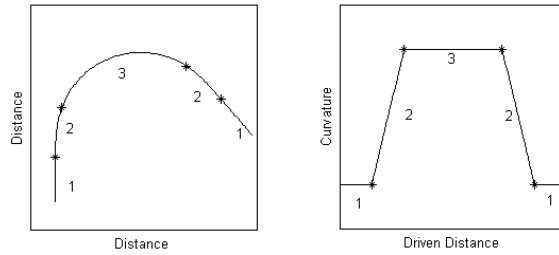


Figure 3. To the left: A straight part before entering the curve (1), an adaptation area where the radius decreases (2), and an area of constant radius (3). To the right: The curvature for the same curve.

The trapezoid, which describes the curvature, is here expressed with the following equation:

$$f(x) = \begin{cases} k_1 \cdot (x - (x_0 - L/2 - h/k_1)), & x_0 - L/2 - h/k_1 \leq x < x_0 - L/2 \\ h, & x_0 - L/2 \leq x < x_0 + L/2 \\ k_2 \cdot ((x_0 + L/2 + h/k_2) - x), & x_0 + L/2 \leq x \leq x_0 + L/2 + h/k_2 \end{cases} \quad (3)$$

where the different parameters can be seen in Figure 4 below:

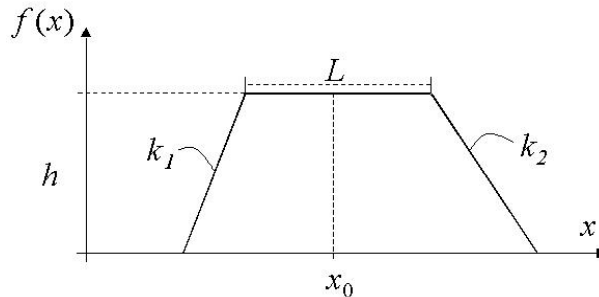


Figure 4. The mathematical model of the curvature as a trapezoid, where h is the height, L is the length of the top, x_0 is the driven distance of the middle of the trapezoid, and k_1 and k_2 are the slopes of the sides.

In [16] an algorithm for estimating the curvature using measurements of the yaw rate and the speed of a vehicle is described. Curves are detected using simple threshold criteria for some signals (speed, lateral acceleration and wheel angle), then for each detected curve a trapezoid is fitted to the signal corresponding to the curvature. Proving ground measurements, as well as video recordings from field measurement, were used to verify the algorithm.

Using this algorithm it is possible to estimate the curvature of each curve. A statistical distribution can then be fitted to the estimated maximal curvatures. It was suggested in [16] that the lognormal distribution might be a good distribution to fit to the data. However, from the result in [16] it was also clear that the data could not be described with a single distribution. The reason for this is that there are very different characteristics of the curves in a city compared to those in the countryside. Therefore, it would be reasonable to have one description for city driving and one for secondary roads and highways. To test this, a series of measurements performed in Brazil was used. The curves in the city stretch were separated from the rest, and the estimated maximal curvatures were fitted to different distributions.

The fact that there is a minimal turning radius sets a natural limit to the curvature distributions. Due to this limit no curvature can be higher than the inverse of the minimal turning radius. In order to find distributions for the curvature, it is therefore suitable to transform the maximal curvature in the following way:

$$Y_j = C_j^{-1} - r_{turn} \quad (4)$$

where C_j is the maximal curvature in curve j and r_{turn} stands for the minimal turning radius. It turns out that the lognormal distribution well describes the transformation (Y_j) of the curvature. However, as mentioned above, different distributions must be used for different kinds of roads. See Figure 5 below:

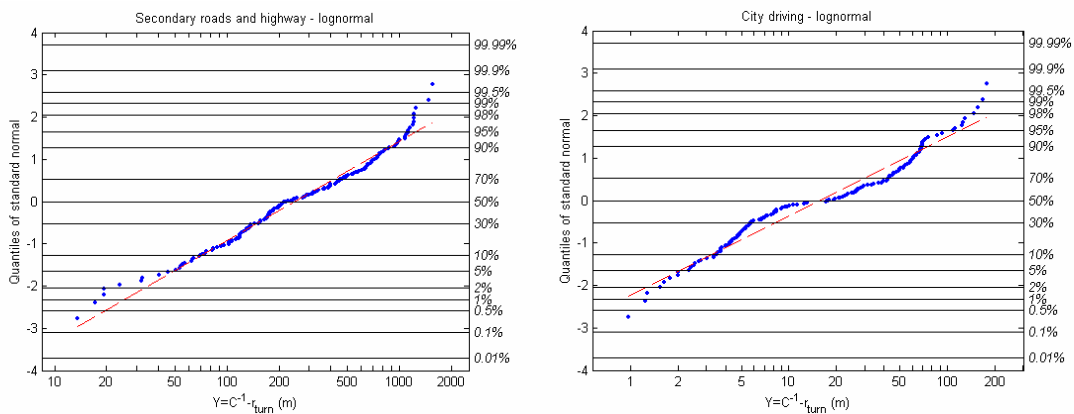


Figure 5. The transformed curvature appears to follow a lognormal distribution, for secondary roads and highway. A lognormal distribution could also be applied to curvature in city driving although the fit appears to be somewhat worse in this case.

In Figure 5, it is worth noticing that the scales of the x-axes in the two plots are very different. It can be seen that more than half of the curves on secondary roads and highways have a radius of more than 200m, while a majority of the curves in the city have a radius of less than 50m. The separation is hence reasonable, since it gives simpler forms for the distribution than a combined description would give.

The fact that it is possible to describe the variability in Y_j with lognormal distribution gives us the following probability density function for the maximal curvature, C_j :

$$f_{C_j}(c) = \frac{1}{\sqrt{2\pi\sigma_c^2}} \cdot \frac{1}{c(1-r_{turn}c)} \cdot \exp\left(-\frac{1}{2} \frac{\left(\ln\left(\frac{1}{c} - r_{turn}\right) - \mu_c\right)^2}{\sigma_c^2}\right) \quad (5)$$

where the parameters μ_c and σ_c are the two parameters in the lognormal distribution for Y_j , i.e. $\log(Y_j) \in N(\mu_c, \sigma_c^2)$. We now have a statistical distribution describing the maximal curvature using 3 parameters.

4. The speed model

There are two different reasons why a speed model is necessary: there is a need to understand the driver's behaviour, and of course it is also necessary to model the speed to be able to relate the curvature to acceleration in order to be able to calculate the cumulative fatigue damage.

If a driver chooses to drive at the same speed through a narrow curve as a broad curve, the lateral acceleration will be greater in the narrow curve due to centripetal acceleration. In order to avoid this it is necessary for the driver to have some strategy when choosing the speed depending on the curvature. There are studies on modelling the relationship between the radius of a curve and the speed at which the driver choose to drive through the curve, (see for instance [17]) but most such studies appear to focus on passenger cars. Three different models were tried out here, according to the following:

$$v_j = ae^{-bC_j + \epsilon_j} \quad \text{model (1)}$$

$$v_j = aC_j^{-b} \cdot e^{\epsilon_j} \quad \text{model (2)}$$

$$v_j = \begin{cases} aC_j^{-b} \cdot e^{\epsilon_j}, & C_j \geq C_{lim} \\ aC_{lim}^{-b} \cdot e^{\epsilon_j}, & C_j < C_{lim} \end{cases} \quad \text{model (3)}$$

Here v_j is the average speed in curve j taken over the part of the curve, where the maximal curvature can be found. (See Figure 2.) The maximum curvature found in

curve j is denoted by C_j . We have seen above that the curvature can be found as $C_j = 1/r_j$. The entities a and b are the regression parameters and ε_j is a random deviation from the linear model, which is assumed to have zero mean and constant variance σ_ε^2 for all curves. The deviations $\{\varepsilon_j\}$ are assumed to be independent. Here C_{lim} is the smallest curvature for which the driver has to adopt the speed.

Model (1) above assumes an exponential relationship between the speed and the curvature, while model (2) assumes a power relationship and model (3) assumes a power relationship along with a cut-off radius, above which the speed is a constant times a stochastic deviation. The physical explanation for the last model is that it is reasonable to assume that for broad curves (low curvature) other effects rather than the curvature will determine the driver's choice of speed, such as the surrounding traffic, speed limits and the engine momentum. Below some curvature C_{lim} , the driver is therefore no longer assumed to adopt the speed to the curve, but rather to other phenomena. This parameter can simply be found through the mean velocity during the straights as $C_{\text{lim}} = (a/v_{\text{lim}})^{1/b}$, where the mean velocity v_{lim} is the mean velocity that the driver uses when he is not adapting to the curvature of the road.

As the parameters a and b in the model depend on the driver they are in a sense random. The same holds for C_{lim} , which is estimated from the measurement, but will mainly depend on the speed limits and traffic situation of the particular market.

The parameters a and b in the two first models can be found using simple linear regression. In the third model the standard linear regression no longer applies. However, a maximum likelihood technique can still be used to estimate the parameters of the model. The likelihood function for model (3) can be written as

$$L(a, b, \sigma_\varepsilon^2) = \prod_{i=1}^n \left(\frac{1}{\sqrt{2\pi\sigma_\varepsilon^2}} e^{-\frac{(\ln v_j - \ln a + b \ln C_j)^2}{2\sigma_\varepsilon^2}} I_{(C_j < C_{\text{lim}})} + \frac{1}{\sqrt{2\pi\sigma_\varepsilon^2}} e^{-\frac{(\ln v_j - \ln a + b \ln C_{\text{lim}})^2}{2\sigma_\varepsilon^2}} I_{(C_j \geq C_{\text{lim}})} \right) \quad (6)$$

where C_{lim} is as above. Estimates for the parameters can be found by maximising the likelihood function, which in this case has to be done numerically.

The models were applied to a series of measurements from Brazilian roads. It turns out that the model (1) gives very poor fit, and can be excluded. The second and third models appear to give good and similar results, which is reasonable since they are very similar in structure. (The cut-off curvature only applies to a small number of the detected curves.) The variability of the deviations ε_i in the second and third models are well described by a normal distribution, and appear to give results with small influence of the radius. See figures below.

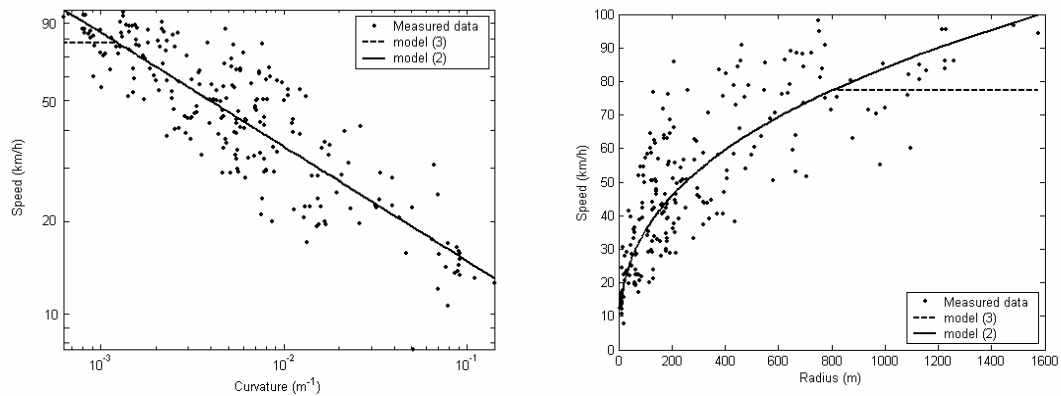


Figure 6. The speed models plotted together with measured data. To the left the curvature versus the average speed, showing what the actual relationship in log log scale looks like and to the right the radius (the inverse of the curvature) versus the speed in linear scale.

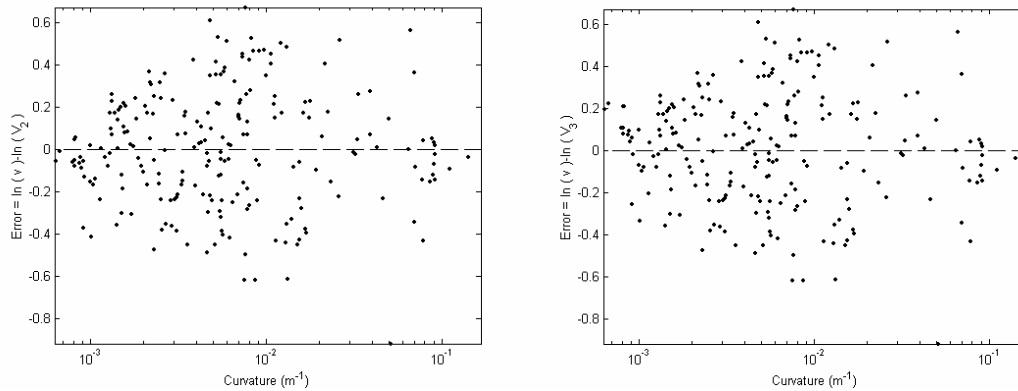


Figure 7. The errors plotted for model (2), to the left, and for model (3) to the right. The errors seem to have some influence from the curvature. There appear to be somewhat smaller errors when the curvature is small. The differences between the figures can be seen in the left parts.

The second model has the advantage of being simple. However, the physical interpretation of very broad curves is questionable. The model suggests that if the radius is large (i.e. the curvature is small) the speed should be large. Thus, in principal if the radius goes to infinity the average speed also has to go to infinity. It can also be noted from Figure 6 that according to model (2) the average speed at a curve of a radius of 1600m would be above 100km/h, which seems fairly unreasonable. It therefore seems like a good idea to choose model (3) as the one to use. Using model (3) we now have four parameters describing the relation between curvature and mean speed.

One way of creating a subtler model for the velocity given the radius would be to use the above model but to include such physical restrictions as speed limits and the limiting lateral acceleration for the vehicle to turn over.

5. Modelling the acceleration signal

Using the equation for centripetal acceleration we can find the part of the acceleration corresponding to the actual curvature from the curvature model and the speed relation in the following way:

$$a_{trap}(t) = \frac{v^2(t)}{r(t)} = v^2(t) \cdot C_{trap}(t), \quad (7)$$

where $v(t)$ is constant over each curve and equal to the average speed along the part of the curve, where the maximal curvature is found. The measured acceleration can be seen as determined by the acceleration from the curvature and a residual on top of that, or as two random processes corresponding to the curvature and the residual, which are modelled as being independent of each other. The residual part mainly corresponds to the driver's response to other factors than the road, the effect of the vehicle and the unevenness of the road. It will be denoted a_{res} . The additive relation can be seen in the following way:

$$a_{meas}(t) = a_{trap}(t) + a_{res}(t) = v^2(t)C_{trap}(t) + a_{res}(t) \quad (8)$$

We will from now on use model (3) for the speed presented above. The curvature and the speed, as described above, can now be combined to model the trapezoidal part of the acceleration, that is the maximum centripetal acceleration in any curve j is:

$$a_{trap,j} = v_j^2 C_j = \begin{cases} a^2 C_j^{1-2b} e^{2\varepsilon_j}, & C_j \geq C_{lim} \\ a^2 C_{lim}^{-2b} C_j e^{2\varepsilon_j}, & C_j < C_{lim} \end{cases} \quad (9)$$

This expression relates to the expressions for $a_{trap}(t)$, $C_{trap}(t)$ and $v(t)$ in such a way that $a_{trap}(t) = a_{trap,j}$, $C_{trap}(t) = C_j$, and $v(t) = v_j$ if t is within the interval over curve j where maximal curvature C_j is found. The remaining part of the acceleration that cannot be described with the trapezoidal part can be thought of as a random process. It turns out that it is reasonable to model this residual acceleration as a transformation of a normal process in the following way:

$$X(t) = \text{sign}(a_{res}(t)) \cdot \sqrt{a_{res}(t)} \in N(0, \sigma_{res}^2) \quad (10)$$

See Figure 8 below. This implies that $a_{res}(t) = \text{sign}(X(t)) \cdot X^2(t)$, where $X(t) \in N(0, \sigma_{res}^2)$, and σ_{res}^2 is the variance of $X(t)$. Unfortunately, there is no physical explanation for this expression, but it could still be argued from Figure 8 below that the fit looks very good for the vast majority of the values, where in total roughly $2 \cdot 10^6$ are considered.

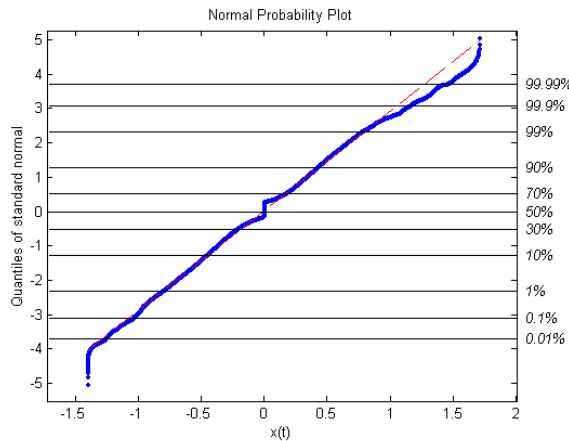


Figure 8. The transformation of the residual appears to follow a normal distribution.

It remains to be seen if the assumption of independence between the residual and the centripetal acceleration holds. It turns out that the variance estimated from the curves is only 8% greater than the variance of the straight parts, and the sample correlation between the sample variance of the residual and the centripetal acceleration over the curves is -0.03 . From these results it appears to be justified to assume that the residual is independent of the centripetal acceleration. Hence, the variance is from now on assumed to be constant over the entire signal.

The idea of the division of the acceleration into two parts is that the lateral acceleration can be seen as a two-folded signal, one part coming from the construction of the road and one part from the way the particular driver uses the vehicle.

We now have a parameterisation of the lateral acceleration into a small number of parameters that describe the measurement. In order for such a parameterisation to be useful it must be possible to calculate the fatigue damage from the parameterisation, as we need to be able to compare the damage that different markets cause.

6. The cumulative fatigue damage for curvature

6.1. A damage approximation

The damage caused by a load is often calculated using the rainflow count algorithm and damage rules such as the Palmgren-Miner rule. (See appendix A1.) As can be seen from the Palmgren-Miner rule, the cumulative fatigue damage, which a component will experience, can be determined from the stress applied to the particular component. The stress is directly proportional to the force, and therefore also to the acceleration. According to the trapezoid model above we can divide the measured acceleration into two parts, one corresponding to the fitted trapezoids, and one corresponding to the residual, see eq. (8).

A natural question to ask is: How much of the damage can be explained by the road and the choice of speed, and to what extent does the residual affect the damage? If we just calculated the acceleration corresponding to the trapezoid and add that to the damage

from the acceleration from the residual, according to eq. (11) below, there would be an error;

$$D(a_{meas}(\cdot)) \approx D(a_{trap}(\cdot)) + D(a_{res}(\cdot)) \quad (11)$$

where $D(x(\cdot))$ is the damage caused by the process $\{x(t)\}$. The problem with this method is twofold. First of all cumulative damage when calculated from rainflow cycles is not a linear function, so this addition is not correct. However, in the special case that we have here, where we have two processes that vary with very different derivatives over the signal, see Figure 9 below, the approximation works well.

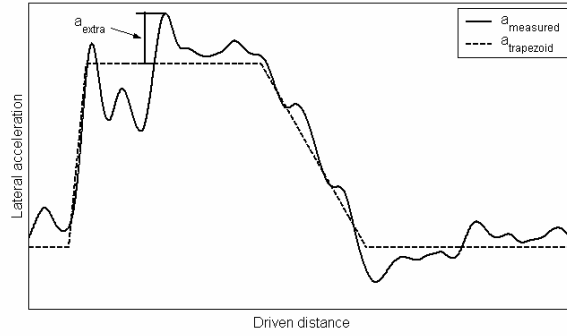


Figure 9. The derivatives for the residual is much larger than the derivatives for the centripetal acceleration on the straight parts and where the curvature is constant, while the opposite is true on the part at the beginning and the end of the curves. The largest residual over the curve is denoted a_{extra} .

The reason for this is the following: in the straight parts of the road and in the parts with a constant curvature the derivative of the residual is obviously much greater than the derivative for the centripetal acceleration, which is zero. On the other hand, through the parts of the curve, where the curvature increases, the centripetal acceleration has a much greater derivative. For this reason the assumption that is made of linearity will work fairly well, despite the approximation.

The second problem with eq. (11) is that it does not take into consideration the fact that the largest cycles of the actual measured signal will be due to the interaction between the trapezoids and the peaks of the residual acceleration. (See Figure 9.) A way of correcting for this error is to model the maximum of the residual over a curve and then add that to the curvature part (that is a_{trap}). Thus we can use the acceleration from the trapezoid model added with the extra loads coming from the maxima of the residual over each curve (here denoted a_{extra}), and let this correspond to the largest cycles. We can, however, still see the effect of the trapezoid acceleration with the following rearrangement:

$$D_{meas} \approx D_{trap} + D_{res} \quad (12)$$

where

$$D_{meas} = D(a_{meas}(\cdot)), \quad D_{trap} = D(a_{trap}(\cdot)) \quad (13)$$

and

$$D_{res} = D(a_{res}(\cdot)) + [D(\hat{a}_{trap}(\cdot)) - D(a_{trap}(\cdot))] \quad (14)$$

where

$$\hat{a}_{trap}(t) = a_{trap}(t) + a_{extra}(t). \quad (15)$$

The last term in eq. (14), i.e. $[D(\hat{a}_{trap}(\cdot)) - D(a_{trap}(\cdot))]$, takes care of the problem of missing the largest loads over the curve. This explains what effect the interaction between the trapezoid and the residual has. The entity a_{extra} is, as mentioned above, the maximum of the residual over each curve.

This entity a_{extra} is fixed for each curve, and thus with the addition in eq. (15) we get that over the whole curve $\hat{a}_{trap}(t)$ increases with the value a_{extra} . However, with the assumption that damage is a rate independent process the only important part is the maxima over each curve, and thus the addition in eq. (15) works. This is true no matter whether we look at the centripetal acceleration a_{trap} or include the maximum of the residual, i.e. look at \hat{a}_{trap} . It should be noted that when there are two curves in the same direction, a similar extra term to a_{extra} could also be included for the largest value in the opposite direction to the curves through the straight part in between them, but this is not included in the model.

The overshoot a_{extra} is here assumed to be independent of the centripetal acceleration a_{trap} . This can be justified by the fact that in the measurements used here the correlation between these two variables was found to be less than 0.8%, i.e. it seems as if the maximum residual acceleration over each curve is independent of the centripetal acceleration governed by the curvature of that curve. From the measurements, it turns out that the variability of the extra loads is well described by the exponential distribution. See Figure 10 below.

The exponential distribution will be used to model a_{extra} from here on. Knowing the distributions for a_{trap} and a_{extra} it is also possible to find the distribution for \hat{a}_{trap} .

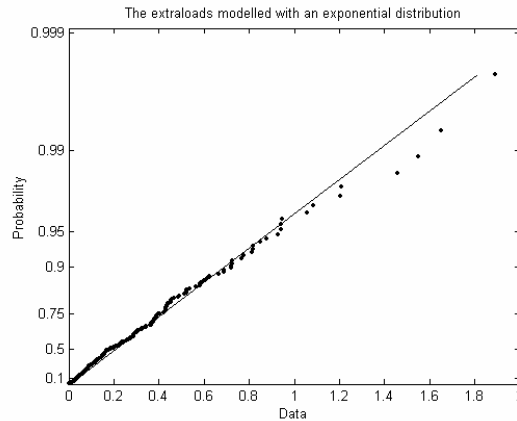


Figure 10. Extra loads plotted on an exponential distribution paper.

The method of dividing the damage into the two classes mentioned above can be illustrated by Figure 11, showing the range spectrum for the measured lateral acceleration a_{meas} , along with the sum of the range spectra for the measured maximal lateral accelerations over the curves and the residual acceleration. It should be noted that this summation is done in the x-direction of Figure 11. At each range, it can be seen that the sum of number of cycles from the residual and the trapezoids with the extra loads is slightly greater than the number of cycles for the measured signal.

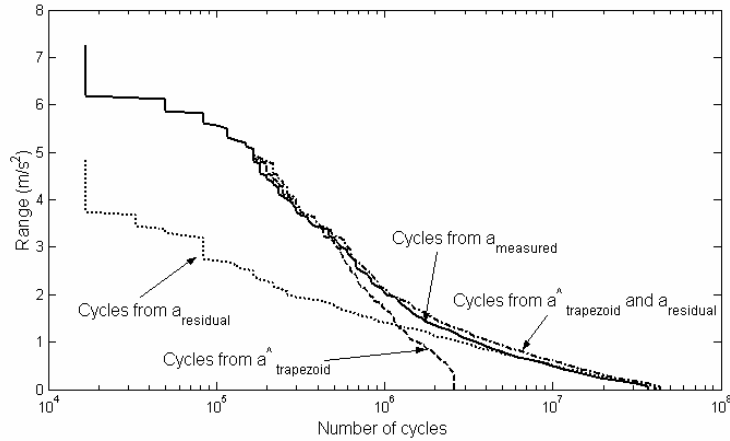


Figure 11. The range spectrum for the trapezoids with the extra loads and the range spectrum for the residual are shown. Adding the cycles from the two yields a result very close to the cycles from the original measurements, justifying the approximation in eq. (12).

As can be seen in the figure the combined ranges are very close to the measured ones. It follows that the cumulative fatigue damage for the two parts summed together also should be close to the damage coming from the measurement. It is also worth noticing in Figure 11 that the residual actually contributes quite a lot to the range spectrum and thus the damage from this part cannot be ignored. In the particular measurement depicted in Figure 11, $D(a_{res}(\cdot))$ explains more than 20% of D_{meas} .

6.2. Rainflow cycles

As already mentioned the most important measure that we are working with is the cumulative fatigue damage. In order to verify that the model describes the loads it is therefore necessary to investigate how damaging (in terms of cumulative fatigue damage) the modelled loads are.

Over the years various methods of extracting fatigue relevant data from random load-time histories have been developed. One way of dealing with this problem is to form equivalent load cycles and then use damage accumulation methods, such as the Palmgren-Miner rule [18, 19]. The most common counting methods are the range-pair counting method, the peak counting method, the level crossing counting method and the rainflow counting method. The method that has shown best results is the rainflow counting method. (See for instance [20].) The rainflow counting method was introduced by Endo 1967 in a series of papers by Endo et al. [21, 22] and Matsuishi and Endo [23]. It has become the most commonly used counting method in engineering. The rainflow cycle algorithm was designed to catch both slow and fast variations of the loading by

forming cycles that pair high maxima with low minima even if they are separated by intermediate extremes. The way of constructing the cycles is based on counting hysteresis cycles for the load in the stress-strain plane. One possible definition is the following, first presented by Rychlik [24]:

Definition 1:

From the i :th local maximum (value M_k) one looks at the lowest values in forward and backward directions between M_k and the nearest point in the forward direction at which the load exceeds (or equals) M_k and the nearest point in the backward direction at which the load exceeds M_k . The larger (less negative) of those two values, denoted by m_k^{rfc} , is the rainflow minimum paired with M_k , i.e. m_k^{rfc} is the least drop before reaching the value M_k again on either side. Thus the i :th rainflow pair is (m_k^{rfc}, M_k) and the rainflow amplitude is $H_k^{rfc} = M_k - m_k^{rfc}$.

This definition is probably best understood from a figure:

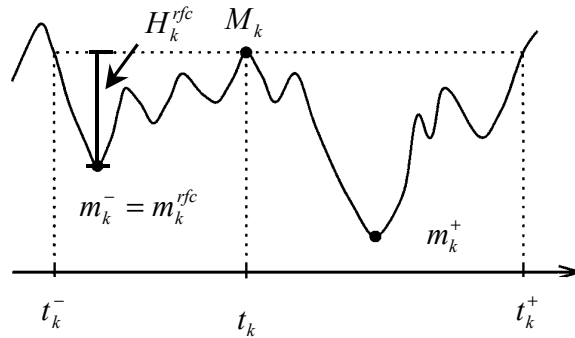


Figure 12. The definition of the rainflow cycle. The rainflow cycle is denoted H_k^{rfc}

We have already seen that a load can be considered a sequence of cycles, which are formed by a combination of local maxima and minima. The cycles can be constructed using the rainflow counting method. The aim now is to find the expected damage for the different parts in eq. (16) and (17) trapezoid acceleration signal $a_{trap}(\cdot)$, the trapezoid acceleration when the extra loads are considered $\hat{a}_{trap}(\cdot)$ as well as for the residual $a_{res}(\cdot)$. The distribution for the trapezoid acceleration is now useful. As we will see it provides a possibility to make exact calculations of the expected damage and the range spectrum for the cases when we consider $a_{trap}(\cdot)$ and $\hat{a}_{trap}(\cdot)$. For the more difficult $a_{res}(\cdot)$ an upper bound will be found.

6.3. Expected damage for the trapezoid acceleration

We can, from eq. (9) calculate the distribution of the amplitude of the trapezoid acceleration in each curve, using our knowledge of the distribution of the curvature and the errors. Since we also know the distribution of the extra loads, the distribution for

$\hat{a}_{trap,i}$ in each curve i can also be calculated. Since we only need to consider the local maxima and minima the load, no matter whether we look at $a_{trap}(\cdot)$ or $\hat{a}_{trap}(\cdot)$, can now be described as a sequence of random variables $\{X_i\}$, where every second value is zero and the values in between are either positive or negative with probability $1/2$ each, and whose amplitude is decided according to the distribution of the trapezoid acceleration. This can be seen in the following way, that each X_i has the following distribution:

$$X_i = \begin{cases} 0, & \text{if } i = 0, 2, 4, \dots \\ Z, & \text{with prob. } 1/2, \text{ if } i = 1, 3, 5, \dots \\ -Z, & \text{with prob. } 1/2, \text{ if } i = 1, 3, 5, \dots \end{cases} \quad (18)$$

where Z is distributed according to the distribution of the amplitude of the trapezoid acceleration, i.e. when not considering the extra loads we have that

$$Z = C_j \cdot v_j^2 = \begin{cases} a^2 C_j^{1-2b} e^{2\varepsilon_j}, & C_j \geq C_{lim} \\ a^2 C_{lim}^{-2b} C_j e^{2\varepsilon_j}, & C_j < C_{lim} \end{cases} \quad (19)$$

and when also considering the extra loads $a_{extra,j}$ we get

$$Z = C_j \cdot v_j^2 + a_{extra,j} = \begin{cases} a^2 C_j^{1-2b} e^{2\varepsilon_j} + a_{extra,j}, & C_j \geq C_{lim} \\ a^2 C_{lim}^{-2b} C_j e^{2\varepsilon_j} + a_{extra,j}, & C_j < C_{lim} \end{cases} \quad (20)$$

Note in eq. (18) that the zeros are necessary to include since there are extremes, which have value zero. This is for instance the case when we have two curves in the same direction as can also be seen in Figure 13, where an example of a sequence is depicted, and we have a zero local maximum for $i = 4$.

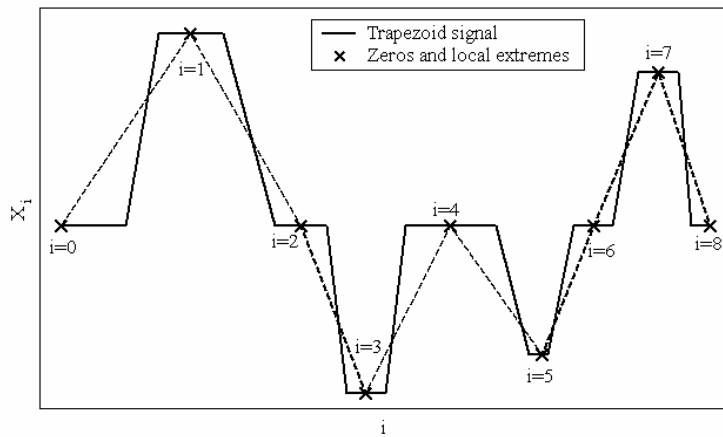


Figure 13. Trapezoid signal with marked zeros and local extreme values, which build up a sequence. The amplitude of each local extreme value is distributed according to the distribution of the amplitude of the trapezoid acceleration.

In the following, the amplitudes of the curves are assumed to be independent of each other, and that the direction of the curves are also independent. Assume now that we study a signal containing n curves. We can then study a sequence of $2n$ elements $(X_0, X_1, \dots, X_{2n-1})$, where the element X_i can be found according to eq. (18).

Our wish is now to apply this sequence to the rainflow count method in order to find the cycles, and the expected damage. This can be done using a technique from Rychlik [24], but in order to do this we need the following definition:

Definition 2:

Let $L(t)$, $0 \leq t \leq T$, be a load and $\{(x, y)_{t_i}\}$ a cycle count. Let $N_T(u, v)$, $u \geq v$, denote a counting distribution of a cycle count $\{(x, y)_{t_i}\}$ defined as follows: $N_T(u, v) = \#\{(x, y)_{t_i}; t_i \leq T \text{ and } x > u \geq v > y\}$, i.e. the number of cycles with top higher than u and through lower than v . This can also be seen as interval up-crossings of the interval $[v, u]$.

Using this definition Rychlik [24] stated the following theorem:

Theorem 1 (Rychlik):

Consider a countable cycle count $\{(x, y)_{t_i}\}$ obtained from a load $L(t)$, $0 \leq t \leq T$, with a counting distribution $N_T(u, v)$ and let the damage caused by a cycle $(x, y)_{t_i}$, $f(x, y)$, be a twice continuously differentiable function such that $\partial^2 f(x, y) / \partial x \partial y \leq 0$ for all $x \geq y$ and $f(x, x) = 0$. Then the total damage $D(T)$ is finite and given by

$$D(T) = -\iint_{u \geq v} N_T(u, v) \frac{\partial^2 f(u, v)}{\partial u \partial v} du dv - \int_{-\infty}^{\infty} N_T(u, v) \frac{\partial f(u, v)}{\partial v} \Big|_{u=v} du \quad (21)$$

For a proof of Theorem 1, see [25]. We are here assuming that the damage for one cycle is given by eq. (A4), with $\beta > 2$. (See appendix A1.) This means that we get the following damage function:

$$f(u, v) = K(u - v)^\beta \quad (22)$$

Using eq. (22) in eq. (21) and simplifying leads to the following result in our case:

$$D(T) = K\beta(\beta - 1) \iint_{u \geq v} N_T(u, v) \cdot (u - v)^{\beta-2} du dv \quad (23)$$

Now, we are mainly interested in the expected damage caused by the signal up to time T . Let $\mu_T(u, v) = \mathbf{E}[N_T(u, v)]$, i.e. the expected number of up-crossings of the interval $[v, u]$ for the sequence until time T . Then, taking the expected value of eq. (23) leads to

$$\mathbf{E}[D(T)] = K\beta(\beta - 1) \iint_{u \geq v} \mu_T(u, v) \cdot (u - v)^{\beta-2} dudv \quad (24)$$

where K and β are the constants in the Wöhler curve according to eq. (A1) in appendix A1. In order to be able to find the expected damage in our particular case we thus need to find $\mu_T(u, v)$, for $u \geq v$.

Let us now consider the sequence of length $2n$, where we have n curves, where the different values in the sequence are found according to eq. (18), and study three different cases for $\mu_T(u, v)$. We here assume that n is a large number so that the boundary effects are negligible.

First assume that $0 < v \leq u$. Since all local minima in our sequence will be ≤ 0 , we can conclude that all cycles that manage to exceed u will have started from a value less than the positive v . The maximum values for the sequence (see Figure 13) can either be positive lateral acceleration or zero lateral acceleration. At all odd indexes, the probability of having a positive lateral acceleration, i.e. having $X_i > 0$ is $1/2$. Hence with a sequence of length $2n$ the average number of positive maximum values of the sequence is $n/2$. Finally, the probability for a curve with positive lateral acceleration to exceed u can simply be found as $\mathbf{P}(Z > u)$. Combining this lead to the following expression for $\mu_{2n}(u, v)$ for the case when $0 < v \leq u$:

$$\mu_{2n}(u, v) = \frac{n}{2} \cdot \mathbf{P}(Z > u) \quad (25)$$

Next consider the case when $v \leq u < 0$. For our sequence all local maxima will be ≥ 0 , we can conclude that all cycles that start from a value below v will always exceed the negative u . With the same reasoning as above it can be concluded that the average number of negative minima over the sequence must be $n/2$. The probability of having a curve with negative lateral acceleration less than v is $\mathbf{P}(-Z < v) = \mathbf{P}(Z > -v)$. Thus, for the case when $v \leq u < 0$ we get

$$\mu_{2n}(u, v) = \frac{n}{2} \cdot \mathbf{P}(Z > -v) \quad (26)$$

The last case that we need to consider, which is the most difficult is when $v \leq 0 \leq u$. It can be shown, see appendix A.2, that this case leads to

$$\mu_{2n}(u, v) = \frac{n}{2} \cdot \frac{\mathbf{P}(Z > u) \cdot \mathbf{P}(Z > -v)}{\mathbf{P}(Z > u) + \mathbf{P}(Z > -v)} \quad (27)$$

To summarise we have now seen that the expected number of crossing of the interval $[v, u]$, where $u \geq v$ can be written as

$$\mu_{2n}(u, v) = \begin{cases} \frac{n}{2} \cdot \mathbf{P}(Z > u), & \text{if } u \geq v > 0 \\ \frac{n}{2} \cdot \frac{\mathbf{P}(Z > u) \cdot \mathbf{P}(Z > -v)}{\mathbf{P}(Z > u) + \mathbf{P}(Z > -v)}, & \text{if } u \geq 0 \geq v \\ \frac{n}{2} \cdot \mathbf{P}(Z > -v), & \text{if } 0 > u \geq v \end{cases} \quad (28)$$

This expression can now be applied to eq. (24). First, notice the symmetry between the two cases $0 < v \leq u$ and $v \leq u < 0$, and then since for a random variable such that $Z > 0$ we have that $\int_0^{\infty} \beta \cdot u^{\beta-1} \cdot \mathbf{P}(Z > u) du = \mathbf{E}[Z^\beta]$. With a few simplifications we can then state the following theorem:

Theorem 2:

For the assumptions made above, and a sequence of length $2n$, we get the following expected damage:

$$\mathbf{E}[D(2n)] = K \cdot n \cdot \mathbf{E}[Z^\beta] + \frac{K \cdot n \cdot \beta \cdot (\beta - 1)}{2} \int_{u=0}^{\infty} \int_{v=-\infty}^0 \frac{\mathbf{P}(Z > u) \cdot \mathbf{P}(Z > -v)}{\mathbf{P}(Z > u) + \mathbf{P}(Z > -v)} \cdot (u - v)^{\beta-2} dv du \quad (29)$$

Eq. (29) can now be evaluated numerically for a particular measurement in order to find the expected damage for the set of parameters of that measurement.

We have not included any dependence for the direction of two consecutive curves. It could of course be argued that it is more likely that a curve to the left will follow one to the right. There are several ways on which this could be incorporated. One possibility is to model the load as a Markov chain, and let a regime process determine the direction. Theoretical results for this could be found in Johannesson [26]. However, it might also be possible to find relatively simple expressions for the expected damage using the same kind of arguments as those used here.

6.4. Range spectrum evaluation

Apart from the damage it is also interesting to see results in terms of range spectra for the modelled loads and compare that with the results for measured loads. The plots of range spectra show in principle the number of cycles, whose ranges exceed a certain level plotted against that level. In the plots the number of cycles are found on the x-axis, and the level on the y-axis.

Let $\kappa(h)$ be the average number of cycles, whose ranges exceed level h . In our case we have three types of cycles, one with negative minima and positive maxima, another with negative minima and zero maxima and the last one having zero minima and positive maxima. By calculating the average number of cycles having a range exceeding the level h for each of these three cases and then add them together the following theorem can be shown that

Theorem 3:

For the assumptions made above and a sequence of length $2n$, we get the average number of cycles, whose ranges exceed h as:

$$\kappa(h) = n \cdot \frac{\mathbf{P}(Z > h)^2}{1 + \mathbf{P}(Z > h)} + \frac{n}{4} - n \cdot \int_{u=0}^h \int_{y=0}^{h-u} \frac{\mathbf{P}(Z > u) \cdot \mathbf{P}(Z > y) \cdot g_z(u) \cdot g_z(y)}{(\mathbf{P}(Z > u) + \mathbf{P}(Z > y))^3} dy du \quad (30)$$

where $g_z(\cdot)$ is the probability density function for the distribution of trapezoid accelerations. For a proof of this result, please consult appendix A.3. An interesting observation of this formula is to let h tend to zero. The first term in $\kappa(h)$ then tends to $n/2$, while the last term vanishes and hence $\kappa(h)$ tends to $3n/4$, which is also the total number of rainflow cycles according to the model. (See appendix A.3.)

Through the results in sections 6.3 and 6.4 we now have a possibility to get the expected damage and the range spectrum for the trapezoid acceleration, and it is also possible to do the same calculations for the trapezoid acceleration when considering the extra loads, with the only change that the distribution for the accelerations becomes somewhat more complicated.

6.5. An upper bound for the expected damage from the residual

As part of the acceleration is described by a residual, (see eq. (1) above) there also has to be a description of how to get the damage for this signal, i.e. the $D(a_{residual}(\cdot))$. That the residual actually is quite important for the total damage can be seen from Figure 11, which shows that although the residual gives only few very high cycles it still makes up a considerable part of the range spectrum.

It is in general difficult to find the expected damage from a non-Gaussian random process. For Gaussian load cases there are some results such as [25], and there are also some approximations for more general cases such as in [27]. However, as mentioned above (see eq. (10)) the residual can be seen as a transformation of a Gaussian process. For such a transformation an upper bound can be found according to Rychlik [28]. For the particular transformation here we get that the following corollary shows the upper bound for the damage intensity:

Corollary:

If a random process $W(t)$ can be modelled as a transformed normal process with the following transformation: $W(t) = sign(X(t)) \cdot X^2(t)$, where

$X(t) \in N(0, \sigma_{res}^2)$, then an upper bound for the damage intensity that the process causes can be seen as

$$d_w \leq \nu \cdot 2^{2\beta} \cdot K \cdot \sigma_{res}^{2\beta} \cdot \Gamma(\beta + 1) \quad (31)$$

where d_w is the damage intensity of the process $W(\cdot)$, ν is the intensity of zero-crossings, β is the slope in the Wöhler curve, K is the maximum load in the Wöhler curve (see appendix A1), σ_{res}^2 is the variance of $X(t)$ and $\Gamma(\cdot)$ is the gamma-function.

This corollary now indicates a simple way of getting an upper bound for the damage from the residual process, where we only need to estimate ν and σ_{res}^2 from the measurements. In the estimates of the damage caused by the residual acceleration this method will be used. For a proof of the corollary, see appendix A.4. It could be argued that it is necessary to consider that we have removed a number of the cycles caused by the residual since we have used one maximum of the residual for each curve, and thus we should decrease the intensity ν , but the total number of cycles for the residual is much larger than the amount of curves, roughly 50 times, and hence this effect is negligible.

7. Results

A series of measurements performed in Brazil and Germany were used to compare the modelled load with the actual measured ones. The parameters for the curvature, speed, residual and extra load were estimated from the measurements. From these it is then possible to find an approximation for the damage and range spectrum according to the ideas in section 6. The results can then be compared with the range spectra and damage directly estimated from the measurements.

Three of the measurements used here, were performed on the same stretches of roads in Brazil. These measurements are denoted measurement 1-3. The measurement denoted Brazil comes from a transport of sand on secondary roads in Brazil. The measurement denoted Germany comes from a highway in the Eastern parts of Germany.

7.1. Range spectra comparison

In the figures over range spectra below, the range spectra for the actual measurements are plotted together with the range spectra from the model using the estimated parameters. (The range spectra for the model have a smoother shape, and will also allow for greater ranges.)

In Figure 14, range spectra, on the basis of the trapezoid acceleration (a_{trap}) only, over each measurement can be seen. From the measurements the trapezoid acceleration was found, and the range spectrum was calculated from this signal. Then the parameters in the curvature and the speed model were estimated and from these estimated parameters (2 for the curvature and 4 for the speed model) the range spectrum for the model was calculated. The three different measurements used here are the measurements 1-3,

which were performed on the same stretches of roads, but with three different drivers. For this reason, it can be seen that the total number of cycles (x-axis) are very close, while the effect of the driver can be seen in the way that driver 1 generally chooses a higher lateral acceleration than driver 3, while the most careful driver is driver 2. This is obviously also reflected in the results for the fitted models.

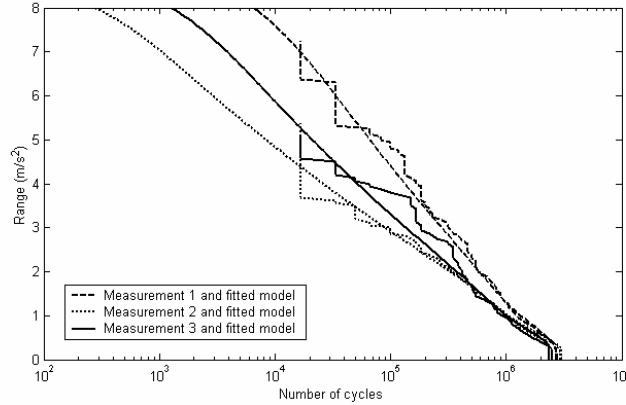


Figure 14. Range spectra for the trapezoid acceleration for three different measurements on the same road using different drivers.

In Figure 15, range spectra on the basis of the maximum acceleration over each curve can be seen. This corresponds to trapezoid acceleration when the extra loads are considered (i.e. \hat{a}_{trap}). The three different measurements again refer to the three measurements on the same road using different drivers. As the only difference from Figure 14 is the inclusion of the extra loads, the difference is rather small, and we can once again see that the driver in Measurement 1 generally chooses the highest lateral acceleration and that the fitted models (the smoother curves) work well.

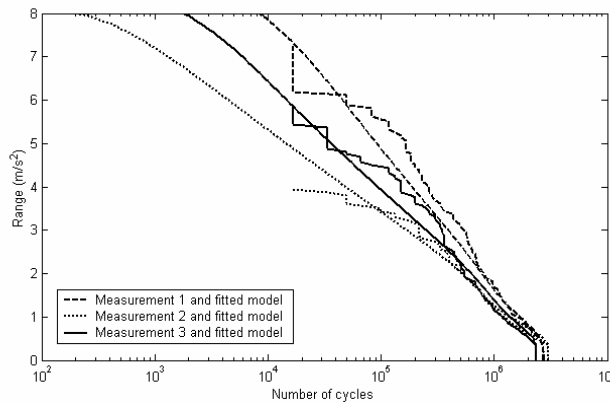


Figure 15. Range spectra for the trapezoid acceleration together with the extra loads for three different measurements on the same road using different drivers.

In Figure 16, range spectra for the whole measurements can be seen. These range spectra are compared with the spectra when the cycles from the model for $\hat{a}_{trap}(\cdot)$ are considered together with the cycles from $a_{res}(\cdot)$. The cycles from the residual is here only the measured ones and are thus not modelled, but the purpose is to show how the result for a whole measurement would look. According to eq. (12) this should be

roughly the same, which could also be seen in Figure 11. The results in Figure 16 once again come from the three measurements on the same road.

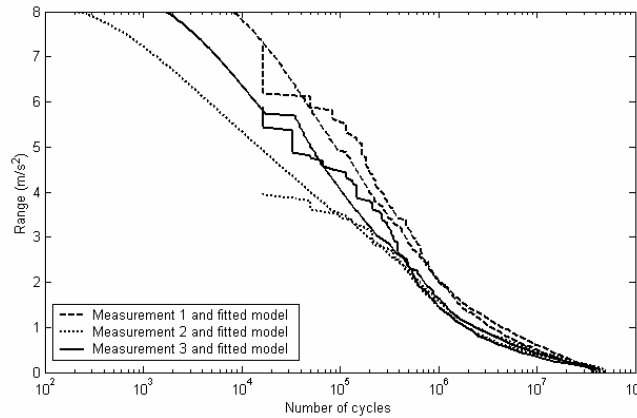


Figure 16. Range spectra for the model and the measured lateral acceleration.

Figure 17 shows the range spectra for the whole measurement for two different measurements performed in Germany and Brazil. The German measurement comes from a highway in the eastern parts of the country, and the Brazilian measurement is a transport of sand in the countryside. For reference purposes measurement 3 from Figure 16 is also included in Figure 17. It can be seen that the main difference is in the middle of the ranges (around $2m/s^2$).

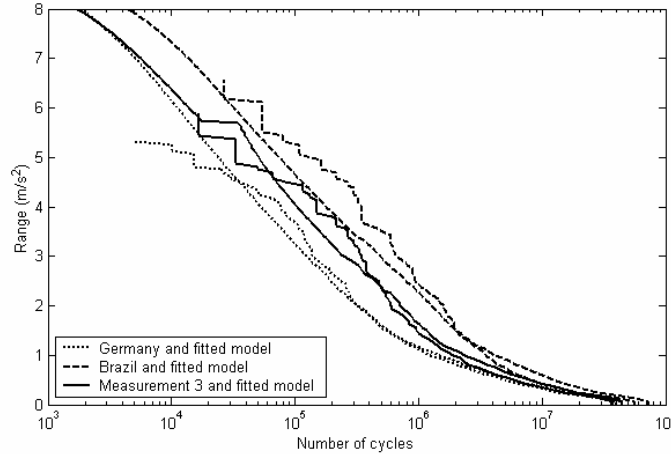


Figure 17. Range spectra for different measurements from Germany and Brazil.

7.2. Damage calculations for the residual approximation

The upper bound for the damage from the residual acceleration $D(a_{res}(\cdot))$, as can be seen in section 6.5, was calculated for the different measurements used above. The values are normalised by the damage for the observed loads in measurement 1.

It can be seen in Table 1 that although the model, which is an upper bound, yields larger damage than the measurement loads, the order of the measurements in terms of damage

is preserved. (The loads in measurement 1 is the most damaging, followed by those in Meas. 3, Germany, Meas. 2, and the least damaging are the loads in the measurement denoted Brazil.)

		Meas. 1	Meas. 2	Meas. 3	Brazil	Germany
$\beta = 3$	Meas.	1	0.35	0.57	0.47	0.22
	Model	1.56	0.66	1.01	0.77	0.38
$\beta = 4$	Meas.	1	0.25	0.76	0.32	0.11
	Model	1.36	0.41	0.78	0.43	0.21

Table 1. The damage from the residual acceleration together with the upper bound for the different measurements. The calculations are made for two common slopes in the Wöhler curve.

7.3 Damage calculations for modelled and observed loads

In order to see how the model works for the entire measurements, the damage was calculated from the observed loads as well as using eq. (29) and (31). The results are presented in Table 2 below. All results are normalised by the damage caused by the measured lateral acceleration for the particular measurement. The entity D_{total} is defined as $D_{total} = D_{trap} + D_{res}$. Thus we can also see how well this approximation works in numbers.

$\beta = 3$		Meas. 1	Meas. 2	Meas. 3	Brazil	Germany
D_{trap}	<i>meas.</i>	<i>0.50</i>	<i>0.49</i>	<i>0.51</i>	<i>0.75</i>	<i>0.63</i>
	model	0.54	0.57	0.51	0.58	0.66
D_{res}	<i>meas.</i>	<i>0.60</i>	<i>0.61</i>	<i>0.64</i>	<i>0.31</i>	<i>0.38</i>
	model	0.67	1.20	0.97	0.51	0.63
D_{total}	<i>meas.</i>	<i>1.10</i>	<i>1.10</i>	<i>1.15</i>	<i>1.06</i>	<i>1.01</i>
	model	1.21	1.78	1.48	1.09	1.56
D_{meas}		<i>1</i>	<i>1</i>	<i>1</i>	<i>1</i>	<i>1</i>

Table 2. The damage from the different parts of the damage approximation in eq. (12). The measured signals are compared to the parameterised model. The calculations are made for $\beta = 3$ a common slope in the Wöhler curve. All results are normalised with the damage from their measured loads, respectively.

Table 3 is constructed to show how well the order of the damage for the measured loads is preserved when using the parameterised model rather than the observed loads.

$\beta = 3$	Meas. 1	Meas. 2	Meas. 3	Brazil	Germany
D_{meas}	1	0.29	0.49	1.17	0.25
D_{total}	1.21	0.52	0.72	1.27	0.39

Table 3. The damage from the damage approximation in eq. (12), compared to the damage from the measured loads. All values are normalised with the original damage of observed loads measurement 1. Once again the slope in the Wöhler curve is assumed to be $\beta = 3$.

Noteworthy in Table 3 is that the order of the measurements is preserved, though the fitted model gives too high damage in all cases. It is also interesting to notice that the damage caused by the residual load process for the Brazilian measurement is roughly half of the damage caused by the residual for measurement 1, but the total damage is actually greater for the loads in the Brazilian measurement.

8. Discussion and conclusion

As can be seen from the results the model appears to work rather well. The model provides a technique to determine the damage from one market and application to another. It is also possible to see the effects of the road in terms of the curvature and the driver. The distribution of the curvature and knowledge about the driver's behaviour also makes it possible to use the model for computer simulations.

It seems, from Figures 14-16, that the effect of the way the driver is driving the vehicle is very important. Although the measurements are performed on the same road, there is a striking difference between the different drivers' behaviour. This appears to be especially pronounced at high acceleration, which is in fact the most important load in terms of fatigue damage.

When the effects of different markets are also applied, as can be seen in Figure 17, the differences between the measurements appear when looking at the number of load cycles at lower lateral accelerations. For instance there is a rather big difference between the numbers of cycles for ranges around $2m/s^2$, while it appears as if the markets have less influence on higher ranges. The fact that the difference is more pronounced for lower lateral acceleration is rather natural since there is a great difference in the number of curves for different roads. (Highways will obviously have fewer curves than urban streets.)

One possible weakness of the model is the difficulty in describing the higher accelerations. It can for instance be seen in Figure 17 that the number of large cycles found in the Brazilian measurement is higher than what the model suggest. This error probably comes from the difficulty in predicting the tails of the distribution for the lateral acceleration. Although most of the accelerations are modelled well, there might very well be an error at the tails. This is especially unfortunate in the case of fatigue when the uppermost loads are the most important. One of the possible reasons for this error can be found in Figure 7, where it can be seen that the errors are, at least to some extent, depending on the curvature. It seems as if the variation increases somewhat as the curvature increases. Another possible reason is that this particular measurement is the one, which has the lowest proportion of two curves in the same direction. The current method, which does not include this proportion will lead to an overestimate of the total number of cycles and an underestimate of the number of large cycles.

Table 1 shows that the upper bound for the residual signal is relatively large for most measurements, typically being 150-200% of the measured damage. On the other hand the upper bound has the interesting property that it preserves the order of the measurements in terms of damage. This is an important fact since one of the main purposes of the project is to be able to compare the expected damage for different markets.

The problem of overestimation from Table 1, is also an important part of the explanation for the overestimate in Table 2 and Table 3. It can also be seen in Table 2 that the approximation of the damage according to eq. (12) appears to overestimate the damage by a few per cent.

Although deviations from the measurements obviously can be found, it seems as if the model is relatively robust. The most sensitive parts appear to be in the speed model, and possibly also the upper bound for the damage of the residual, where the estimate of the standard deviation of the transformed normal process (σ_{res}) has a big effect on the model. (See eq. (31).) On the other hand it is worth noticing that the measurements are very different in nature and it appears as if the model works well for all measurements studied. It is also important to note that despite the approximations the order of the measurements is still kept in the model.

9. Future Work

The above model gives little insight into the residual signal. It is of great interest to understand what part of the residual comes from the effects of the vehicle, and what part is due to other effects such as the driver. This can be done by running the trapezoid signal through a simple vehicle model and studying the effects of the signal to see what part of the residual the vehicle is responsible for. Naturally the driver takes into consideration the vehicle responses, but studying the problem as an open loop problem will still lead to some understanding of the loads, not least when it comes to understanding the frequency content.

Another interesting aspect is to include the proportion of two curves in the same direction in the model for the trapezoid acceleration. There might also be a possibility to find at least an asymptotic variance for the damage, and describe the number of curves as a Poisson process, which would give an increased understanding for the variability. A natural way of studying the variability would also be to use parametric bootstrap techniques and simulate sequences.

An important step is also to collect more data. The measured loads studied here only come from a single vehicle. Although tried out in different environments and with different loading conditions and drivers, naturally only a very small part of the possible markets is covered. New techniques for logging signals have been developed over the last couple years and a very interesting aspect of the model is to adapt it to so called on-board logging, which makes it possible to log much larger amounts of data than what is currently possible.

A fourth interesting aspect would be to study the effects of different drivers more closely in order to see if it is possible to find a statistically significant difference between the drivers. In the same way it would be of great interest to study different markets. Another interesting part to be investigated is the robustness of the model. Finally it would of course be of great interest to extend the concept to other loads such as those coming from the topography of the road, and naturally also to continue the work with vertical excitations such as potholes and road vibration.

Acknowledgement

This work has been a joint work between Volvo Truck Corporation, Fraunhofer-Chalmers Research Centre for Industrial Mathematics (FCC), and the Department of Mathematical Statistics at Chalmers University of Technology, where the author is a graduate student. The author wishes to express his gratitude towards his supervisors Dr. Thomas Svensson, FCC, Prof. Jacques de Maré, Chalmers and Dr. Bengt Johannesson, Volvo. Prof. Igor Rychlik also deserves special thanks for reading the manuscript of the second paper and supplying valuable comments, which greatly improved the paper. He also provided the ideas behind large parts of section 6. The project is funded by the Swedish Agency for Innovation Systems.

References

1. Berger, C., Eulitz, K. -G., Heuler, P., Kotte, K. -L., Naundorf, H., Schütz, W., Sonsino, C. M., Wimmer, A., Zenner, H.: Betriebsfestigkeit in Germany – an overview, *International Journal of Fatigue*, Vol. 24, pp. 603-625, 2002.
2. Klemenc, J., Fajdiga, M.: An Improvement to the Methods for Estimating the Statistical Dependencies of the Parameters of Random Load States, *International Journal of Fatigue*, Vol. 26, pp. 141-154, 2004.
3. Grubisic, V., Fischer, G.: Methodology for Effective Design Evaluation and Durability Approval of Car Suspension Components, *SAE Technical Paper 970094*, 1997.
4. Olofsson, M.: *Evaluation of Estimates of Extreme Fatigue Load – Enhanced by Data from Questionnaires*. Licentiate of Engineering Thesis, Chalmers University of Technology, Göteborg, Sweden, 2000.
5. Niemand, L.: *Probabilistic Establishment of Vehicle Fatigue Test Requirements*. Master of Engineering Thesis, University of Pretoria, Pretoria, 1996.
6. Thomas, J.J., Perroud, G., Bignonnet, A., Monnet, D.: Fatigue Design and Reliability in the Automotive Industry. In Marquis, G. Solin, J. (editors), *Fatigue Design and Reliability, ESIS Publication 23*. Oxford, UK: Elsevier Science, pp.1-12, 1999.
7. Edlund, S., Fryk P.O.: The Right Truck for the Job with Global Truck Application Descriptions, *SAE Technical Paper 2004-01-2645*, 2004.
8. Fischer, G.: Design and Quality Assurance of Vehicle Components based on the Usage Related Stress Analysis. *XXIX Convegno Nazionale dell'Associazione Italiana per l'Analisi delle Sollecitazioni*, Lucca, 6-9 Sept. 2000.
9. Dini, A., Rupp, A.: Comparison of Procedures for Experimental and Theoretical Durability Approval of a Truck Axle, *SAE Technical Paper 982787*, 1998.
10. Aurell J., Edlund S.: Operating Severity Distribution a Base for Vehicle Optimization, *11th IAVSD-Symposium on the Dynamics of Vehicles on Roads and Tracks*, Kingston, Canada, 1989.
11. Aurell J., Edlund S.: Prediction of Vibration Environment in Real Operations Described by Q-distributions, *14th IAVSD - Symposium on the Dynamics of Vehicles on Roads and Tracks*, Ann Arbor, USA, 1995.
12. Öijer, F., Edlund, S.: Complete Vehicle Durability Assessments Using Discrete Sets of Random Roads and Transient Obstacles Based on Q-distributions, *17th IAVSD - Symposium on the Dynamics of Vehicles on Roads and Tracks*, Lyngby, Denmark, 2001.
13. Öijer, F., Edlund, S.: Identification of Transient Road Obstacle Distributions and Their Impact on Vehicle Durability and Driver Comfort, *18th IAVSD- Symposium on the Dynamics of Vehicles on Road and Trucks*, Atsugi, Japan, 2003.
14. Vägverket: Vägutformning-94 version S-1, del 6 Linjeföring. *Vägverket Publikation 1994-52*, Borlänge, 1994. (In Swedish).
15. Bauer, O., Mayr, R.: Road Database Design for Velocity Profile Planning, *IEEE Conference on Control Applications – Proceedings*, Istanbul, Turkey, 2003.
16. Karlsson, M.: Driver Independent Road Curve Characterisation, *18th IAVSD- Symposium on the Dynamics of Vehicles on Road and Trucks*, Atsugi, Japan, 2003.
17. Felipe, E., Navin, F.: Automobiles on Horizontal Curves. Experiment and Observations, *Transportation Research Record*, No. 1628, pp. 50-56, 1998.
18. Palmgren, A.: Die Lebensdauer von Kugellagern. *Zeitschrift des Vereins Deutscher Ingenieure*, 68:339-342, 1924.
19. Miner, M.A.: Cumulative Damage in Fatigue, *Journal of Applied Mechanics*, 12:A159-A164, 1945.
20. Dowling, N.E.: Fatigue predictions for complicated stress-strain histories, *Journal of Materials*, 7:71-87, 1972.
21. Endo, T., Mitsunaga, H., Nakagawa, H.: Fatigue of metals subjected to varying stress – prediction of fatigue lives. In *Preliminary Proceedings of the Chugoku-Shikoku District Meeting*, pp. 41-44. The Japanese Society of Mechanical Engineers, November 1967. (In Japanese)
22. Endo, T., Mitsunaga, H., Nakagawa, H., Ikeda, K.: Fatigue of metals subjected to varying stress – low cycle, middle cycle fatigue. In *Preliminary Proceedings of the Chugoku-Shikoku District Meeting*, pp. 41-44. The Japanese Society of Mechanical Engineers, November 1967. (In Japanese)
23. Matsuishi, M., Endo, T.: Fatigue of metals subjected to varying stress, paper presented to Japan Society of Mechanical Engineers, March 1968. (In Japanese)

24. Rychlik, I.: A new definition of the rainflow cycle counting method, *International Journal of Fatigue*, 9:119-121, 1987.
25. Rychlik, I.: Extremes, rainflow cycles and damage functionals in continuous random processes, *Stochastic Processes and their Applications*, Vol 63, pp. 97-116, 1996.
26. Johannesson, P.: Rainflow Cycles for Switching Processes with Markov Structure, *Probability in the Engineering and Informational Sciences*, 12:143-175, 1998.
27. Bishop, N.W.M., Sheratt, F.: A theoretical solution for the estimation of “rainflow” ranges from power spectral density data, *Fatigue and Fracture of Engineering Materials and Structures*, Vol 13, No. 4, pp. 311-326, 1990.
28. Rychlik, I. Rainflow Cycles, Markov Chains and Electrical Circuits, In Spencer, B.F., Johnson, E.A., Balkema, A.A. (editors), *Stochastic Structural Dynamics*, ISBN 90 5809 0248, pp. 229-234, 1999.
29. Samuelsson, J.: *Fatigue Design of Vehicle Components: Methodology and Applications*, PhD Thesis, Royal Institute of Technology, Stockholm, 1988.
30. Schütz, W.: A History of Fatigue. *Engineering Fracture Mechanics*, Vol 54, pp. 263-300, 1996.
31. Johannesson, P., Svensson, T., and de Maré, J.: Fatigue life prediction based on variable amplitude tests - Methodology, *Cumulative Fatigue Damage*, Seville, 2003.

Appendix

A.1. Cumulative fatigue damage

Since this work deals with fatigue loads, there has to be a measure of how damaging the loads are. This measure is the cumulative fatigue damage. It is generally agreed that fatigue is a rate independent process, i.e. the most important properties of the load are the local extreme values and the order of these. Therefore the load can be seen as a sequence of cycles formed by the local extremes. The sequence of cycles must then be transformed into a measure of the cumulative fatigue damage. In order to relate a load sequence to the damage it inflicts the material, some kind of counting method is often used, together with a damage accumulation rule. The accumulated fatigue damage can be calculated for constant amplitude loading with the Wöhler curve, that is

$$N^{-1} = \begin{cases} KS^\beta, & S > S_f \\ 0, & S \leq S_f \end{cases} \quad (\text{A1})$$

where N is the number of cycles to fatigue failure, and S is the stress amplitude of the applied load. The material parameters are: K , describing the fatigue strength of the material, β , the damage exponent and S_f , the fatigue limit. The next thing is to consider block loading, i.e. blocks of constant amplitude loading one following the other. The Palmgren-Miner rule [18, 19] then states that each cycle with the amplitude S_i uses a fraction $1/N_i$ of the total lifetime. Thus the total fatigue damage is given by

$$D = \sum \frac{n_i}{N_i} \quad (\text{A2})$$

where n_i is the number of cycles with amplitude S_i . Fatigue failure occurs when the damage D exceeds one.

For the more general case of variable amplitude loading, with stress amplitudes $\{S_k\}$, where S_k is the amplitude of the k :th cycle, the fatigue damage can be calculated in accordance with the Palmgren-Miner rule as

$$D(T) = \sum_{t_k \leq T} \frac{1}{N_{S_k}} \quad (\text{A3})$$

where the sum is extended over all cycles completed at time T . The cycle life N_s can be obtained from $S - N$ data tests with the constant amplitude S . In the same way as above the fatigue failure will occur when $D(T)$ exceeds one. The cycles in this case can be obtained using a number of different cycle counting methods, e.g. the rainflow count method.

Studies have shown that the Palmgren-Miner rule can lead to both conservative and non-conservative results, although the latter is more common. A number of

modifications of the rule have been tried out, carrying names such as relative Palmgren-Miner and Miner consistent. Other approaches have also been used such as the local strain concept. However, neither Samuelsson [29] nor Schütz [30] supports this method. Berger et al. [1] rely more on the relative-Miner, while Schütz [30] who created the method claims the accuracy is insufficient. A generalisation of the relative-Miner was suggested in [31], which is based on variable amplitude testing. Although not tested to a great extent it appears to be a possible way in the future. However, so far it seems as if the simplicity of the Palmgren-Miner rule keeps it in much use. It is also important to keep in mind that the simplification of the load history to accumulated fatigue damage (just one measure) is a rather rough simplification and therefore the models themselves can be rather simple.

In the calculations used in this work the Palmgren-Miner hypothesis will be used together with the commonly used S-N curve

$$N_{S_k}^{-1} = K \cdot S_k^\beta \quad \text{with} \quad S_k = (M_k - m_k^{rfc}) \quad (\text{A4})$$

where M_k and m_k^{rfc} are as in definition 1, and K and β are the parameters in eq. (A1). Since the fatigue limit S_f is dependent of the material we have here for simplicity calculated the results using $S_f = 0$. However, the calculations for arbitrary S_f can of course without any difficulty be studied with the same technique.

A.2. Proof of eq. (27)

Our wish is to show that $\mu_{2n}(u, v) = \frac{n}{2} \cdot \frac{\mathbf{P}(Z > u) \cdot \mathbf{P}(Z > -v)}{\mathbf{P}(Z > u) + \mathbf{P}(Z > -v)}$, where Z is distributed

according to eq. (19) or (20), depending on whether we take the extra load into consideration or not. We start with calculating the expected number of up-crossings when $v \leq 0 \leq u$. For fixed values $v \leq 0 \leq u$, the expected number of up-crossings of the interval $[v, u]$ can be found as the number of cycles with a minimum below v multiplied with the probability that the sequence exceeds u before going back to v . Denote this probability $p(u, v)$. The expected number of cycles with minimum below v is the expected number of cycles with a minimum below zero multiplied with the probability of having a minimum below v , i.e. $(n/2) \cdot \mathbf{P}(Z > -v)$. We thus get that for fixed $v \leq 0 \leq u$,

$$\mu_{2n}(u, v) = (n/2) \cdot \mathbf{P}(Z > -v) \cdot p(u, v) \quad (\text{A5})$$

Since the first value after a negative value in the sequence will always be zero, the sequence will in this step be within the interval $[v, u]$. The step after this will either be a step with positive trapezoid acceleration or one with negative each with probability $1/2$. The probability of exceeding u in the first attempt can therefore be calculated as $(1/2) \cdot \mathbf{P}(Z > u)$. However, if the sequence fails to exceed u , but given that it stays within the interval $[v, u]$, there will be another chance with exactly the same probability

of success. (See Figure A1.) The probability for staying in the interval $[v, u]$ is $(1/2) \cdot \mathbf{P}(Z \leq u) + (1/2) \cdot \mathbf{P}(-Z \geq v)$. Thus, we can write $p(u, v)$ as

$$p(u, v) = \frac{1}{2} \cdot \mathbf{P}(Z > u) + \frac{1}{2} \cdot [\mathbf{P}(Z \leq u) + \mathbf{P}(Z \leq -v)] \cdot p(u, v) \quad (\text{A6})$$

which simplifies to

$$p(u, v) = \frac{\mathbf{P}(Z > u)}{\mathbf{P}(Z > u) + \mathbf{P}(Z > -v)} \quad (\text{A7})$$

and hence we see that for fixed values $v \leq 0 \leq u$ we get using eq. (A7) in eq. (A5) that

$$\mu(u, v) = \frac{n}{2} \cdot \frac{\mathbf{P}(Z > u) \cdot \mathbf{P}(Z > -v)}{\mathbf{P}(Z > u) + \mathbf{P}(Z > -v)}. \quad (\text{A8})$$

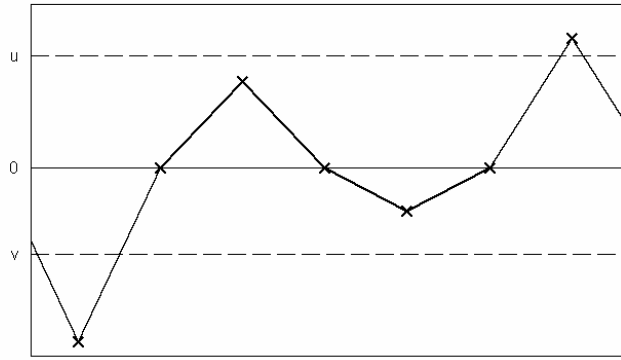


Figure A1. The sequence starts below level v and does not manage to up-cross level u until the third time, but for the points in between the sequence stays in the interval $[v, u]$ so this counts as an up-crossing of the interval.

A.3. Proof of Theorem 3

We would here like to prove that the average number of cycles having range exceeding h could be found as

$$\kappa(h) = n \cdot \frac{\mathbf{P}(Z > h)^2}{1 + \mathbf{P}(Z > h)} + \frac{n}{4} - n \cdot \int_{u=0}^h \int_{y=0}^{h-u} \frac{\mathbf{P}(Z > u) \cdot \mathbf{P}(Z > y) \cdot g_Z(u) \cdot g_Z(y)}{(\mathbf{P}(Z > u) + \mathbf{P}(Z > y))^3} dy du \quad (\text{A9})$$

As mentioned earlier we have three different types of cycles, one having negative minima and zero maxima, another one having zero minima and positive maxima and the last one having negative minima and positive maxima. We can therefore write $\kappa(h)$ as a sum of the contributions from each of these three cases:

$$\kappa(h) = \kappa_{0,-}(h) + \kappa_{+,0}(h) + \kappa_{+,-}(h) \quad (\text{A10})$$

With the same kind of signal as above with $2n$ points, it was argued that there will on average be $n/2$ positive maxima as well as $n/2$ negative minima. The average number of zero maxima can be found as follows: since the direction of a curve is independent of the direction of the previous one, the probability of having a curve to the left given that the previous one was also to the left is $1/2$. Thus, half of the negative minima will be followed by a zero and then another negative minima. Each such combination leads to a zero local maximum, and thus the average number of zero maxima must be $n/4$. By symmetry it can be argued that the average number of zero minima must also be $n/4$. Since every minima has to be combined with a maxima, and zero minima cannot be combined with zero maxima, we get that there will on average be $n/4$ cycles of each of the three different types of cycles stated above, giving a total of $3n/4$ cycles.

Let us start with considering the cycles with maximum at zero and negative minimum. Let M , m^- and m^+ be as in definition 1. It follows that $H^{rfc} = \min\{m^-, m^+\}$, so assuming that we have a cycle with zero maximum, we get

$$\begin{aligned} \mathbf{P}(H^{rfc} > h | M = 0) &= \mathbf{P}(\min\{m^-, m^+\} > h | M = 0) = \\ &= \mathbf{P}(\{m^- > h\} \cap \{m^+ > h\} | M = 0) = \\ &= \mathbf{P}(m^- > h | M = 0) \cdot \mathbf{P}(m^+ > h | M = 0) \end{aligned} \quad (\text{A11})$$

Definition 1 states that m^+ is the minimum value between the maximum and the nearest point in the forward direction at which the load reaches the maximum. Since we have maximum at zero this will happen immediately after the first minima. Thus we get that

$$\mathbf{P}(m^+ > h | M = 0) = \mathbf{P}(Z > h) \quad (\text{A12})$$

We are now interested in the first factor i.e. $\mathbf{P}(m^- > h | M = 0)$. This cannot be found as easily as for the forward direction, since we demand that the load must exceed the maximum in the backward direction. (See definition 1.) We are thus interested if we have at least one local minimum, which goes lower than $-h$ in the backward direction before encountering a maximum above zero. Since the sequence is time-reversible, we can just as well study this as if it would have taken place in the forward direction. Hence, let $p(h)$ denote the probability of down-crossing $-h$ before having a positive local maximum, given that the sequence start at zero and are going down from there. We note that $p(h) = \mathbf{P}(m^- > h | M = 0)$. The probability of reaching below $-h$ in the first curve is $\mathbf{P}(Z > h)$. If the sequence does not reach below $-h$ then there is probability $1/2$ that the next point will give a minimum, and if it does we are again back in the situation where we started at zero and are going down, and want to find the probability that we are going below $-h$. (See Figure A2.)

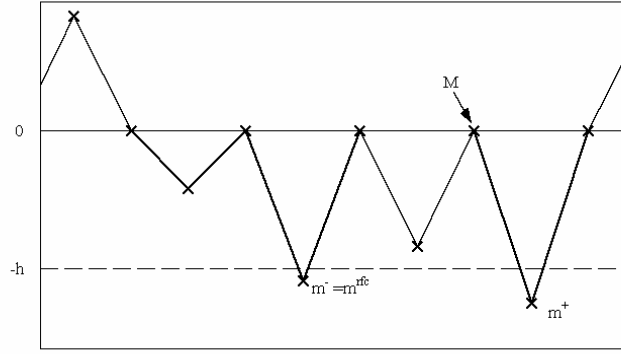


Figure A2. The case with maximum at zero. The first negative value before the maxima does not down-cross the level $-h$, but the second does and hence the range for this cycle is larger than h .

Hence, we can now write $p(h)$ as

$$p(h) = \mathbf{P}(Z > h) + \mathbf{P}(Z \leq h) \cdot \frac{1}{2} \cdot p(h) \quad (\text{A13})$$

And rewriting this leads to the following expression:

$$p(h) = \frac{\mathbf{P}(Z > h)}{1 - \frac{1}{2}\mathbf{P}(Z \leq h)} = \frac{2 \cdot \mathbf{P}(Z > h)}{1 + \mathbf{P}(Z > h)} \quad (\text{A14})$$

Since we on average have $n/4$ cycles of this type we get, by inserting eq. (A14) and eq. (A12) into eq. (A11), the following result:

$$\kappa_{0,-}(h) = \frac{n}{2} \cdot \frac{\mathbf{P}(Z > h)^2}{1 + \mathbf{P}(Z > h)} \quad (\text{A15})$$

Now assume that we have a cycle with zero minimum. Since we have time reversibility and this case is symmetrical to the one where we had zero maximum it follows that

$$\kappa_{+,0}(h) = \frac{n}{2} \cdot \frac{\mathbf{P}(Z > h)^2}{1 + \mathbf{P}(Z > h)} \quad (\text{A16})$$

For the last case where we have a cycle with positive maximum and negative minimum, note first that since the minima is always negative the range of the rainflow cycle can be seen as the sum of two positive random variables. This follows since $H^{rfc} = M - m^{rfc} = M + (-m^{rfc})$, where $M > 0$, and $(-m^{rfc}) > 0$. In order to find the cumulative probability function for H^{rfc} it is of interest to find the bivariate distribution for the pair $(M, -m^{rfc})$. First, note that in this case we have

$$\mathbf{P}(M > u, -m^{rfc} > y) = \mathbf{P}(M > u, m^{rfc} < -y) = \frac{\mu_{2n}(u, -y)}{n/4} = 2 \cdot \frac{\mathbf{P}(Z > u) \cdot \mathbf{P}(Z > y)}{\mathbf{P}(Z > u) + \mathbf{P}(Z > y)} \quad (\text{A17})$$

This holds since $\mu_{2n}(u, -y)$ is the expected number of cycles, which have a maximum above u and a minimum below $-y$, when $u \geq 0 \geq -y$, and $n/4$ is the expected number of cycles, which have a maximum above zero and minimum below zero.

The bivariate cumulative distribution function for the pair $(M, -m^{rfc})$, i.e. the maximum and minimum can thus be found as

$$\begin{aligned} G(u, y) &= \mathbf{P}(M \leq u, -m^{rfc} \leq y) = \\ &= 1 - \mathbf{P}(M > u) - \mathbf{P}(-m^{rfc} > y) + \mathbf{P}(M > u, -m^{rfc} > y) = \\ &= 1 - \mathbf{P}(M > u) - \mathbf{P}(-m^{rfc} > y) + 2 \cdot \frac{\mathbf{P}(Z > u) \cdot \mathbf{P}(Z > y)}{\mathbf{P}(Z > u) + \mathbf{P}(Z > y)} \end{aligned} \quad (\text{A18})$$

Eq. (A18) can now be differentiated with respect to u and y to find the probability density function $g(u, y)$. This leads to the following result:

$$g(u, y) = \frac{\partial^2 G(u, y)}{\partial u \partial y} = 4 \cdot \frac{\mathbf{P}(Z > u) \cdot \mathbf{P}(Z > y) \cdot g_Z(u) \cdot g_Z(y)}{[\mathbf{P}(Z > u) + \mathbf{P}(Z > y)]^3}, \quad u, y \geq 0 \quad (\text{A19})$$

Thus, we can find the cumulative distribution function for the rainflow cycles of this kind as

$$\mathbf{P}(H^{rfc} \leq h) = \int_{u=0}^h \int_{y=0}^{h-u} g(u, y) dy du = \int_{u=0}^h \int_{y=0}^{h-u} 4 \cdot \frac{\mathbf{P}(Z > u) \cdot \mathbf{P}(Z > y) \cdot g_Z(u) \cdot g_Z(y)}{[\mathbf{P}(Z > u) + \mathbf{P}(Z > y)]^3} dy du \quad (\text{A20})$$

The probability of a cycle larger than h can simply be found by taking 1 minus the result in eq. (A20). Finally, since we on average have $n/4$ cycles of this type we get

$$\begin{aligned} \kappa_{+,-}(h) &= \frac{n}{4} [1 - \mathbf{P}(H^{rfc} \leq h)] = \\ &= \frac{n}{4} - n \cdot \int_{u=0}^h \int_{y=0}^{h-u} \frac{\mathbf{P}(Z > u) \cdot \mathbf{P}(Z > y) \cdot g_Z(u) \cdot g_Z(y)}{[\mathbf{P}(Z > u) + \mathbf{P}(Z > y)]^3} dy du \end{aligned} \quad (\text{A21})$$

Thus, bringing eq. (A15), eq. (A16) and eq. (A21) together leads to eq. (A9) and we are done with the proof of Theorem 3.

A.4. Proof of Corollary:

For a process $W(t)$ the damage intensity d_w can be found in the following way:

$$d_w = (\text{intensity of cycles}) \cdot K \cdot E\left[\left(H^{rfc}\right)^\beta\right], \quad (\text{A22})$$

where β and K are material constants as in the corollary and H^{rfc} is the rainflow amplitude. Rychlik showed in [28] that an upper bound for the different moments $E\left[(H^{rfc})^\beta\right]$ can be found through the level crossing intensity using the fact that the load can be described as a transformed Gaussian process. (This upper bound also explains the relation between the actual damage and the so-called Rayleigh approximation.) The upper bound for $E\left[(H^{rfc})^\beta\right]$ is according to [28]:

$$E\left[(H^{rfc})^\beta\right] \leq \alpha E\left[(G(R) - G(-R))^\beta\right] \quad (\text{A23})$$

$\beta > 1$, where R is a Rayleigh distributed random variable with the probability density function $f_R(r) = r \exp\left(-r^2/2\right)$, α is the irregularity factor, found as the ratio between the intensity of zero-up-crossings (ν) and the intensity of local maxima, and G is a transformation that transforms a standard Gaussian process ($Z(t)$) into the process of interest. We have in our case that $W(t) = X^2(t) \cdot \text{sign}(X(t))$, where $X(t) \in N(0, \sigma_{res}^2)$, and thus we get that

$$W(t) = X^2(t) \cdot \text{sign}(X(t)) = \sigma_{res}^2 \cdot Z^2(t) \cdot \text{sign}(Z(t)) = G(Z(t)) \quad (\text{A24})$$

Using the fact that the intensity of cycles has to be equal to the intensity of local maxima, and that a Rayleigh distributed variable is always positive, we can simplify the expression for the damage intensity to:

$$\begin{aligned} d_w &\leq \nu \cdot K \cdot E\left[(G(R) - G(-R))^\beta\right] = \\ &= \nu \cdot K \cdot E\left[\left(\sigma_{res}^2 \cdot R^2 \cdot \text{sign}(R) - \sigma_{res}^2 \cdot (-R)^2 \cdot \text{sign}(-R)\right)^\beta\right] = \\ &= \nu \cdot K \cdot E\left[\left(2\sigma_{res}^2 \cdot R^2\right)^\beta\right] = \\ &= \nu \cdot K \cdot 2^\beta \cdot \sigma_{res}^{2\beta} \cdot E\left[R^{2\beta}\right] \\ &= \nu \cdot K \cdot 2^{2\beta} \cdot \sigma_{res}^{2\beta} \cdot \Gamma(\beta + 1) \end{aligned} \quad (\text{A25})$$

where $\Gamma(\cdot)$ is the gamma-function. The last equality holds since the moment for a Rayleigh distributed variable can be found as $E[R^k] = 2^{k/2} \cdot \Gamma\left(\frac{2+k}{2}\right)$, and hence we get the result in eq. (31).

IMECE2005-79868

EVALUATION OF APPROXIMATIVE METHODS FOR RAINFLOW DAMAGE OF BROAD-BANDED NON-GAUSSIAN RANDOM LOADS

Magnus Karlsson
Volvo Truck Corporation
Durability & Reliability, Dept 26780 A2,
SE-405 08 Göteborg, Sweden,
Department of Mathematical Statistics,
Chalmers University of Technology
Telephone: +46 31 668 286
Telefax: +46 31 508 764
magnus.k.karlsson@volvo.com

ABSTRACT

Two different methods for approximating the fatigue damage of broad banded non-Gaussian random loads using the rainflow cycle count method are evaluated using loads measured on a truck. Results for Gaussian loads are summarized, and transformations for non-Gaussian loads are discussed. One of the two methods is based on the spectral moments of the process, and the results are obtained as a linear combination of an upper and lower bound. The second method is based on the assumption that the sequence of turning points of the load can be considered a Markov chain, for which results can be obtained. Measurements performed on different markets are used to study the two methods. Results are presented in terms of expected damage and amplitude spectra. Problems and possible improvements of the models are discussed.

Keywords: Fatigue, Rainflow method, broad banded, non-Gaussian random loads.

NOMENCLATURE

Latin symbols

C = parameter in the damage function.
 $E[X]$ = expected value of the random variable X .
 $G(x)$ = transformation function.
 H_i^{RFC} = the rainflow range of the i :th rainflow cycle.
 M_i = local maximum i of the random process.
 $R_X(\tau)$ = autocorrelation function.
 $S_X(\omega)$ = spectral density.
 W_p = random peak.
 W_t = random trough.

b = linear combination parameter.
 c_1, c_2 = parameters in the spectrum approximation.
 $f(u, v)$ = damage function of a load cycle with maximum at u and minimum at v .
 $h_{CC}(u, v)$ = joint density function for maximum at u and minimum at v for a load cycle from cycle count method CC .
 k = parameter in the damage function.
 m_i^{RFC} = the rainflow minimum belonging to maximum M_i .
 $p_p(u)$ = density function for peaks.
 $p_t(u)$ = density function for troughs.

Greek symbols

$\Gamma(x)$ = gamma function.
 α_1, α_2 = bandwidth parameters.
 $\delta(x)$ = Dirac delta function.
 $\kappa_{CC}(s)$ = expected number of cycles from cycle count method CC having amplitude greater than s .
 λ_i = i :th spectral moment.
 $\mu_{CC}(u, v)$ = intensity of cycles from cycle count method CC having maximum at u and minimum at v .
 $\mu(u)$ = intensity of upcrossings of level u .
 ν_p = intensity of cycles.

Subscripts and superscripts

RFC = index for rainflow cycle count method.
 RC = index for rangepair cycle count method.

LC = index for level crossing cycle count method.

INTRODUCTION

For many engineering structures the primary mode of failure can be attributed to fatigue damage resulting from the application of time varying loading. Rainflow cycles are often used to describe the variability of loads and stresses and are assumed to be relevant for estimating the fatigue damage caused by loads acting on vehicle components. A common way to evaluate measured time histories is to regard them as samples of random processes and for Gaussian random load processes explicit expressions for the expected fatigue damage have been presented.

Several different methods exist, which aim to approximately model the damage using a small number of parameters, often estimated from the spectral moments of the process. These methods appear to work well for Gaussian loads. See for instance [1,2,3,4]. Therefore, for non-Gaussian loads the methods generally start with a transformation of the process, with the intention of making the load more Gaussian, then the transformed load is evaluated and conclusions can be drawn about the original load, for instance an upper bound for the expected damage can be found using the so-called narrow-band approximation. There are also suggested methods for linear combinations of upper and lower bounds, where the coefficient in the linear combination is determined from the estimated spectral parameters. [1]

An alternative approach for a broad banded process with short memory in time is to model the turning points of the process as coming from a Markov chain. The transition matrix of the Markov chain may then be approximated with a small number of parameters, which once again can be done from the spectrum. Having the transition matrix an exact expression for the expected fatigue damage exists. [5,6,7,8]

The purpose of this work is to compare these two approaches in an application of measured lateral acceleration on trucks, where the load process has been found broad-banded and non-Gaussian, but may be assumed to be stationary and ergodic. The aim is to be able to classify truck markets depending on a small set of parameters, which control the fatigue damage. Thus, it is important being able to describe the damage accurately, but at the same time the model must be parsimonious enough for performing rough classifications.

In the following sections, there will first be a section on rainflow cycles and damage, and then we will go through results obtained for Gaussian loads. A discussion on possible ways of transforming the non-Gaussian load process in order to make it approximately Gaussian will follow. Then a method based on estimating the spectral moments and finding a linear combination of upper and lower bounds of the damage will be presented. After this a section on how to use the Markovian techniques will follow. The two approaches are then applied to a set of measurements performed in Brazil and Germany on a Volvo truck. Results are shown in terms of fatigue damage and amplitude spectra.

RAINFLOW CYCLES AND DAMAGE

Over the years various methods of extracting fatigue relevant data from random load-time histories have been developed. One way of dealing with this problem is to form equivalent load cycles and then use damage accumulation methods, such

as the Palmgren-Miner rule. This rule assumes that the total life may be estimated by merely adding up the percentage of life consumed by each stress cycle. The cycle counting method that has shown best results is the rainflow cycle counting method. See for instance Dowling [9]. The method was introduced in Endo et al. [10]. It has since then become the most commonly used counting method in engineering. The rainflow cycle algorithm was designed to catch both slow and fast variations of the loading by forming cycles that pair high maxima with low minima even if they are separated by intermediate local extremes. The way of constructing the cycles is based on counting hysteresis cycles for the load in the stress-strain plane. A definition more suitable for mathematical analysis is the following, presented by Rychlik [11]:

Definition:

Starting at the local maximum M_i at time point t_i , one looks at the next time point of the same value backward (at t_i^-) and forward (at t_i^+). Let m_i^- the minimum in $[t_i^-, t_i]$ and m_i^+ the minimum in $[t_i, t_i^+]$. The i :th rainflow cycle is defined as (m_i^{RFC}, M_i) , where $m_i^{RFC} = \max(m_i^-, m_i^+)$. The rainflow range is defined as $H_i^{RFC} = M_i - m_i^{RFC}$.

This definition is probably best understood from Fig. 1:

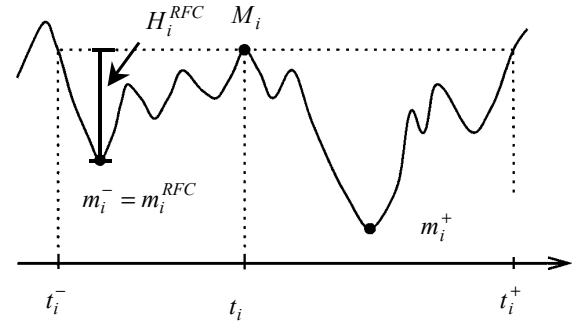


Figure 1. The definition of the rainflow cycle from a load time history.

Assume that the Palmgren-Miner rule holds and the damage for one load cycle, having maximum u and minimum v , is given by the following damage function corresponding to the Basquin equation:

$$f(u, v) = C^{-1}(u - v)^k \quad (1)$$

where C and k are two constants and $f(u, v)$ is the damage caused by a load cycle with maximum u and minimum v . The expected damage intensity, disregarding mean effects, can then be found as:

$$E[D_{RFC}] = C^{-1} \cdot v_p \iint_{u \geq v} (u - v)^k \cdot h_{RFC}(u, v) dudv \quad (2)$$

where $h_{RFC}(u, v)$ is the joint density function for maximum u and minimum v and ν_p denotes the intensity of cycles. Alternatively, it is possible to use an expression from Rychlik [11]:

$$E[D_{RFC}] = C^{-1}k(k-1) \iint_{u \geq v} \mu_{RFC}(u, v) \cdot (u-v)^{k-2} du dv \quad (3)$$

where $\mu_{RFC}(u, v)$ denotes the intensity of cycles having minimum below v , and maximum above u . When considering another cycle counting method, it is possible to replace the joint density function in eq. (2) or the intensity of cycles in eq. (3). The problem of estimating the expected damage can now be regarded as the problem of finding ν_p and $h_{RFC}(u, v)$ or equivalently $\mu_{RFC}(u, v)$.

THEORETICAL RESULTS FOR GAUSSIAN LOADS

As was mentioned in the introduction, both methods that will be applied here are based on characteristics of the power spectrum. The spectral density $S_X(\omega)$ of a stationary stochastic process is defined as the Fourier transform of the autocovariance function $R_X(\tau)$:

$$S_X(\omega) = \int_{-\infty}^{\infty} R_X(\tau) \cdot e^{-i\omega\tau} d\tau \quad (4)$$

where

$$R_X(\tau) = E[X(t) \cdot X(t+\tau)] \quad (5)$$

and $X(t)$ is a zero-mean random load process. One way of characterizing the spectral density is through the spectral absolute moments. The spectral absolute moments of the spectral density can be found as

$$\lambda_m = \int_{-\infty}^{\infty} |\omega|^m S_X(\omega) d\omega \quad (6)$$

Some of the moments can be related to important time-domain characteristics, e.g. the variance of the process $X(t)$, and its derivatives $\dot{X}(t)$ and $\ddot{X}(t)$. These are

$$\lambda_0 = \sigma_X^2, \quad \lambda_2 = \sigma_{\dot{X}}^2, \quad \lambda_4 = \sigma_{\ddot{X}}^2 \quad (7)$$

It is also common in many problems to measure bandwidth parameters such as α_1 and α_2 , which are defined as:

$$\alpha_1 = \frac{\lambda_1}{\sqrt{\lambda_0 \cdot \lambda_2}}, \quad \alpha_2 = \frac{\lambda_2}{\sqrt{\lambda_0 \cdot \lambda_4}}, \quad 0 \leq \alpha_1, \alpha_2 \leq 1 \quad (8)$$

In a narrowband process α_1 and α_2 tend to unity, while in a broadband process they tend to zero. In the case of a Gaussian process α_2 equals the irregularity factor, i.e. the ratio between

the number of mean up-crossings, and the number of load cycles.

For the case when the load process can be modeled as a Gaussian process many results have been presented. Rychlik [12] showed that for a stationary, ergodic Gaussian process it is possible to relate the expected damage due to the rainflow cycle counting method $E[D_{RFC}]$ to the expected damage due to the level crossing and the range pair counting methods $E[D_{LC}]$ and $E[D_{RC}]$ (Two other common cycle counting methods) in such a way that the damage from the level crossing method is an upper bound and the damage from the range pair method is a lower bound for the damage from the rainflow method.

$$E[D_{RC}] \leq E[D_{RFC}] \leq E[D_{LC}] \quad (9)$$

The damage due to the level crossing method is in the Gaussian case the same as for the so-called narrow-band approximation [2], which can be written as

$$E[D_{LC}] = \nu_p C^{-1} \alpha_2 (\sqrt{2\lambda_0})^k \Gamma\left(1 + \frac{k}{2}\right), \quad (10)$$

where the parameters k , C are from the Basquin equation, ν_p is the intensity of cycles, λ_0 is the zeroth spectral moment, and $\Gamma(x)$ is the gamma function. Furthermore the distribution of counted cycles can be represented by means of a joint density function for maxima at u and minima at v . For the level crossing counting method this joint density function can be found as (see [1]):

$$h_{LC}(u, v) = \begin{cases} [p_p(u) - p_t(v)] \cdot \delta(u+v) + p_t(u) \cdot \delta(u-v), & u > 0 \\ p_p(u) \cdot \delta(u-v), & u \leq 0 \end{cases} \quad (11)$$

where $p_p(u)$ and $p_t(v)$ are the probability distributions of peaks and troughs respectively, and $\delta(x)$ is the Dirac delta function. For a Gaussian process

$$p_p(u) = \frac{\sqrt{1-\alpha_2^2}}{\sqrt{2\pi\lambda_0}} e^{-\frac{(u-m)^2}{2\lambda_0(1-\alpha_2^2)}} + \frac{\alpha_2 u}{\lambda_0} e^{-\frac{(u-m)^2}{2\lambda_0}} \Phi\left(\frac{\alpha_2 u}{\sqrt{\lambda_0(1-\alpha_2^2)}}\right) \quad (12)$$

and

$$p_t(v) = p_p(-v), \quad (13)$$

where m is the mean of the random process.

For the range pair cycle counting method, there exist no exact formulas, such as (10). Attempts have been made to find an approximation for the damage. The most frequently used approximation dates back to the 1960s. (See for instance Sjöström [4], Kowalewski[13]) The approximation is based on

the fact that the height of a local maximum W_p for a Gaussian process can be written in the following way:

$$W_p = \alpha_2 \cdot \sqrt{\lambda_0} \cdot R + \sqrt{(1 - \alpha_2^2) \cdot \lambda_0} \cdot Z \quad (14)$$

i.e. as a linear combination of a standard Rayleigh distributed variable R and a standard normal distributed variable Z . These two variables are independent of each other. In the same way a trough W_i can be written as:

$$W_i = -\alpha_2 \cdot \sqrt{\lambda_0} \cdot R + \sqrt{(1 - \alpha_2^2) \cdot \lambda_0} \cdot Z \quad (15)$$

Assuming that the relationship between the trough and the adjacent peak is strong and thus that the normal distributed variable as well as the Rayleigh distributed are the same in the above two equations leads to the following joint density function for the adjacent maxima and minima:

$$h_{RC}(u, v) = \frac{u - v}{4\alpha_2^2 \lambda_0 \sqrt{2\pi\lambda_0(1 - \alpha_2^2)}} e^{-\frac{(u-v)^2 + 4uv\alpha_2^2}{8\alpha_2^2(1 - \alpha_2^2)\lambda_0}} \quad (16)$$

For this joint density function the damage can be calculated as

$$E[D_{RC}] = \nu_P C^{-1} \alpha_2^k (\sqrt{2\lambda_0})^k \Gamma\left(1 + \frac{k}{2}\right) = E[D_{LC}] \cdot \alpha_2^{k-1} \quad (17)$$

In order to be able to use these results it is necessary that the load can be well approximated with a stationary ergodic Gaussian process. A definition of a Gaussian process can be found in any textbook on random processes. See for instance [14].

Definition of a Gaussian process:

A real-valued continuous time process X is called a Gaussian process if each finite-dimensional vector $(X(t_1), X(t_2), \dots, X(t_n))$ has the multivariate normal distribution $N(\mathbf{\mu}(\mathbf{t}), \mathbf{V}(\mathbf{t}))$ for some mean vector $\mathbf{\mu}$ and some covariance matrix \mathbf{V} , which may depend on $\mathbf{t} = (t_1, t_2, \dots, t_n)$.

As a consequence of this definition, it is not only necessary that the values point-by-point follow a normal distribution, but it is also necessary that any finite linear combination of the values does so. Thus, in order to investigate whether the sample at hand might be well modeled by a Gaussian process, it is also important to see whether linear combinations of measured values follow a normal distribution. One simple way of getting a good picture of the normality of a sample is to use normal probability paper. This should be done both for the sample points and linear combinations of them. Another useful test is to plot the empirical level crossing for the sample path at hand and compare that with the result in the Rice formula, which describes the level crossing intensity. For a stationary Gaussian process with mean m , Rice formula says that, the intensity of upcrossings of the level u can be found as:

$$\mu(u) = \frac{1}{2\pi} \sqrt{\frac{\lambda_2}{\lambda_0}} \cdot e^{-(u-m)^2 / 2\lambda_0} \quad (18)$$

Non-Gaussian Loads - Gaussian transformations

However, in most cases it is obvious that the Gaussian process is not a good model for the measured load histories. One possibility to circumvent this fact is to transform the load process at hand so that it becomes more Gaussian. This was first discussed for fatigue problems in the mid-80s by Holm and de Maré [15]. The transformed load can then be evaluated as if it would be Gaussian and then the results can be transformed back in a suitable way to get results for the non-Gaussian loads. Several such transformations are suggested in the literature. In order for such a transformation to work it is necessary that the transformation have a unimodal level crossing intensity. Rychlik et al. [16] suggest a non-parametric transformation based on the empirical level-crossing intensity function. Benasciutti and Tovo [1] use a parametric expression based on the skewness and kurtosis. There is also an attempt by Kihl et al. [3]. The transformation, which will be used here, was suggested by Karlsson [17]:

$$G(x) = \frac{\text{sign}(x) \cdot x^2}{\sigma_{res}^2} \quad (19)$$

where σ_{res}^2 is a constant giving the transformed signal the correct variance. The same verification methods as was suggested to check whether the load process is Gaussian, can of course also be applied to verify that the transformed signal is Gaussian, i.e. that the transformation is appropriate. (See section on definition of a Gaussian process.) Rychlik [2] showed that the Rice formula could also be found for transformed Gaussian loads as

$$\mu(u) = \mu(0) \cdot e^{-(G^{-1}(u))^2 / 2} \quad (20)$$

and furthermore for a non-Gaussian process $Y(t)$ with unimodal level crossing intensity it is possible to find a non-linear transformation $G(\cdot)$ from a standard Gaussian process $X(t)$. Having the transformation $G(\cdot)$, Rychlik showed that the damage due to the level crossing could be found as

$$E[D_{LC}] = \nu_P C^{-1} \alpha_2 E[(G(R) - G(-R))^k] \quad (21)$$

where R is a standard Rayleigh distributed variable. In fact having $G(x) = \sqrt{\lambda_0} \cdot x - m$, as is the case with a general Gaussian process, using the expression in eq. (20) leads to eq. (10).

Similar we have the equivalence of eq. (17) as

$$E[D_{RC}] = \nu_P C^{-1} \alpha_2 E[(G(W_p) - G(W_i))^k] \quad (22)$$

where W_p and W_i are as in eq. (14) and (15).

SPECTRAL MOMENT TECHNIQUES

In the case of a narrowband process the upper bound as suggested in eq. (21) would give a reasonable approximation of the damage. However, in our case we have a broad banded process and hence this approximation does not hold.

On the other hand from eq. (9) it can be seen that a natural approach for estimating the damage from the rainflow cycles would be to use a linear combination of the result for the damage from the level crossing and the result from the range pair cycle counting, in the following way:

$$E[D_{RFC}] = b \cdot E[D_{LC}] + (1-b) \cdot E[D_{RC}] \quad (23)$$

The main task then becomes to find a suitable linear combination, i.e. to find an appropriate b . Some suggestions based on empirical observations can be found in the literature. These empirical expressions usually contain estimates of the spectral moments measuring the irregularity of the process and grouping of large cycles. Tovo suggests in [18]:

$$b_1 = \min \left\{ \frac{\alpha_1 - \alpha_2}{1 - \alpha_1}, 1 \right\} \quad (24)$$

and in another paper by Benasciutti and Tovo [1]:

$$b_2 = \frac{(\alpha_1 - \alpha_2) \cdot (1.112 \cdot (1 + \alpha_1 \alpha_2 - (\alpha_1 + \alpha_2)) e^{2.11 \alpha_2} + (\alpha_1 - \alpha_2))}{(\alpha_2 - 1)^2} \quad (25)$$

The parameters α_1 and α_2 are calculated from the estimates of the spectral moments as suggested in eq. (8). It is worth noticing that they should be estimated from the spectrum of the transformed load. However, both of these empirical formulas have the rather questionable property that b can be outside the interval $[0,1]$. This could of course be corrected in the following way:

$$\tilde{b}_1 = \begin{cases} 0, b_1 \leq 0 \\ b_1, b_1 \in (0,1) \end{cases} \quad \text{and} \quad \tilde{b}_2 = \begin{cases} 0, b_2 \leq 0 \\ b_2, b_2 \in (0,1) \\ 1, b_2 \geq 1 \end{cases} \quad (26)$$

As the parameter b_2 in eq. (25) was shown to give better results in [1], we will here use the corrected parameter \tilde{b}_2 above as our estimate of the linear combination parameter. Using the corrected parameter \tilde{b}_2 in eq. (23) gives the expected damage.

For comparison, it is also interesting to find approximations for the amplitude spectra of the limits. The joint density functions $h_{RC}(u,v)$ and $h_{LC}(u,v)$ can be found using the fact that the transformation G in eq. (19) is differentiable and strictly monotonic. Using these properties the joint density functions for the non-Gaussian case can be found from the joint densities in the Gaussian case (i.e. eq. (11) and

eq. (16)) simply by using the standard method of finding the density of functions of random variables. Having the joint densities for the non-Gaussian case for the level crossing count and the range-pair count, it is reasonable to assume that the relationship in eq. (23) holds also for the distribution of the rainflow cycle counting distribution as:

$$h_{RFC}(u,v) = b \cdot h_{LC}(u,v) + (1-b) \cdot h_{RC}(u,v) \quad (27)$$

Using eq. (27) the expected number of rainflow cycles having amplitude above a certain level s can be calculated. Let $\kappa_{RFC}(s)$ denote this expected number for the level s . The entity $\kappa_{RFC}(s)$ can now be found as

$$\kappa_{RFC}(s) = \int_{u-v > 2s} h_{RFC}(u,v) du dv \quad (28)$$

Similarly, the expected number of level crossing cycles and range pair cycles having amplitude above a certain level s can be calculated as

$$\kappa_{RC}(s) = \int_{u-v > 2s} h_{RC}(u,v) du dv, \quad \kappa_{LC}(s) = \int_{u-v > 2s} h_{LC}(u,v) du dv, \quad (29)$$

respectively.

MARKOV CHAIN TECHNIQUES

An alternative to the spectral moments technique is to model the sequence of turning points of the load process as a Markov chain. The reasoning behind this is that the most important property of the load is the local extremes, thus we only need to model the sequence of local extremes or turning points. See for instance [5,6,7,8]. For a Markov chain, the expected damage can be found exactly depending on the transition matrix for the Markov chain. Obviously then the transition matrix has to be estimated.

For a Gaussian process, notice that the same equations for the marginal distributions of the maxima and minima also should hold here. The approximative formulas for the distribution of the adjacent maxima and minima as in eq. (16) can then provide an approximation of the transition probabilities for the Markov chain. This is the method suggested in [5]. It could then be possible to find a result using the transformation as suggested in eq. (19), but the approximation in eq. (16) is not necessarily that accurate in our case. There does however exist a method developed by Rychlik and Lindgren [19,20,21], which gives an accurate approximative method to compute densities of different wave characteristics of Gaussian processes, and also in the case of simple transforms such as eq. (19) (see [16]). This algorithm uses the spectral density to estimate for instance the joint density of maximum and adjacent minimum, with a regression approximation method using the Slepian model. No assumptions about the relationship of the maximum and minimum as in eq. (16) are necessary, and thus the model is less sensitive than the one suggested in [5]. The algorithm is implemented in the Matlab toolbox WAFO – Wave Analysis in Fatigue and Oceanography –, which can be downloaded free of charge from the following website:

<http://www.maths.lth.se/matstat/wafo/>. In order to use this model it is necessary to get an approximate expression for the spectral density. We have previously used the spectral moments to characterize the spectral density. We are now interested in describing the entire curve. For our load histories a suitable model for the spectral density appears to be:

$$S_X(\omega) = c_1 \cdot e^{-c_2|\omega|} \quad (30)$$

where c_1 and c_2 are two constants that need to be estimated for the different measurements. Our spectral density is now characterized by the two parameters c_1 and c_2 . This can be compared to the characterization by the spectral moments that were previously used. See Fig. (2) for an example of a spectrum estimated from a measurement and the fitted spectrum in accordance with eq. (30).

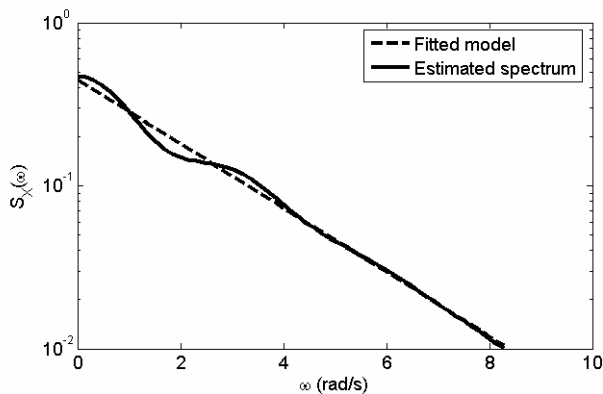


Figure 2. Estimating an approximative spectral density

From the joint density of the maximum and adjacent minimum the rainflow intensity $\mu_{RFC}(u, v)$ can be found. See Theorem 2 in [7]. Using the expression for the rainflow intensity and eq. (31), the expected damage can be derived. Having the rainflow intensity it is also easy to find the expected intensity of rainflow cycles having amplitude greater than s , i.e. the amplitude spectrum.

There are alternative approaches for the case of broad-banded load processes such as the one by Dirlik [22], which uses a semi-empirical model which is a mixture of one exponential and two Rayleigh distributed variables to model the ranges in the rain-flow cycles. This model, which assumes that the load process is Gaussian appears to work well for this case [23], but cannot be used in non-Gaussian cases according to [1]. There are also other methods, which aim to directly model the range distribution (e.g. [24]), but using these methods generally leads to estimating a large number of parameters, and will not be considered here.

EXAMPLE FROM MEASUREMENTS ON TRUCKS

In previous papers [17,25], it has been shown that a reasonable way of modeling the lateral acceleration acting on a truck is to consider it a sum of two random processes. One, which is due to the centripetal acceleration in the curve and one, which is due to the driver response to other factors than the curvature as well as the road vibration and vehicle dynamics. Using a

simplified model of the centripetal acceleration it has been shown that the accumulated fatigue damage for the first part can be described with reasonable accuracy [17]. However, it still remains to get a good understanding for the process due to other factors than the curvature. This load process can be regarded as a stationary, non-Gaussian, broad banded process.

In this section, the results for the transformation, which is used for both methods, will first be presented. Then, the spectral moments methods are used to calculate an upper limit as well as an approximative lower limit. The parameter for the linear combination is estimated and the results for the damage using the spectral moment method are obtained. Using the Markov method the damage is approximated. Finally the range spectra is computed for the different techniques and compared to the one found directly from the measurement.

Results for the transformation

The different transformations, mentioned in earlier sections were all tried out, but no significant difference in the results was found and hence it appears to be better to use the simplest possible model, i.e. the one suggested in eq. (19).

The parameter σ_{res}^2 in the model is estimated directly from the data as the value that makes the variance of the transformed data equal one. In Fig. 3, the data points from one of the measurements are plotted on normal probability paper. As can be seen from the figure the transformed data is rather well approximated with the normal distribution point wise. The dashed line represents the line, which the data should follow according to the normal distribution.

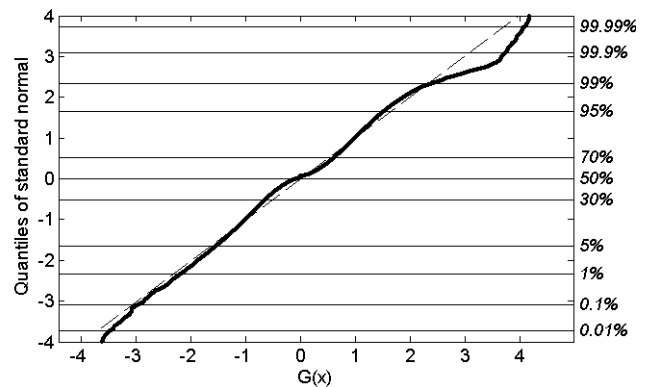


Figure 3. Transformed data plotted on normal probability paper.

In order for the transformed process to be well modeled by a Gaussian process, it is also necessary that linear combinations of the data follow a normal distribution. One such linear combination is shown in Fig. 4. Here, the differences of each pair of data points separated by 0.5 seconds are plotted. As can be seen from the figure the result is not as good as for the case in Fig. 3.

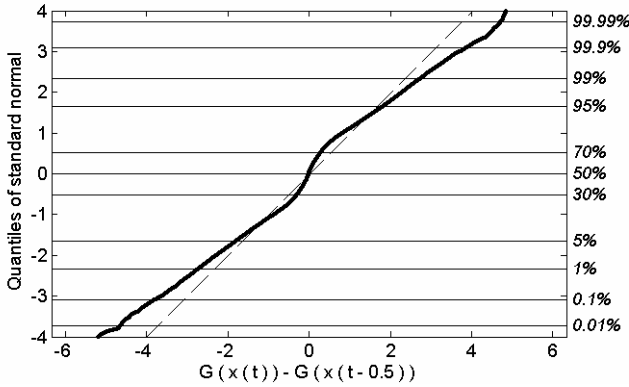


Figure 4. Linear combination of transformed data plotted on normal probability paper.

Finally, in Fig. 5, the level upcrossing from a measurement is plotted with the fitted model, using eq. (20). It seems as if the result is not so good.

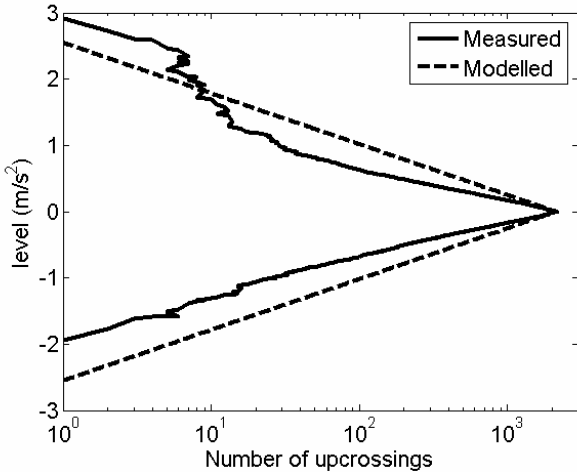


Figure 5. Number of level upcrossings for one of the measurements together with the result for the fitted model.

Expected damage for the two methods

Despite the far from perfect results for the transformation, the measured load histories are transformed in accordance with the transformation in eq. (19). After this, the upper bound is calculated using the transformation and eq. (21). An approximative lower bound is also obtained using the approach suggested in eq. (22). Furthermore, from the spectral parameters, the linear combination parameter \tilde{b}_2 is estimated as well as the expected damage from the rainflow cycle count.

For the Markov chain approach, the parameters in the model for the spectral density are fitted to the estimated spectral density of the transformed load. The transition matrix is then calculated from the spectral density of eq. (30) using the algorithm suggested in [21]. From the transition matrix, the expected damage is calculated. The results for the two methods are presented in Table 1 for five different measurements performed in Brazil and Germany.

No.	Meas.	Upper	Lower	Comb.	Markov
1	137	473	0.25	292	250
2	61	227	0.11	128	128
3	99	383	0.21	219	213
4	39	146	0.04	79	68
5	125	347	0.15	199	170

Table 1. Results for the expected damage calculations for the methods.

The results in Table 1 show clearly that both the spectral moment method and the Markov method leads to overestimates of the measured accumulated damage. It should however be noted that they both allow for greater cycle ranges, than the maximal range found in the measurements, which might be a reason why the overestimates are as great as they are. In other words, the method gives an extrapolation of the loads to a region, which we have not found in measurements. From a physical point of view it is still reasonable to have loads in this region, and thus the extrapolation is reasonable. This fact can also be seen in Fig. (6).

The lower bound is in all cases so small that it hardly contributes at all to the linear combination. In one sense this is good as it is an approximative lower bound, but on the other hand it shows in a way that this method is very sensitive to the parameter in the linear combination. This part can also be seen in the result for the amplitude spectra.

Amplitude spectra

For the spectral moment method, the amplitude spectra are also calculated for the level crossing, range pair and rainflow cycle count techniques in accordance with eq. (28) and (29).

From the transition matrix it is also possible to get the joint distribution of rainflow maxima and minima under the assumption that the load is a Markov chain. From the rainflow matrix, the intensity of cycles having amplitude greater than a certain level s can be calculated. The result for one of the five measurements can be seen in Fig. 6. The results for the other measurements show similar characteristics.

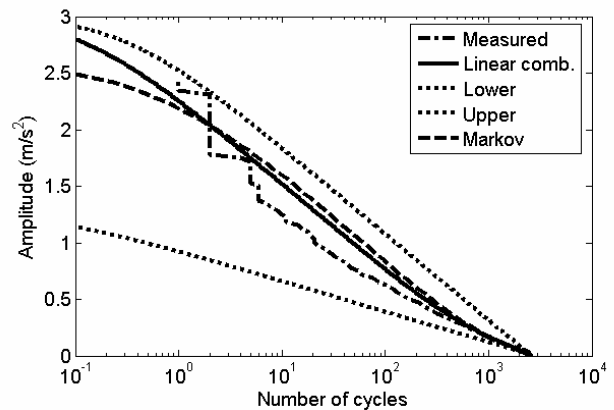


Figure 6. The amplitude spectra for measurement 1.

It is worth noticing that the upper and lower limit captures the measured amplitude spectrum as we expect, but that they are very spread apart, and therefore not too informative. It is also interesting to see that the shape of the curve for the linear combination using the spectral moment method and the shape of the curve for the Markov method are rather similar. The

reason for this might be that the error from the transformation is so large that the differences between the two methods drown. As can be seen from the Fig. 6, both the Markov method and the spectral moment method yield convex curves, whereas the measured amplitude spectrum appears to be concave.

CONCLUSIONS

It can be concluded that the methods studied here actually have many similarities. They are both based on the assumption that the load is Gaussian. If this assumption is violated, results can still be found using a transformation. The results are then found by approximating the spectral density in a suitable way, either by the different spectral moments or by approximating the whole curve. For the spectral moment case, we find an upper and a lower bound and then find our result through a linear combination. With this technique, we need to find a suitable transformation and estimate four spectral moments. In the case of the Markov techniques we perform the transformation and use a model for the spectral density using two parameters. From the two parameters it is possible to find approximative results using the algorithm from Rychlik and Lindgren.

It can be seen from this that one of the most crucial points is to find a reasonable transformation. This can in particular be seen in Fig. 6, since the results for the two methods differ from the measurement in a very similar way. It appears, as most of the current transformations are based on fitting the measured data point-by-point to a normal distribution. However, from the definition of the Gaussian process, this is not enough since also every linear combination should be distributed according to the normal distribution. Furthermore, from a damage point of view it may be more reasonable to base the transformation on the level crossing intensity and Rice formula.

The advantage that can be seen in the spectral moment techniques is that it is rather straightforward and if we get a too large discrepancy between the correct answer and the approximation, it is rather easy to detect where the method fails. On the other hand, there is no exact expression for the lower bound and it is necessary to find a better expression for the parameter in the linear combination. The parameter used here is developed for another transform than the one used and the expression is relatively complicated.

The advantage of the Markov techniques is that it directly gives the transition matrix from which it is possible to find an exact expression of the rainflow matrix and the expected damage. On the other hand there is no general way of approximating the spectral density. Another disadvantage of the technique is that it is relatively difficult to get a good picture of the computations involved and hence it is more difficult to determine possible errors.

It has been shown that the two methods give similar results. It is possible that the transparency of the spectral moment method makes it slightly more attractive, but it is necessary to improve the transformation techniques before any real conclusions can be drawn about the two methods.

Finally, the results in Table 1 might appear as worse than they are, since the models used allow for extrapolation to load levels, which have not been found in the measurements, but still are reasonable. These loads will obviously be damaging and thus increase the expected damage.

FUTURE WORK

It appears as if the most crucial part to work with in the future for both techniques is to find a good transformation. An approach, which has not been studied, but may give good results is the one suggested in [26]. This transformation is also based on the intensity of upcrossings, which already been pointed out as an interesting characteristic. Furthermore, the linear combination parameter, b , suggested here, needs improvement, and can possibly be fitted from data.

As we could see in the 2nd section, the problem of finding the damage of rainflow cycles is to a great extent the problem of finding the joint distribution between the maximum and minimum in the rainflow cycle. In the case of Gaussian load processes, the marginal distribution is known for the maximum and minimum respectively. A possible approach to find the joint distribution would then be to use the copula technique outlined in for instance [27]. This has to author's knowledge not been applied within the fatigue analysis and would be an interesting area to investigate. In the case of non-Gaussian loads a transformation technique could be used, although as has been seen in this paper, large errors can be made using transformation in a careless way.

ACKNOWLEDGMENTS

This work has been a joint work between Volvo Truck Corporation, Fraunhofer-Chalmers Research Centre for Industrial Mathematics (FCC), and the Department of Mathematical Statistics at Chalmers University of Technology, where the author is a graduate student. The author wishes to express his gratitude towards his supervisors Dr. Thomas Svensson, FCC, Prof. Jacques de Maré, Chalmers and Dr. Bengt Johannesson, Volvo, as well as Prof. Igor Rychlik, Lund Institute of Technology and Chalmers. The project is funded by the Swedish Agency for Innovation Systems.

REFERENCES

- [1] Benasciutti D., Tovo R., 2005, "Cycle distribution and fatigue damage assessment in broad-band non-Gaussian random processes," *Prob. Eng. Mech.*, **20**, pp. 115-127.
- [2] Rychlik I., 1999, "Rainflow cycles, Markov chains, and electrical circuits", *Proc., 4th International Conference on Stochastic Structural Dynamics*, E. A. Johnson et al., eds., Taylor & Francis, pp. 229-234.
- [3] Kihl D. P., Sarkani S., Beach J. E., 1995, "Stochastic fatigue damage accumulation under broadband loadings," *Int. J. Fatigue*, **17**, pp. 321-329.
- [4] Sjöström S., 1961, "On random load analysis", *Trans. of the Royal Institute of Technology*; **161**, pp. 1-41.
- [5] Sherratt F., Bishop N. W. M., 1990, "A theoretical solution for the estimation of 'rainflow' ranges from power spectral density data", *Fatigue Fract. Engng Mater. Struct.*, **13**, pp. 311-326.
- [6] Rychlik I., 1996, "Simulation of load sequences from rainflow matrices: Markov method", *Int. J. Fatigue*, **18**, pp. 429-438.

- [7] Fren Dahl M., Rychlik I., 1993, "Rainflow analysis: Markov method", *Int. J. Fatigue*, **15**, pp.265-272.
- [8] Rychlik I., Lindgren G., Lin Y. K., 1995, "Markov based correlations of damage cycles in Gaussian and non-Gaussian loads", *Prob. Eng. Mech.*, **10**, pp. 103-115.
- [9] Dowling N. E., 1972, "Fatigue predictions for complicated stress-strain histories", *Journal of Materials*, **7**, pp. 71-87.
- [10] Endo T., Mitsunaga K., Nakagawa H., 1967, "Fatigue of metals subjected to varying stress – prediction of fatigue lives", *Preliminary Proceedings of the Chugoku-Shikoku district meeting, The Japan. Soc. Mech. Engrs.*, pp. 41-44.
- [11] Rychlik I., 1987, "A new definition of the rainflow cycle counting method". *Int. J. Fatigue*, **9**, pp. 119-121.
- [12] Rychlik I., 1993, "Note on cycle counts in irregular loads". *Fatigue Fract. Eng. Mater. Struct.*, **16**, pp. 377-390.
- [13] Kowalewski J., 1963, "On the relationship between component life under irregularly fluctuating and ordered load sequences", Part 2, DVL Rep. 249. MIRA Transl. No. 60/66.
- [14] Grimmett G., Stirzaker D., 2004, *Probability and random process, 3rd ed.*, Oxford University Press, King's Lynn, UK.
- [15] Holm S., de Maré J., 1985, "Generation of random processes for fatigue testing", *Stochastic Processes and their Applications*, **20**, pp. 149-156.
- [16] Rychlik I., Johannesson P., Leadbetter M. R., 1997, "Modelling and statistical analysis of ocean-wave data using transformed Gaussian processes," *Mar. Struct.*, **10**, pp. 13-47.
- [17] Karlsson M., 2005, "Modelling of lateral vehicle loads for fatigue life calculations", to be presented at the 9th International Conference on Structural Safety and Reliability, Rome, Italy.
- [18] Tovo R., 2002, "Cycle distribution and fatigue damage under broad-banded random loading", *Int. J Fatigue*, **24**, pp. 1137-1147.
- [19] Rychlik I., 1987, "Regression approximations of wavelength and amplitude distributions", *Adv. Appl. Prob.*, **19**, pp. 396-430.
- [20] Lindgren G., Rychlik I., 1991, "Slepian models and regression approximations in crossing and extreme value theory", *International Statistical Review*, **59**, pp. 195-225.
- [21] Rychlik I., Lindgren G., 1993, "CROSSREG, a technique for first passage and wave density analysis", *Probability in Engng. Inform. Sciences*, **7**, pp. 125-148.
- [22] Dirlik T., 1985, "Application of computers in fatigue analysis", Ph.D. thesis, University of Warwick, Warwick, UK.
- [23] Bouyssy V., Naboishikov S. M., Rackwitz R., 1993, "Comparison of analytical counting methods for Gaussian processes", *Structural Safety*, **12**, pp. 35-57.
- [24] Nagode M., Fajdiga M., 1998, "On a new method for prediction of the scatter of loading spectra", *Int. J. Fatigue*, **20**, pp. 271-277.
- [25] Karlsson M., 2004, "Parameterisation of lateral vehicle loads for fatigue assessments", Thesis of Licentiat of Eng., Chalmers University of Technology, Göteborg, Sweden.
- [26] Machado U. B., 2003, "Probability density functions for non-linear random waved and responses", *Ocean Eng.*, **30**, pp. 1027-1050.
- [27] Salvadori, G., 2004, "Bivariate return periods via 2-Copulas", *Statistical Methodology*, **1**, pp. 129-144.

Evaluation of Road Load Classification for Fatigue Assessments

Magnus Karlsson*^{†‡}

*Volvo 3P, Durability & Reliability, Dept 26780, SE-405 08 Göteborg, Sweden

[†] Mathematical Sciences, Chalmers University of Technology, SE-41296 Göteborg, Sweden

[‡] Mathematical Sciences, Göteborg University, SE-41296 Göteborg, Sweden
magnus.k.karlsson@volvo.com

Abstract

A way of modelling customer usage for fatigue life considerations is discussed. Based on a parametric vehicle independent load model, parameters are estimated using measurement data. The variation of the parameters over the measurements is studied using the analysis of variance method. In order to find a global description of customer loads, a road classification is considered, which is compared to the effect of more local factors such as market and driver. Practical considerations in the design of experiments to gather data for the models are addressed. A case study with a vehicle independent description for lateral loads is then presented. The analysis technique is applied to the load model using data from a field study made in three different markets. Conclusions are drawn on the possibilities of classifying road loads and the need for design of experiments to use field measurements more efficiently.

Keywords: Fatigue, customer correlation, road load modelling, design of experiments, vehicle independent load models.

1. Introduction

Improved measurement equipment and computers have created a possibility to increase the information about the load situation for vehicles. More data can be collected with greater accuracy and the data can be handled more easily in a computer. The natural way of taking advantage of the increased amounts of data is to create mathematical models based on the load situation found in the measurements. From these models, conclusions can be drawn and comparisons can be made about the service loads.

Much of the traditional work on describing the service loads has been focused on measuring and describing the most severe customers. For instance, Conle and Landgraf (1983) declare that it is important to anticipate as closely as possible the extremes of the field. Tests of vehicles have then been conducted comprising all possible most damaging service load states (See Berger et al. (2002)). The result is handled in such a way that if the tested vehicle/system/component can manage these extreme loads, then it is supposed to work also in the field. This holds as long as all possible loading phenomena are taken into account. Having an insufficient amount of data, which has been the case, it can at least be concluded with this policy that the components should last the design life. The great problem is, however, that it is more or less impossible to say how long they will last, and according to Olofsson (2000) this method has often resulted in components becoming unnecessarily over-dimensioned.

With the increased number of measurements, it becomes more interesting not only to model some kind of worst-case customer, but also to model the general load situation for the population of all customers. This information is of great importance when optimising the design of the vehicle towards a specific customer, and is getting even

more important as the truck industry is increasingly characterised by specialisation and customerisation. A methodology which appears to be common in order to describe the usage more generally, is to divide measurements into different classes (See Bignonnet and Thomas (2001), Ledesma et al. (2005), Aoki et al. (2003) and Panse and Awate (2006)). The classification is made depending on different factors, such as road class, topography and quality of the road. For instance, categories can be defined based on whether the road is considered to be uneven or smooth or whether it is a highway, a city street, or perhaps a mountain road. Within each class the conditions are supposed to be relatively constant. Each class of roads is then described by summarising the loads from the class. The loads can be summarised using rain-flow cycle counts on the measured load signals. Furthermore, if the interest is to quantify the load level and to get just one number to compare, it is possible to calculate a pseudo-damage from the rain-flow matrices using the Palmgren-Miner rule and the Basquin equation. With a description of each class of roads, a customer can be modelled by considering how long a distance the customer drives or how much time he or she spends in each of the different classes.

There are, however, some disadvantages of this way of describing customer loads. First of all, the most common way to determine the distance driven in each class for different customers is to use questionnaires. Unfortunately, this technique is very sensitive to the kind of questions asked and the subjective judgement of the participants. Another difficult problem is how to treat non-responses. A possible way of dealing with this problem is to use so-called easy-to-measure channels. The use of sensors in different kinds of electronic control systems in today's vehicles gives a possibility to register at least fairly accurate load signals in many more vehicles compared to what was previously possible. Although the accuracy of these sensors is lower than that of the conventional ones, there is still a great potential in logging valuable information from them. Using threshold values it might be possible to register in a more objective way the distance the vehicle is driven in each of the classes. Albeit interesting, this problem will not be treated here.

A possibly more severe problem is the way each road class is defined and described. According to Hughes et al. (2005), an important trend in the industry is to shorten the developing time and reduce the dependency on the expensive physical prototype vehicles. This means that fatigue considerations have to be moved into earlier stages of the design process, where the vehicle only exists as a computer model. The input data for these models still need to be found from measurements at service, but the vehicles used during the measurements will obviously be different from those considered in the design. (See Figure 1 for a methodology of how to consider fatigue in such earlier stages of design process.) Consequently, also the forces and strains acting on the vehicle structure will be different. Therefore, rather than modelling the forces and strains through rain flow matrices, it would be preferable to have some sort of vehicle-independent description of the load situation. One example of a vehicle-independent description is the modelling of road profile data. (See for instance Dodds and Robson (1973), Öijer and Edlund (2004) and Bogsjö (2005).) However, in order to be able to use such descriptions as input data, it is also necessary to have a model for the speed, and this problem still seems to be addressed.

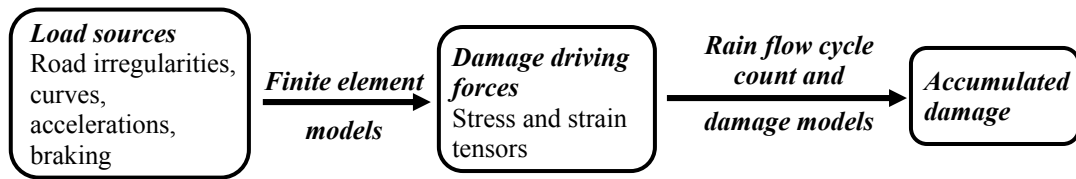


Figure 1. Methodology for considering fatigue in earlier phases of the vehicle design process.

Another great problem is to find a way of verifying that the classification is made in a proper way. As the vehicle industry is becoming increasingly global, it is important to be able to describe customers all over the world. Thus, it is necessary that the classification is also made global in some sense. In doing this a comparison has to be made with effects of more local nature, such as market effects and drivers. Such a comparison means that data have to be collected in a suitable manner and therefore there is a great need for statistical design of experiments in order to collect data in the most efficient way.

The aim of this work is to use the idea of road classification, but based on a parametric vehicle-independent load model. In the next section, a way of analysing a parametric model is considered. Based on analysis of variance method, a factor effect model is built up for each parameter in the model. In order to find a global description, a road classification is considered, and this is compared to the effect of more local factors such as market and driver. Practical considerations in the design of experiments to gather data for the models are then addressed. After this, a case study with a vehicle-independent description for lateral loads is presented. The model, which is described in detail in a series of articles by Karlsson (2004, 2005a and 2005b), is here summarised. The analysis technique is then applied to the load model using data from a field study made in three different markets. Conclusions are drawn on model complexity and possible improvements.

2. Analysing parametric load models

In this section, we will assume that we have a parametric vehicle-independent model of the loads with p parameters $(y^{(1)}, y^{(2)}, \dots, y^{(p)})$, which controls the different aspects of the load. Our model of the load is based on measurements. The parameters that are included in the model can be estimated from each separate measurement, leading to a set of parameters for each measurement. We assume that these parameters may vary between the measurements depending on several different factors and therefore we can treat them as random variables. In a sense they are load measures as they all influence the final damage according to our load model. Thus, an appropriate name for the parameters is **random load measures**. Our primary interest is to find a global classification of the loads based on road classes and to study how complex it should be. In order to do this we study the influence of road classes on the load measures, but also the influence from the local factors such as the market and the driver.

The parametric model will here be analysed using the following step-wise procedure:

1. Estimate the parameters/load measures in the model from measurements.
2. If necessary, transform the load measures in suitable ways to get a constant variance.

3. Estimate the effects of the road class, market, driver, etc., for each load measure.
4. Estimate which load measure has the largest effect on the damage.
5. Orthogonalise the load measures based on the most important measure.
6. Repeat the procedure from step 3 until all load measures are orthogonal.
7. Reduce the model based on how influential the load measures are.

We will now go through these steps in more detail. In order to estimate the effects of different factors, we will use a factor effect model for each load measure. Such a model can be studied through the analysis of variance. In a factor effect model, the variance for the model error is assumed to be the same, independent of the levels of the different factors. Consequently, some of the load measures may need to be transformed, and modelled in their transformed form.

In the factor effect models we will consider three different factors: road class, market and driver. The markets we consider here are relatively small (regions/countries), which means that it is impossible to measure all markets. Thus, ideally we can think of the markets as randomly chosen among the populations of all markets and the drivers as randomly chosen among the population of drivers driving within the market. The driver effect is thus nested within the market effect. The road class is a fixed effect since we have a limited number of road classes and measure on all of them. In the design we get drivers nested in the market levels, whereas the road classes and markets are arranged in a factorial. A factor effect model for one of the load measures $y^{(m)}$ in our parametric description of the loads is therefore:

$$y_{ijkl}^{(m)} = \mu^{(m)} + \tau_i^{(m)} + \beta_j^{(m)} + \gamma_{k(j)}^{(m)} + (\tau\beta)_{ij}^{(m)} + (\tau\gamma)_{ik(j)}^{(m)} + \varepsilon_{(ijk)l}^{(m)}, \quad m = 1, \dots, p \quad (1)$$

In eq. (1), $\mu^{(m)}$ is the mean level of the load measure over all road classes, markets and drivers. The parameters $\tau_i^{(m)}$ and $\beta_j^{(m)}$ stand for the effects of the i th road class and the j th market, respectively. The interaction effect between a road class and a market is represented by $(\tau\beta)_{ij}^{(m)}$. The effect of the driver within the market can be found in $\gamma_{k(j)}^{(m)}$ and the possible interaction between driver and road class within the market in $(\tau\gamma)_{ik(j)}^{(m)}$. Finally, $\varepsilon_{(ijk)l}^{(m)}$ is the variation due to the particular measurement.

In the above model, we have assumed that the effect of market and driver is random. Furthermore, we assume that the contributions are zero-mean normally distributed and are independent of each other. Let σ_β^2 denote the variance for the market effect, $\sigma_{\tau\beta}^2$ denote the variance for the road class/market interaction, σ_γ^2 denote the variance for the driver effect within the market, and let $\sigma_{\tau\gamma}^2$ be the variance for the interaction between drivers and road classes within a market. Finally, σ^2 is the variance for the effect of the particular measurement. We also assume that we have a different road classes, that we pick b different markets, use c different drivers in each market and make n different measurements with each driver on each road class. This means that we are using a balanced design. Using these assumptions, we can get the following table for the

expected mean squares for the different effects, following the rules of Montgomery (2005) pp. 502-503:

Model term	Degrees of Freedom	Sums of squares	Expected mean square
τ_i	$a - 1$	$bcn \sum_i (\bar{y}_{i\dots} - \bar{y}_{\dots})^2$	$\frac{bcn \sum_{i=1}^a \tau_i^2}{a - 1} + cn\sigma_{\tau\beta}^2 + n\sigma_{\tau\gamma}^2 + \sigma^2$
β_j	$b - 1$	$acn \sum_j (\bar{y}_{\cdot j \dots} - \bar{y}_{\dots})^2$	$acn\sigma_{\beta}^2 + an\sigma_{\gamma}^2 + \sigma^2$
$(\tau\beta)_{ij}$	$(a - 1)(b - 1)$	$cn \sum_{ij} (\bar{y}_{ij\dots} - \bar{y}_{i\dots} - \bar{y}_{\cdot j\dots} + \bar{y}_{\dots})^2$	$cn\sigma_{\tau\beta}^2 + n\sigma_{\tau\gamma}^2 + \sigma^2$
$\gamma_{k(j)}$	$b(c - 1)$	$an \sum_{ijkl} (\bar{y}_{\cdot jk\cdot} - \bar{y}_{\cdot j\cdot\cdot})^2$	$an\sigma_{\gamma}^2 + \sigma^2$
$(\tau\gamma)_{ik(j)}$	$(a - 1)b(c - 1)$	$n \sum_{ijk} (\bar{y}_{ijk\cdot} - \bar{y}_{ij\cdot\cdot} - \bar{y}_{\cdot jk\cdot} + \bar{y}_{\cdot j\cdot\cdot})^2$	$n\sigma_{\tau\gamma}^2 + \sigma^2$
$\varepsilon_{(ijk)l}$	$abc(n - 1)$	$\sum_{ijkl} (y_{ijkl} - \bar{y}_{ijk\cdot})^2$	σ^2

Table 1: Expected mean squares for the different model terms

In Table 1, the different sums of squares contains mean values of the collected data, e.g. $\bar{y}_{\cdot jk\cdot}$, which stands for the mean of the load measures over all measurements for market j and driver k . From this table we can find estimates of the variance components by replacing the expected mean squares with the estimated mean squares and extracting the different variance components.

One problem with this method is the possibility of estimating negative variance components. In the case of such estimates, the original estimates are replaced with 0. Finally, this results in estimated variance components for each load measure. However, a problem with even a very simple parametric load model is that there are several parameters or load measures, which can vary depending on factors such as road class, market, driver, etc., but they can also be dependent on each other, e.g. if the road has unusually many curves it is likely that the curves are also narrower. It would be preferable if the load measures were independent of each other since it would be easier to determine which of them are of importance for the damage, and to see how they are affected by the road class, market and driver.

Orthogonalisation of the load measures

In order to remove possible dependency between the load measures, we orthogonalise them in a step-by-step procedure. The order in which this orthogonalisation is made is based on the influence the load measures have on the expected damage. One alternative would be to use principal component analysis, but we are interested in keeping the physical understanding of the load measures to the greatest extent possible. By initially assuming that the load measures are in fact independent and studying the effect they have on the expected damage through a sensitivity study, the most important load measure can be selected. For the sensitivity study, the effects of the different road classes are estimated. The random effects on the load measures are chosen at a high and

a low level. These levels were set as ± 2 standard deviations, where the standard deviations were found from the estimates of the variance components. The effects of the different load measures on the expected damage were then estimated based on a fractional factorial design. To estimate the influence on the variation on the damage, the Gauss approximation formula has been used in the following way:

$$\begin{aligned} \text{Var}(E[D | (y_1, y_2, \dots, y_p)]) &= \text{Var}(f(y_1, y_2, \dots, y_p)) \\ &\approx \left(\frac{\partial f}{\partial y_1}\right)^2 \text{Var}(y_1) + \left(\frac{\partial f}{\partial y_2}\right)^2 \text{Var}(y_2) + \dots + \left(\frac{\partial f}{\partial y_p}\right)^2 \text{Var}(y_p) = \\ &= c_1^2 \sigma_1^2 + c_2^2 \sigma_2^2 + \dots + c_p^2 \sigma_p^2 \end{aligned} \quad (2)$$

where y_1, y_2, \dots, y_p are the load measures and the influence of these effects can be found as $c_1^2 \sigma_1^2, c_2^2 \sigma_2^2, \dots, c_p^2 \sigma_p^2$. These can also be approximated from the fractional factorial design. The load measure, which shows the largest influence on the variance, is selected. All other measures can then be made uncorrelated to this by removing the linear effect of the selected measure. (See Appendix A.1 for more details.)

We then repeat the procedure, by again assuming the residual parts of all measures to be independent, and select the second most influential load measure through a sensitivity study and make all remaining measures uncorrelated to this by removing the linear effect. By repeating this procedure through all measures, they can be made uncorrelated. This procedure will not remove all correlation between the different effects such as driver and market as would be preferable. (See Appendix A.1.) However, large parts will be removed and we will treat the resulting load measures as if they were independent. As this procedure is based on the influence on expected damage, some of the load measures will have very little influence, and reductions of the model can be made based on the influence of these measures compared to the most influential of the load measures. In this study, attention should also be paid to whether the effects are significant or not. Tests for significance for the different effects can be made based on Table 1. After the reduction, the remaining model can be used to determine whether the classification is good enough. In particular, the market effects can be studied to see that they are small enough to be of no importance.

3. Practical problems in the design of an experiment

In order to be able to use the analysis technique suggested in Section 2, measurement data need to be recorded. From the data, the load measures are extracted. We have assumed above that the market and driver effects are random. This means that in order to fulfil the requirement of the model in principal the markets should be randomly selected. Within each market the drivers should be randomly selected and for each driver and road class, roads should be randomly picked from the population of roads for the driver and road class. In practice, this procedure is naturally difficult to follow, but it is of importance to follow it as closely as possible. For instance, for each market we have chosen to measure, haulage contractors can be picked and two drivers per contractor be selected as randomly as possible. Each driver can then be followed over a

short period of time and then road segments can be randomly picked along the route for measurements.

Further problems to be resolved in a practical situation are how long a distance should be measured and how large a sample should be picked in order to get a sufficiently accurate description of the customer population. With the factor effect model suggested in eq. (1) the sample size problem comes down to determining the constants a , b , c , and n in Table 1. The value for a is predetermined by the number of road classes that we want to study, which means that in practice we are left with choosing the number of markets to investigate, the number of drivers on each market and the number of measurements for each driver on each road class. By putting requirements on, for instance, the variability of the estimated expected values for the load measures for each road class, and considering costs for measuring at additional markets, with additional customers and at more roads, it is possible to get a rough idea about the sample size and configuration. Another concern is the distance to measure. In our model we have included the estimation error in the remaining variance term, but this error and the remaining variance could possibly be separated, if there were an estimate of the variance of the estimation error. The total cost K_{tot} for the entire experiment can be calculated as

$$K_{tot}(b, c, n, L) = b \cdot (k_b + c \cdot (k_c + an(k_L \cdot L + k_n))) \quad (3)$$

where L is the length of a measurement, k_b is the additional cost for measuring at a market, k_c is the additional cost for measuring an extra customer, k_n is the additional cost for performing an extra measurement, k_L is the cost per km to perform a measurement. Knowing the contribution to the variability in expected damage from the different effects, we can find the set of parameters b, c, n , and L that minimise the total cost of an experiment. As the variability is not known in advance, these variance components have to be replaced with estimates. Such estimates can be found from smaller pre-studies, older measurements or using engineering judgement.

In our case we have not considered the estimation error separately, but we could choose a long enough distance and then study the variability of the estimated expected values for the load measure. Assume that we do not allow the variance for a load measure to be greater than a certain threshold Var_{th} . The estimate of the expected value for a load measure for a certain road class is $\bar{y}_{i,\dots}$. The variance of this estimate can be found based on the model in eq. (1) as:

$$Var(\bar{y}_{i,\dots}) = \frac{nc\sigma_\beta^2 + nc\sigma_{\alpha\beta}^2 + n\sigma_\gamma^2 + n\sigma_{\alpha\gamma}^2 + \sigma^2}{bcn} \quad (4)$$

Thus, we get that

$$b \geq \frac{nc\sigma_\beta^2 + nc\sigma_{\alpha\beta}^2 + n\sigma_\gamma^2 + n\sigma_{\alpha\gamma}^2 + \sigma^2}{ncVar_{th}} \quad (5)$$

By using eq. (5) in eq. (3) , and optimising, we can find the choice of b, c , and n , which minimises the cost of the experiment based on the threshold. As mentioned above this demands estimates of the variance components included in eq. (5).

4. Vehicle independent parameterisation of lateral loads

We will now go through a model which can be applied to the analysis technique suggested in the previous section. We are here interested in getting a parametric vehicle-independent description of the loads coming into the vehicle in the lateral direction from which it is possible to simulate load data. This description should catch the important features in terms of fatigue as accurately as possible, but also be as simple as possible. The effect of the operating environment on the lateral loads comes mainly from two sources: the unevenness of the road surface creates a primarily high-frequent load and due to the curvature of the road there will be a load which is more low-frequent. (See Aoki et al. (2003) for a comparison). The loads coming from the road profile can be modelled, for example, by considering methods as those suggested in Öjjer and Edlund (2004) or Bogsjö (2005). Thus, the most influential part of the operating environment to model for the lateral loads is the curvature of the road as well as the number of curves. Another important aspect to model would be the speed at which the vehicle is driven through the curves.

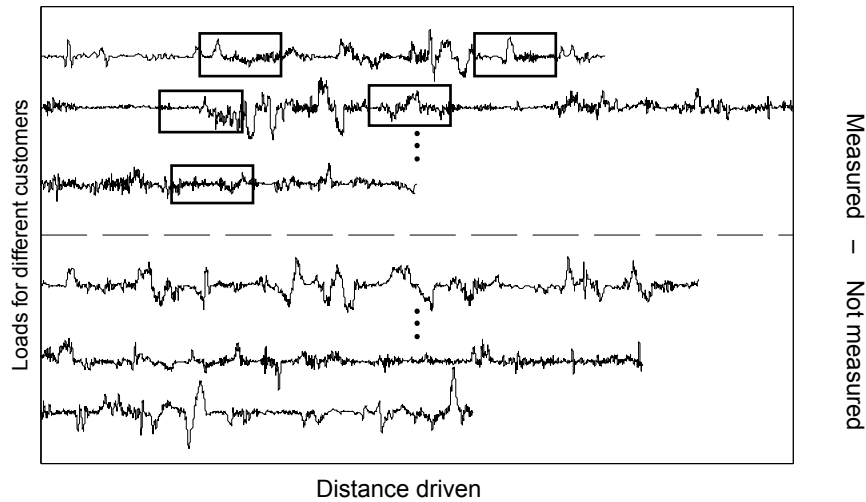


Figure 2. Only a very small number of the customers can be measured. Furthermore, the loads are only measured during a short distance of the vehicles' total lives. (Here exemplified with boxes.)

In the articles by Karlsson (2004, 2005a and 2005b), a model for the lateral loads was established. In this model, curves are detected from measurements on the yaw rate and velocity. For each detected curve an approximate curvature is found, based on road construction requirements on how to build curves suggested by the Swedish National Road Administration (1994). The curvature is modelled as a trapezoid, where the maximum curvature is considered to be most important. The distribution of maximum curvature in each curve is modelled using a transformed lognormal distribution with parameters μ_c and σ_c^2 . The number of curves is assumed to be Poisson distributed with parameter ν_c . These parameters are constants given the road, but they will differ from

one road to another. In terms of fatigue, also the speed is of great importance as the curvature and speed together will cause the lateral acceleration, which will be the load acting on the vehicle. To consider the speed, a regression model is applied, which says that down to a certain curvature, there will be a linear relation between the logarithm of the curvature and the logarithm of the speed. For wider curves, the driver no longer adopts the speed to the curvature, but rather to other sources of information such as traffic density, speed limits, engine capacity, etc. The model for the curvature and the speed can be combined to a model for the centripetal acceleration in each curve j :

$$a_{tr,j} = v_j^2 C_j = \begin{cases} a^2 C_j^{1-2b} e^{2\varepsilon_j}, & C_j \geq C_{\text{lim}} \\ a^2 C_{\text{lim}}^{-2b} C_j e^{2\varepsilon_j}, & C_j < C_{\text{lim}} \end{cases} \quad (6)$$

where the parameters a and b are the parameters in the regression model for the speed, C_{lim} is the cut-off curvature. The entities ε_j consider the random variation in speed from one curve to another, which is not explained by the regression model. They are modelled as independent zero-mean normally distributed with variance σ_ε^2 . These parameters all vary depending on the particular driver.

However, even with a model of the speed and the curvature, not all lateral acceleration coming in to the vehicle is explained. There is also another low-frequent load process which may be due to the driver's ability to follow the road, the unevenness of the road, etc. This is in contrast to Aoki et al. (2003), but may be due to the fact that the responses due to vertical loads are mostly high-frequent. Thus, some of the most low-frequent vertical loads may interfere with the low-frequent curvature loads. In the articles by Karlsson (2005a,b), this residual process is modelled as a transformed Gaussian process. In this process, the two most important parameters are the frequency of cycles ν_{res} and the variance of the transformed process σ_{res}^2 , which are modelled and contribute to the parameter vector. In this work, the spectral moment technique in Karlsson (2005b) has been used although the variance σ_{res}^2 has been fitted based on the level-crossing intensity. The remaining parameter necessary in using that technique are treated as deterministic. This residual process is assumed to be present with the same properties both in curves and on straight parts of the road, whereas the curvature loads obviously only occur in curves. The two processes are further assumed to be independent of each other given the measurement. Figure 3 below shows the measured lateral acceleration split into the two load processes:

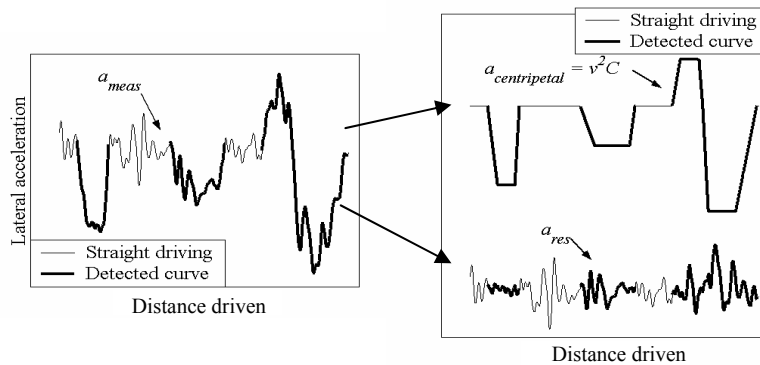


Figure 3. The measured lateral acceleration is due to the centripetal acceleration and a residual.

Using this description of the lateral acceleration, we arrive at a model containing two parameters to describe the distribution of the curvature: μ_C and σ_C^2 . We get four parameters to describe the relationship between speed and curvature a , b , C_{lim} and σ_ε^2 , where C_{lim} is of less importance for the damage, but has some value for the physical reasonability of the model. The parameter C_{lim} is modelled as deterministic. We also have one parameter describing the frequency of curves: ν_C . For the residual process, the two main parameters to consider are ν_{res} and σ_{res}^2 , the frequency of residual cycles and the variability in amplitude.

The model's accuracy has been validated through formulas for expected damage and expected range spectra given the parameter values. In these formulas also the maximum value for the residuals in the curves are considered. This value is assumed to be exponentially distributed with parameter λ . The results of these formulas with the parameter values estimated from measurements have been compared to the pseudo-damage and the range spectra found from the measured load data. (See Karlsson (2005a,b).)

5. A numerical example

The analysis technique suggested in Section 2 has here been applied to data from a field study performed on different markets. This data set was not collected with the analysis in mind and therefore it is severely unbalanced. Thus, the tests based on Table 1 are not applicable in this case as they assume balanced design. Furthermore, the experiment was not randomised and thus there are other problems with the analysis. For instance, many of the measurements in Brazil in the road class "street" were performed simulating a garbage truck whereas no such measurements were made elsewhere. Nevertheless, the results can be seen as an example of what conclusions could be drawn had it been a properly designed experiment, and, furthermore, the data can be used as input for new field studies which can be made based on the analysis techniques.



Figure 4. The truck during a field measurement in Brazil.

The data come from measurements performed in Scandinavia, Germany and Brazil with a Volvo FH12 4x2 truck, which was equipped with a large number of sensors. The sensors all recorded their signals synchronised at a sample rate of 400Hz. Our particular interest is in the lateral acceleration. This entity has been found from the measurements by using a sensor for yaw rate measured just above the front axle as well as a sensor recording the vehicle speed. In order to be able to extract the parameter values from the measurements, the time signals were first cut depending on the different road classes, so that each cut had a unique road class. Since some of the measurements (especially the ones performed on highways were made over long distances) the time signals were cut a second time so that each cut was approximately 30 km long. With this technique, 277 measurement segments were found. Apart from the road class, also the driver and the market were recorded for each segment. All parameter values were then estimated using the parametric model described in the previous section. We will here use the 7-step procedure suggested in Section 2, slightly shifted due to the fact that the data are not balanced.

5.1 Parameter values and transformations

In the model we have identified a number of different parameters which determines the external loads in the lateral direction. As can be seen in Section 4, the most important of these parameters are: the distribution parameters for the curvature μ_c and σ_c^2 , the speed parameters a , b and σ_ε^2 , the curve frequency ν_c , the parameters for the residual ν_{res} and σ_{res}^2 and the maximal residual loads in the curves λ . In this study, the cut-off curvature C_{lim} is supposed to be fixed for each road class. The parameters can be estimated from each measurement. They correspond to the load measures discussed in Section 2.

As mentioned in Section 2, there is an assumption in the factor effect model that the model error variance is homogenous over all factor levels. In order to obtain homogenous variances, transformations of the original load measures may be necessary. A discussion around such variance-stabilising transformation can be found on p. 320 in Rice (1995). As an example we will here study the frequency of curves. We have assumed that the number of curves found in a road segment is Poisson distributed with frequency ν_c curves/km. The estimated curve frequency will thus be $\hat{\nu}_c = N_c / L$, which has variance $Var(\hat{\nu}_c) = \nu_c / L$. The entities N_c and L stand for the number of curves found in the measurement and the length of the measurement. If $Y = f(\hat{\nu}_c)$, it can be shown that $Var(Y) = Var(\hat{\nu}_c) \cdot f'(\nu_c)^2 = \nu_c / L \cdot f'(\nu_c)^2$. Thus if the transformation function f is chosen in such a way that $\nu_c / L \cdot f'(\nu_c)^2$ is constant, the variance of Y will not depend on ν_c . This means that a good choice is $f(\nu_c) = 2 \cdot \sqrt{\nu_c}$ meaning that $f'(\nu_c)^2 = 1/\nu_c$ and $Var(Y) = 2/L$. Consequently, the transformed estimated frequency will be:

$$\tilde{\nu}_c = 2 \cdot \sqrt{\hat{\nu}_c} = 2 \cdot \sqrt{N_c / L} \quad (7)$$

The transformations for the remaining load measures can be found in the appendix A.2.

5.2 Simplifications of the model due to the unbalanced data

Since the available data were unbalanced, it was difficult to get suitable estimates for all effects in the factor effect model suggested in eq. (1) above. As the unbalance was particularly severe between different road classes, a model was constructed for each road class separately. We therefore used the following model to describe the effect on each load measure of the market and driver within market:

$$y_{ijkl} = \tau_i + \beta_{ij} + \gamma_{ik(j)} + \varepsilon_{(ijk)l} \quad (8)$$

This load measure can e.g. be the transformed curve frequency. We will here use the following notation: a is the number of road classes, b is the number of markets, c_{ij} is the number of drivers that have been driving on road class i in market j , and finally n_{ijk} is the number of measurements with driver k on road class i in market j . Our primary interest is to estimate the variance components in the model, of which there are three for each load measure: σ_β^2 , σ_γ^2 , and σ^2 . As the data were unbalanced the simple the results suggested in Table 1 are not applicable. For variance components estimation in the case of unbalanced data there exist several different methods. (See Rao and Heckler (1997).) We have here relied on the analysis of variance method. There are four different road classes for which we have measurements in more than one market. For a given road class, the sums of squares can be found in the following way:

$$\begin{aligned} \sum_{jkl} (y_{ijkl} - \bar{y}_{i\dots})^2 &= \sum_{jkl} (\bar{y}_{ij\dots} - \bar{y}_{i\dots})^2 + \sum_{jkl} (\bar{y}_{ijk\dots} - \bar{y}_{ij\dots})^2 + \sum_{jkl} (y_{ijkl} - \bar{y}_{ijk\dots})^2 = \\ &= \sum_{j=1}^b (\bar{y}_{ij\dots} - \bar{y}_{i\dots})^2 n_{ij\dots} + \sum_{j=1}^b \sum_{k=1}^{c_{ij}} (\bar{y}_{ijk\dots} - \bar{y}_{ij\dots})^2 n_{ijk} + \sum_{j=1}^b \sum_{k=1}^{c_{ij}} \sum_{l=1}^{n_{ijk}} (y_{ijkl} - \bar{y}_{ijk\dots})^2 \\ &= SS_B + SS_{C(B)} + SS_E \end{aligned} \quad (9)$$

In eq. (9), the entities $\bar{y}_{i\dots}$, $\bar{y}_{ij\dots}$, $\bar{y}_{ijk\dots}$, and y_{ijkl} stand for the mean over all measurements in the road class i , the mean over all measurements in the road class i and the market j , the mean over all measurement with driver k in market j and road class i , and the result in measurement l with driver k in market j and road class i , respectively. The numbers $n_{i\dots}$, $n_{ij\dots}$, and n_{ijk} stand for the number of measurements in road class i , the number of measurements in road class i on market j , and the number of measurements with driver k , in road class i on market j , respectively.

5.3 Estimation of variance components

By some calculation it is possible to show that the expected sums of squares are (Also see Rao and Heckler (1997)):

$$E[SS_B] = \sigma_\beta^2 \left(n_{i..} - \frac{\sum_{j=1}^b n_{ij.}^2}{n_{i..}} \right) + \sum_{j=1}^b \sum_{k=1}^{c_{ij}} \left(\frac{n_{i..} - n_{ij.}}{n_{i..} n_{ij.}} \right) n_{ijk} (n_{ijk} \sigma_\gamma^2 + \sigma^2) \quad (10)$$

$$E[SS_{C(B)}] = \sigma_\gamma^2 \left(n_{i..} - \sum_{j=1}^b \sum_{k=1}^{c_{ij}} \frac{n_{ijk}^2}{n_{ij.}} \right) + \sigma^2 \left(\sum_{j=1}^b c_{ij} - b \right) \quad (11)$$

and

$$E[SS_E] = \sigma^2 \left(n_{i..} - \sum_{j=1}^b c_{ij} \right) \quad (12)$$

where the sums of squares SS_B , $SS_{C(B)}$, and SS_E are defined through eq. (9). Estimates of the different variance components can now be found by extracting the variance components from the above eqs. (10-12) and replacing the expectations by their respective sums of squares. (See Appendix A.3 for an example of such variance component estimates for one of the road classes.) It should here be noted that these sums of squares are not in general independent of each other, as is the case for the balanced design.

5.4 Orthogonalisation of the load measures

By studying correlation matrices, it is clear that the load measures are in some cases strongly correlated. Therefore, we will apply the orthogonalisation technique from Section 2 and Appendix A.1. This technique is based on choosing the most important load measure in terms of the effect on the damage and therefore we need to perform a sensitivity study to understand in which order to choose the load measures. Such a study was made for each of the road classes. The order of importance according to the first sensitivity study can be seen below for each of the four identified road classes:

Road class \ Load measure	Highway		Sec. road		Thoroughfare		Street	
	First	Final	First	Final	First	Final	First	Final
Number of curves (ν_C)	1	1	2	2	2	2	2	3
Speed parameter (a)	2	2	1	3	1	1	1	2
Relative speed (b)	3	8	3	4	3	3	3	4
Speed variability (σ_ε^2)	9	4	6	1	8	6	9	6
Median curvature (μ_C)	4	3	4	5	4	4	4	1
Curve variability (σ_C^2)	7	7	8	7	9	8	7	7
Max. res. (λ)	5	5	5	6	7	5	8	9
No. of res. cycles (ν_{res})	6	6	7	8	6	7	5	5
Residual variability (σ_{res}^2)	8	9	9	9	5	9	6	8

Table 2. The order of influence of the load measures for different road classes in the first loop and applying the orthogonalisation procedure. (Influence is decreasing with increasing numbers.)

As can be seen from this table the most influential sources of variation in the first loop appear to be the number of curves and the speed parameter a . The curvature parameters on the other hand seem to be of less importance. A possible explanation to this is that the curvature is very well defined by the road classes we have selected, whereas the other load measures have a tendency to vary also within the road class. After the orthogonalisation procedure has been applied to all of the load measures, it is clear that the number of curves and the speed parameter a still is of great importance, which is reasonable since they were the most influential in the first round, and, consequently, we have based the orthogonalisation on these measures. One should, of course, here also be careful about causality. Since we remove the linear dependency of one of the load measures on the other, there is no causal argument involved. The reasoning behind the orthogonalisation is instead that by using the effect on damage argument we will single out a small number of load measures, which is of great importance and we will still keep some sort of physical explanation behind them.

Looking a little bit more into the details, we can see from Figures 5-8 below that a large number of the effects can be disregarded as they have very little influence on the variance of the expected damage. Again, this is one of the ideas behind the orthogonalisation procedure. In most cases, the most influential of the variability components within each load measure is the remaining variance, i.e. the variability which is explained by neither the market nor the driver.

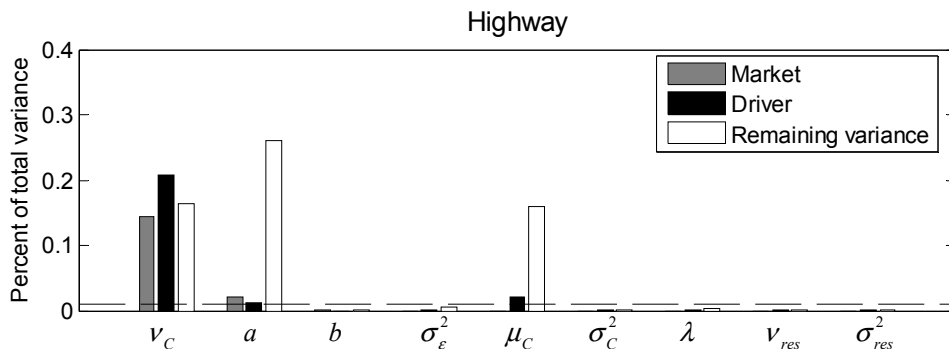


Figure 5. The contribution of the identified load measures to the damage after applying the orthogonalisation procedure. (Highway)

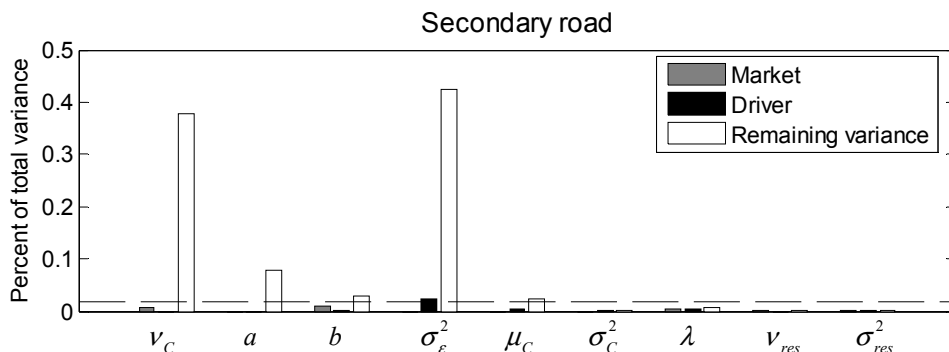


Figure 6. The contribution of the identified load measures to the damage after applying the orthogonalisation procedure. (Secondary road)

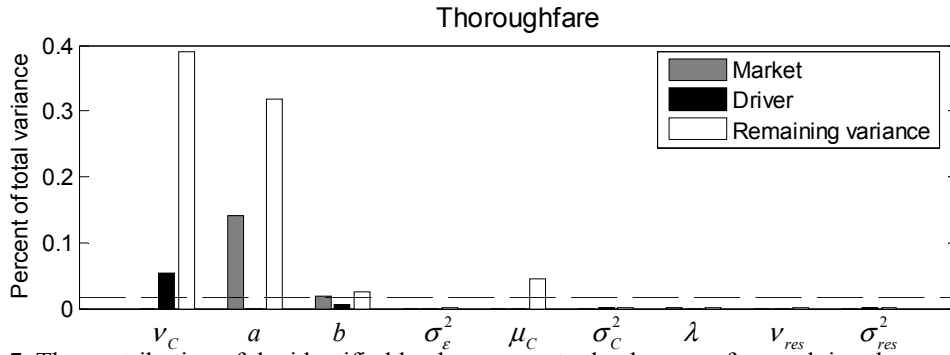


Figure 7. The contribution of the identified load measures to the damage after applying the orthogonalisation procedure. (Thoroughfare)

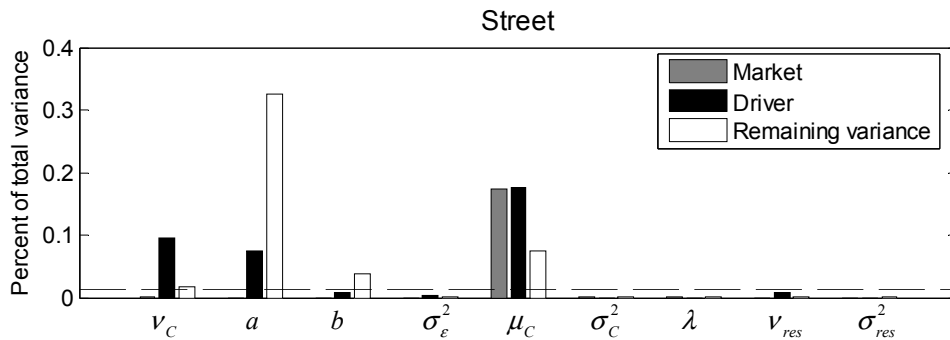


Figure 8. The contribution of the identified load measures to the damage after applying the orthogonalisation procedure. (Street)

The line that is present in all of Figures 5-8 marks the level at which the contribution to the variance of the damage is only 4% of the greatest contribution. Any effect contributing less than this level is not considered. The global load measures are now modelled using the factor effect model of eq. (8), where only the effects contributing more than the level are considered. When describing a customer, these load measures can be transformed back to the original form.

6. Discussion and Conclusions

6.1 Comments on the results

From the results in Figures 5-8, we have found some effects from markets and drivers. In some cases these detected effects may be somewhat questionable. For instance, the market effect of the mean curvature on the road class “Street” is probably due to the fact that some of the measurements in Brazil were performed simulating garbage trucks, which had the effect that the curves were almost exclusively 90 degrees and rather narrow, whereas the more regular streets have another curve distribution. Therefore, we detect a market effect as the Brazilian street curves appear to be narrower. Yet another example is the market effect on the first speed parameter in the road class “Thoroughfare”. Here it seems that the effect is due to the fact that the Brazilian drivers in some cases got stuck in traffic jams outside Sao Paulo. Such an effect can of course be regarded as a market effect as traffic jams may be more likely to occur in Sao Paulo than in Norway. On the other hand, in the case of road class “thoroughfare” only a very limited amount of data was available. Thus, these effects may simply be regarded as random variation within a market. This could be dealt with in a much more efficient way if the data would have been collected using statistical design of experiments.

Balancing the experiments as suggested in Section 2 would have resulted in spending more measurement time in road classes other than “Highway”, which had led to a better possibility of drawing conclusions without increasing the costs for the entire field study. Similarly, using a proper design of experiments the problems due to the garbage truck data mentioned above can be avoided.

On the other hand, one case where there really seems to be a market effect is for the curve frequency on the road class “Highway”. Here, the Brazilian roads were simply straighter than the European ones. This is particularly apparent compared to some measurements in Norway, which were made in hilly terrain. Norway and Sweden were set as one “Scandinavian” market in order to handle some of the unbalance and this might have been the reason for the large driver effect. The effect of the driver on, for instance, the numbers of curves appears to be somewhat odd. On the other hand it can be seen as the effect of the population of roads on which the particular driver is driving. What we see may be the effect of a driver driving on particularly curvy or straight roads within the market.

Another possible explanation here can be the fact that the measurements were cut into smaller parts and therefore the parameter values in one part might have affected the values in the next. Thus, the assumption about independence between different measurements is somewhat questionable. This possible violation of the assumptions can be dealt with by designing new experiments in a more proper way as outlined in Section 3.

The choice of treating the markets as a random factor may seem strange. The problem here is choosing the size of the market, as we cannot measure all markets with our current definition. Rather than choosing markets the size of a country or region, it may also be possible to cluster greater areas, for instance, continents. In such a way it would be possible to measure on all markets and treat them as fixed. However, we also assume that the drivers are picked randomly within the population of drivers in the market. With fewer but greater markets, this may, e.g., regarding Asia as a market, mean that one driver is chosen in Iran whereas another is picked in China. In the present way of defining markets, these would be treated as two separate markets. An example where the market size has an effect already within the current example is the choice of letting Sweden and Norway combine to form one market, which gave the impression that there was a strong driver effect on the number of curves in the road class “Highway”.

The factor effect model considers the factors road class, market and driver. Other factors of interest could be road severity, traffic density, and (as already mentioned) topography and transport mission. These are not studied here, but given that the levels of these factors have been estimated in each measurement it is possible to study their influence through residual plots, i.e. to study whether these factors can explain some of the remaining variation when the effects of road class, market and driver have been removed.

6.2 Customer description based on the model

A customer can be described from the model based on knowing how much of the distance the vehicle is driven in each of the road classes. The expected damage from the

customer can be found by calculating the expected damage for each of the road classes and adding these expectations to get the expected damage for the customer. In order to estimate the variability for the customer, the damage can be simulated from the parametric load model including the variability due to the driver, and estimates of the severe customer can be made.

When selling a truck to a customer, the most proper specification can be chosen by determining how much of the distance the vehicle is to be driven in each of the road classes. Naturally, the number of specifications that can be produced is limited and it is therefore necessary to choose the truck that best meets the requirements. This means that the customers themselves have to be classified by either putting restrictions on the expected damage or possibly the distance driven in the most severe road classes.

6.3 Conclusions

One of the obvious conclusions from the results presented based on the previous measurements is the need for a proper design of the experiments. The unbalance of the available data and the lack of randomisation cause great difficulties in estimating the effects of different factors and drawing conclusions. The information that can be found from such measurements is therefore limited. Nevertheless, the information can be used to determine the approximate number of measurements needed and give us a rough picture of the variations. The older measurements are therefore very useful in the context of serving as a pre-study. This information is of great use when designing further experiments, which can be set to follow a proper design of experiments, as suggested in Section 3.

Based on the vague results that have been produced from the current data set, it still appears as if it is possible to base a classification on road classes. In Figures 5-8 we can see that the driver and the market in most cases have very little influence. On occasion for example in the class denoted “Highway”, we can see an influence of the market, which may be interpreted as that in this case the classification cannot be regarded as global. In this case, further investigations are needed; possibly the class has to be split based on topography considerations.

7. Future Work

Obviously, it would be interesting to make new measurements according to the ideas outlined in Sections 2 and 3. With such a design of experiments, many of the pitfalls in the current measurements can be avoided.

In the future, more data can be available through so-called easy-to-measure channels. These data are not as accurate as the data that can be found through regular field measurements, but the possibility to collect this kind of data through the sensors used in the vast number of control systems in the trucks will be of great importance. Consequently, an interesting challenge in the future will be to find a rational way of updating models fitted through the current measurement type using the data from these on-board-logging activities. There is also a possibility in using warranty data as a source for updating the models. An obvious candidate technique to use is Bayesian updating. One example where warranty data have been used as an input to Bayesian updating in a fatigue context has been given by Torstensson (2004).

Based on the easy-to-measure channels it may also be possible to get more objective information regarding the customer usage and distances the customers drive in each of the road classes. This information is naturally very important for determining the load scenario for customers.

Acknowledgement

This work has been a joint project between Volvo 3P, Fraunhofer- Chalmers Research Centre for Industrial Mathematics (FCC), and the Department of Mathematical Sciences at Chalmers University of Technology and Göteborg University, where the author is a graduate student. The author wishes to express his gratitude towards his supervisors Dr. Thomas Svensson, FCC, Prof. Jacques de Maré, Chalmers and Dr. Bengt Johannesson, Volvo. The project is funded by the Swedish Agency for Innovation Systems.

References

- Aoki, T., Imai, K., Watanabe, S., Yamakawa, S., Nakahara, Y., Haraguchi, M., Uchiyama, Y., (2003) "A Study of Development Indices Established Quantification of Road Load", SAE Technical Paper 2003-01-2843.
- Berger C., Eulitz K. G., Heuler P., Kotte K. L., Naundorf H., Schütz W., Sonsino C. M., Wimmer A., Zenner H., (2002) "Betriebsfestigkeit in Germany – an overview". *Int. J. Fatigue*, 24 pp. 603-625.
- Bignonnet, A., Thomas, J. J., (2001) "Fatigue Assessment and Reliability in Automotive Design", SAE Technical Paper 2001-01-4061.
- Bogsjö, K., (2005) "Stochastic Modelling of Road Roughness", Licentiate of Engineering Thesis, Lund Institute of Technology, Lund, Sweden.
- Conle, A., and Landgraf, R. W., (1983) "A Fatigue Analysis Program for Ground Vehicle Components", *Proc. of the International Conference on Digital Techniques in Fatigue (SEECO '83)*, Society of Environmental Engineers, March 1983, London, pp. 1-28.
- Dodds, C. J., Robson, J. D., (1973) "The Description of Road Surface Roughness", *J. of Sound and Vibration*, 31, pp. 175-183.
- Hughes, S., Jones, R. P., and Burrows, A. J., (2005) "Application of System Modeling to Road Load Data Synthesis for Automobile Product Development", *Proc. of 2005 ASME International Mechanical Engineering Congress and Exposition*, Nov. 5-11, 2005, Orlando, FA.
- Karlsson, M., (2004) "Driver Independent Road Curve Characterisation", *Supp. to Vehicle System Dynamics*, 41, pp. 411-420.
- Karlsson, M., (2005a) "Modelling of Lateral Vehicle Loads for Fatigue Life Calculations", *Proc. of the International Conference on Structural Safety and Reliability*, Rome, Italy, 19-23 June, 2005.
- Karlsson, M., (2005b) "Evaluation of Approximative Methods for Rainflow Damage of Broad-Banded Non-Gaussian Random Loads", *Proc. of 2005 ASME International Mechanical Engineering Congress and Exposition*, Nov. 5-11, 2005, Orlando, FA.
- Ledesma, R., Jenaway, L., Wang, Y, Shih, S., (2005) "Development of Accelerated Durability Tests for Commercial Vehicle Suspension Components", SAE Technical Paper 2005-01-3565.
- Montgomery, D. C., (2005) *Design and Analysis of Experiments*, 6 Ed., Wiley, Hoboken, NJ.
- Öijer, F., Edlund, S., (2004) "Identification of Transient Road Obstacle Distributions and Their Impact on Vehicle Durability and Driver Comfort", *Supp. to Vehicle System Dynamics*, 41, pp. 744-753.
- Olofsson, M., (2000) "Evaluation of Estimates of Extreme Fatigue Load – Enhanced by Data from Questionnaires". Licentiate of Engineering Thesis, Chalmers University of Technology, Göteborg, Sweden.
- Panse, S. M., Awate, C. M., (2006) "Development of Accelerated Structural Durability Test Program for a Mini-truck and its Components", SAE Technical Paper 2006-01-0085.
- Rao, P.S.R.S., Heckler, C.E., (1997) "The three-fold nested random effects model", *Journal of Statistical Planning and Inference*, 64, pp. 341-352.
- Rice, J.A., (1995) *Mathematical Statistics and Data Analysis*, 2 Ed., Duxbury Press, Belmont, CA.
- Swedish National Road Administration, (1994) "Vägutformning-94 version S-1, del 6 Linjeföring". Vägverket Publikation 1994-52, Borlänge. (In Swedish).

Appendices

A.1 Orthogonalisation in detail

Assume again that we have p load measures in our model: $(y_{ijkl}^{(1)}, y_{ijkl}^{(2)}, \dots, y_{ijkl}^{(p)})$. The expected damage given the load measures can be written as a function of these measures:

$$E[D_{ijkl} | y_{ijkl}^{(1)}, y_{ijkl}^{(2)}, \dots, y_{ijkl}^{(p)}] = f_1(y_{ijkl}^{(1)}, y_{ijkl}^{(2)}, \dots, y_{ijkl}^{(p)}) \quad (\text{A.1})$$

If the load measures were independent, it would be relatively easy to relate the variability in the expected damage to the variability in the load measures themselves. However, as the load measures depend on each other, it is more difficult to get an estimate of how much they contribute to the variability, in other words how important they are for the damage. One way of treating the problem with dependency is to orthogonalise the load measures. Since we are assuming everything to be Gaussian it would be sufficient to remove the linear dependency. The orthogonalisation is made in the following way: First, a sensitivity study is performed to see which load measure affects the expected damage the most by initially assuming the load measures to be independent. The most influential load measure is selected and the linear effect of this measure is removed from all other measures. After this the procedure is repeated: through a new sensitivity study the most important measure among the residuals of the remaining measures is selected and the effect of this measure is removed from all other measures. Finally, after all measures are made orthogonal of each other, the resulting measures can be studied to see how they affect the expected damage. The resulting measures can now be regarded as linear combinations of the original, or equivalently that the original measures can be regarded as a linear combination of the resulting measures. Thus, the eq. (A.1) can be written as:

$$\begin{aligned} E[D_{ijkl} | y_{ijkl}^{(1)}, y_{ijkl}^{(2)}, \dots, y_{ijkl}^{(p)}] &= f_1(y_{ijkl}^{(1)}, y_{ijkl}^{(2)}, \dots, y_{ijkl}^{(p)}) = \\ &= f_1(a_1^{(1)} \tilde{y}_{ijkl}^{(1)} + a_1^{(2)} \tilde{y}_{ijkl}^{(2)} + \dots + a_1^{(p)} \tilde{y}_{ijkl}^{(p)}, \dots, a_p^{(1)} \tilde{y}_{ijkl}^{(1)} + a_p^{(2)} \tilde{y}_{ijkl}^{(2)} + \dots + a_p^{(p)} \tilde{y}_{ijkl}^{(p)}) \end{aligned} \quad (\text{A.2})$$

where $\tilde{y}_{ijkl}^{(m)}$, $m = 1, \dots, p$ are the resulting load measures and $a_q^{(m)}$ are coefficients. The orthogonalisation can therefore be seen as a way of moving the variability in one measure that can be explained with a second measure to that second measure. For instance, if there are three measures and a very strong correlation between the two first, the first measure can be used to explain most of the variability caused by the pair of measures. This may therefore lead to another order of importance than what was originally found. Similarly, if the first measure is relatively uncorrelated with the second and third, and there is a strong correlation between the second and third, the resulting second measure may end up explaining more of the variability than the first measure. This can in fact be seen for instance for the road class "secondary street", where the load measure corresponding to speed parameter a appears to be most

important in the first round, but after the orthogonalisation has been applied it is only the third most important measure.

Each of the load measures further depends on the road class, market and driver as specified in eq. (1), but the effects of these factors are latently hidden in the load measures. Thus, the orthogonalisation will not remove all of the correlation structure from the factor effects. To see this, consider the two load measures Y_1 and Y_2 , which can be written as $Y_1 = \mu_1 + X_1 + Z_1 + \varepsilon_1$ and $Y_2 = \mu_2 + X_2 + Z_2 + \varepsilon_2$, respectively, where μ_i are mean values. The components of the triple $(X_i, Z_i, \varepsilon_i)$ are supposed to be independent of each other and the only dependency between the different load measures is that X_1 and X_2 may be dependent, Z_1 and Z_2 may be dependent, and ε_1 and ε_2 may be dependent. One way to make Y_2 orthogonal to Y_1 is with the following transformation:

$$Y'_2 = Y_2 - E[Y_2|Y_1] = X_2 + Z_2 + \varepsilon_2 - E[X_2 + Z_2 + \varepsilon_2|Y_1]. \quad (\text{A.3})$$

We define $X'_2 = X_2 - E[X_2|Y_1]$, $Z'_2 = Z_2 - E[Z_2|Y_1]$, and $\varepsilon'_2 = \varepsilon_2 - E[\varepsilon_2|Y_1]$. We would like to see that X_1 and X'_2 are independent, etc. However, it can be shown that:

$$\begin{aligned} \text{Cov}(X_1, X'_2) &= \text{Cov}(X_1, X_2) \cdot \left(1 - \frac{\text{Var}(X_1)}{\text{Var}(Y_1)}\right) = \\ &= \text{Cov}(X_1, X_2) \cdot \left(1 - \frac{\text{Var}(X_1)}{\text{Var}(X_1) + \text{Var}(Z_1) + \text{Var}(\varepsilon_1)}\right) \end{aligned} \quad (\text{A.4})$$

This means that in general not all correlation is removed, but for the effect which contributes most to the load measure the correlation will be lowered most.

A.2 Variance-stabilising transformation of the parameter values

As was seen in Section 5, there may be a need for transforming the load measures included in the model. This idea was exemplified with the parameter, which identifies the frequency of curves. For the parameters in the curvature distribution, μ_c is estimated by taking the mean of the logarithm of a transformed curvature in the different curves (See [15] for the transformation.). The transformed curvature is assumed to be lognormally distributed. Thus, there is no need for a variance-stabilising transformation in this case. The parameter σ_c^2 corresponds to the variance of the logarithm of the transformed curvature and can therefore be estimated in that way. Based on the χ^2 -distribution, the variance for the estimate can be found as $\text{Var}(S_c^2) = 2\sigma_c^4 / (n-1)$. Applying the variance-stabilising technique, a transformation giving constant variance can be found as $Y = \ln(S_c^2)$. This transformation can also be applied to the variance estimate σ_e^2 for the same reason. The parameter λ is the expected value in an exponential distribution. The variance of the estimate of this parameter is $\text{Var}(\hat{\lambda}) = \lambda^2 / n$. A transformation can be found as $Y = \ln(\hat{\lambda})$. Finally, for the remaining parameters in the regression model for the speed, using the assumption in the model it is clear that the estimate of the slope parameter b needs no transform and

by taking the logarithm of the estimate of the parameter a , the variance will have no mean value dependency. The frequency of residual cycles is transformed using a square-root transform and the variance estimate σ_{res}^2 is transformed using logarithm. To summarise we get the following transformations for the different parameters: $\tilde{\mu}_C = \hat{\mu}_C$, $\tilde{\sigma}_C^2 = \ln(\hat{\sigma}_C^2)$, $\tilde{\sigma}_\varepsilon^2 = \ln(\hat{\sigma}_\varepsilon^2)$, $\tilde{\sigma}_{res}^2 = \ln(\hat{\sigma}_{res}^2)$, $\tilde{b} = \hat{b}$, $\tilde{a} = \ln \hat{a}$, $\tilde{\nu}_C = 2 \cdot \sqrt{\hat{\nu}_C}$, $\tilde{\lambda} = \ln(\hat{\lambda})$ and $\tilde{\nu}_{res} = 2 \cdot \sqrt{\hat{\nu}_{res}}$.

A.3 Example of variance component estimates

An example of variance component estimates for the road class “Highway” is given in Table A.1 below. Negative variance component estimates have been replaced with a 0. Such estimates are marked with a minus sign in the table.

Variance comp. Load measure	Market (σ_β^2)	Driver (σ_γ^2)	Remaining variance (σ^2)
No. of curves (ν_C)	0.39	0.56	0.45
Speed parameter (a)	-0	0.0015	0.0086
Relative speed (b)	-0	0.06	0.72
Speed variability (σ_ε^2)	0.06	0.03	0.77
Median curvature (μ_C)	$0.01 \cdot 10^{-3}$	-0	$0.14 \cdot 10^{-3}$
Curve variability (σ_C^2)	-0	0.007	0.064
Max. res. (λ)	-0	0.02	0.14
No. of res. cycles (ν_{res})	-0	0.074	0.088
Residual variability (σ_{res}^2)	-0	0.006	0.088

Table A.1. Variance components estimates for the different load measures for the road class “Highway”